

# **Analysis of Experimental Data for High-Burnup PWR Spent Fuel Isotopic Validation — Vandellós II Reactor**

**AVAILABILITY OF REFERENCE MATERIALS  
IN NRC PUBLICATIONS**

**NRC Reference Material**

As of November 1999, you may electronically access NUREG-series publications and other NRC records at NRC's Public Electronic Reading Room at <http://www.nrc.gov/reading-rm.html>. Publicly released records include, to name a few, NUREG-series publications; *Federal Register* notices; applicant, licensee, and vendor documents and correspondence; NRC correspondence and internal memoranda; bulletins and information notices; inspection and investigative reports; licensee event reports; and Commission papers and their attachments.

NRC publications in the NUREG series, NRC regulations, and *Title 10, Energy*, in the Code of *Federal Regulations* may also be purchased from one of these two sources:

1. The Superintendent of Documents  
U.S. Government Printing Office  
P.O. Box SSOP  
Washington, DC 20402-0001  
Internet: [bookstore.gpo.gov](http://bookstore.gpo.gov)  
Telephone: 202-512-1800  
Fax: 202-512-2250
2. The National Technical Information Service  
Springfield, VA 22161-0002  
[www.ntis.gov](http://www.ntis.gov)  
1-800-553-6847 or, locally, 703-605-6000

A single copy of each NRC draft report for comment is available free, to the extent of supply, upon written request as follows:

Address: Office of the Chief Information Officer,  
Reproduction and Distribution  
Services Section  
U.S. Nuclear Regulatory Commission  
Washington, DC 20555-0001  
E-mail: [DISTRIBUTION@nrc.gov](mailto:DISTRIBUTION@nrc.gov)  
Facsimile: 301-415-2289

Some publications in the NUREG series that are posted at NRC's Web site address <http://www.nrc.gov/reading-rm/doc-collections/nuregs> are updated periodically and may differ from the last printed version. Although references to material found on a Web site bear the date the material was accessed, the material available on the date cited may subsequently be removed from the site.

**Non-NRC Reference Material**

Documents available from public and special technical libraries include all open literature items, such as books, journal articles, and transactions, *Federal Register* notices, Federal and State legislation, and congressional reports. Such documents as theses, dissertations, foreign reports and translations, and non-NRC conference proceedings may be purchased from their sponsoring organization.

Copies of industry codes and standards used in a substantive manner in the NRC regulatory process are maintained at—

The NRC Technical Library  
Two White Flint North  
11545 Rockville Pike  
Rockville, MD 20852-2738

These standards are available in the library for reference use by the public. Codes and standards are usually copyrighted and may be purchased from the originating organization or, if they are American National Standards, from—

American National Standards Institute  
11 West 42<sup>nd</sup> Street  
New York, NY 10036-8002  
[www.ansi.org](http://www.ansi.org)  
212-642-4900

Legally binding regulatory requirements are stated only in laws; NRC regulations; licenses, including technical specifications; or orders, not in NUREG-series publications. The views expressed in contractor-prepared publications in this series are not necessarily those of the NRC.

The NUREG series comprises (1) technical and administrative reports and books prepared by the staff (NUREG/XXXX) or agency contractors (NUREG/CR-XXXX), (2) proceedings of conferences (NUREG/CP-XXXX), (3) reports resulting from international agreements (NUREG/IA-XXXX), (4) brochures (NUREG/BR-XXXX), and (5) compilations of legal decisions and orders of the Commission and Atomic and Safety Licensing Boards and of Directors' decisions under Section 2.206 of NRC's regulations (NUREG-0750).

**DISCLAIMER:** This report was prepared as an account of work sponsored by an agency of the U.S. Government. Neither the U.S. Government nor any agency thereof, nor any employee, makes any warranty, expressed or implied, or assumes any legal liability or responsibility for any third party's use, or the results of such use, of any information, apparatus, product, or process disclosed in this publication, or represents that its use by such third party would not infringe privately owned rights.

# **Analysis of Experimental Data for High-Burnup PWR Spent Fuel Isotopic Validation— Vandellós II Reactor**

Manuscript Completed: August 2010  
Date Published: January 2011

Prepared by  
G. Ilas and I.C. Gauld

Oak Ridge National Laboratory  
Managed by UT-Battelle, LLC  
Oak Ridge, TN 37831-6170

M. Aissa, NRC Project Manager

NRC Job Code N6540



## ABSTRACT

This report is one of the several recent NUREG/CR reports documenting benchmark-quality radiochemical assay data and the use of the data to validate computer code predictions of isotopic composition for spent nuclear fuel, to establish the uncertainty and bias associated with code predictions. The experimental data analyzed in the current report were acquired from a high-burnup fuel program coordinated by Spanish organizations. The measurements included extensive actinide and fission product data of importance to spent fuel safety applications, including burnup credit, decay heat, and radiation source terms. Six unique spent fuel samples from three uranium oxide fuel rods were analyzed. The fuel rods had a 4.5 wt %  $^{235}\text{U}$  initial enrichment and were irradiated in the Vandellós II pressurized water reactor operated in Spain. The burnups of the fuel samples range from 42 to 78 GWd/MTU. The measurements were used to validate the two-dimensional depletion sequence TRITON in the SCALE computer code system.



# CONTENTS

	<u>Page</u>
ABSTRACT.....	iii
LIST OF FIGURES .....	vii
LIST OF TABLES .....	ix
ACKNOWLEDGMENTS .....	xi
ACRONYMS AND ABBREVIATIONS .....	xiii
1 INTRODUCTION.....	1
2 EXPERIMENTAL PROGRAM.....	3
3 ISOTOPIC MEASUREMENTS .....	5
4 ASSEMBLY DESIGN AND IRRADIATION HISTORY DATA.....	17
5 COMPUTATIONAL ANALYSIS.....	25
5.1 COMPUTATIONAL METHODS .....	25
5.2 MODELS .....	25
6 RESULTS AND DISCUSSION.....	33
7 SUMMARY .....	59
8 REFERENCES.....	61
APPENDIX A TRITON INPUT FILES .....	A-1





## LIST OF FIGURES

	<u>Page</u>
Figure 2.1. Locations of samples from rod WZR0058 (taken from Ref. 4).....	4
Figure 4.1. Assembly layout for Vandellós II samples.....	19
Figure 4.2. Vandellós II core layout. ....	20
Figure 4.3. Boron concentration vs. irradiation time (from Ref. 9).....	23
Figure 5.1. TRITON model for rod WZR0058 – cycle 7. ....	27
Figure 5.2. TRITON model for rod WZR0058 – cycle 8. ....	27
Figure 5.3. TRITON model for rod WZR0058 – cycle 9. ....	28
Figure 5.4. TRITON model for rod WZR0058 – cycle 10. ....	29
Figure 5.5. TRITON model for rod WZR0058 – cycle 11. ....	30
Figure 5.6. Measured data for $^{148}\text{Nd}$ and $^{137}\text{Cs}$ vs. sample location for rod WZR0058. ....	32
Figure 6.1. Calculation-to-measurement comparison for $^{234}\text{U}$ .....	37
Figure 6.2. Calculation-to-measurement comparison for $^{235}\text{U}$ .....	37
Figure 6.3. Calculation-to-measurement comparison for $^{236}\text{U}$ .....	38
Figure 6.4. Calculation-to-measurement comparison for $^{238}\text{Pu}$ . ....	38
Figure 6.5. Calculation-to-measurement comparison for $^{239}\text{Pu}$ . ....	39
Figure 6.6. Calculation-to-measurement comparison for $^{240}\text{Pu}$ . ....	39
Figure 6.7. Calculation-to-measurement comparison for $^{241}\text{Pu}$ . ....	40
Figure 6.8. Calculation-to-measurement comparison for $^{242}\text{Pu}$ . ....	40
Figure 6.9. Calculation-to-measurement comparison for $^{237}\text{Np}$ .....	41
Figure 6.10. Calculation-to-measurement comparison for $^{241}\text{Am}$ .....	41
Figure 6.11. Calculation-to-measurement comparison for $^{243}\text{Am}$ .....	42
Figure 6.12. Calculation-to-measurement comparison for $^{244}\text{Cm}$ .....	42
Figure 6.13. Calculation-to-measurement comparison for $^{246}\text{Cm}$ .....	43
Figure 6.14. Calculation-to-measurement comparison for $^{140}\text{Ce}$ . ....	43
Figure 6.15. Calculation-to-measurement comparison for $^{142}\text{Ce}$ . ....	44
Figure 6.16. Calculation-to-measurement comparison for $^{144}\text{Ce}$ . ....	44
Figure 6.17. Calculation-to-measurement comparison for $^{142}\text{Nd}$ .....	45
Figure 6.18. Calculation-to-measurement comparison for $^{143}\text{Nd}$ .....	45
Figure 6.19. Calculation-to-measurement comparison for $^{145}\text{Nd}$ .....	46
Figure 6.20. Calculation-to-measurement comparison for $^{146}\text{Nd}$ .....	46
Figure 6.21. Calculation-to-measurement comparison for $^{148}\text{Nd}$ .....	47
Figure 6.22. Calculation-to-measurement comparison for $^{150}\text{Nd}$ .....	47

## LIST OF FIGURES (continued)

	<u>Page</u>
Figure 6.23. Calculation-to-measurement comparison for $^{147}\text{Sm}$ . .....	48
Figure 6.24. Calculation-to-measurement comparison for $^{148}\text{Sm}$ . .....	48
Figure 6.25. Calculation-to-measurement comparison for $^{149}\text{Sm}$ . .....	49
Figure 6.26. Calculation-to-measurement comparison for $^{150}\text{Sm}$ . .....	49
Figure 6.27. Calculation-to-measurement comparison for $^{151}\text{Sm}$ . .....	50
Figure 6.28. Calculation-to-measurement comparison for $^{152}\text{Sm}$ . .....	50
Figure 6.29. Calculation-to-measurement comparison for $^{154}\text{Sm}$ . .....	51
Figure 6.30. Calculation-to-measurement comparison for $^{153}\text{Eu}$ . .....	51
Figure 6.31. Calculation-to-measurement comparison for $^{154}\text{Eu}$ . .....	52
Figure 6.32. Calculation-to-measurement comparison for $^{155}\text{Eu}$ . .....	52
Figure 6.33. Calculation-to-measurement comparison for $^{154}\text{Gd}$ . .....	53
Figure 6.34. Calculation-to-measurement comparison for $^{155}\text{Gd}$ . .....	53
Figure 6.35. Calculation-to-measurement comparison for $^{156}\text{Gd}$ . .....	54
Figure 6.36. Calculation-to-measurement comparison for $^{158}\text{Gd}$ . .....	54
Figure 6.37. Calculation-to-measurement comparison for $^{160}\text{Gd}$ . .....	55
Figure 6.38. Calculation-to-measurement comparison for $^{133}\text{Cs}$ . .....	55
Figure 6.39. Calculation-to-measurement comparison for $^{134}\text{Cs}$ . .....	56
Figure 6.40. Calculation-to-measurement comparison for $^{135}\text{Cs}$ . .....	56
Figure 6.41. Calculation-to-measurement comparison for $^{137}\text{Cs}$ . .....	57
Figure 6.42. Calculation-to-measurement comparison for $^{106}\text{Ru}$ . .....	57
Figure 6.43. Calculation-to-measurement comparison for $^{139}\text{La}$ . .....	58
Figure 6.44. Calculation-to-measurement comparison for $^{99}\text{Tc}$ . .....	58

## LIST OF TABLES

	<u>Page</u>
Table 1.1. Summary of spent fuel measurements .....	2
Table 2.1. Vandellós II fuel samples.....	3
Table 3.1. Experimental techniques and isotopic concentrations (in %g/g <sup>238</sup> U) for 1 <sup>st</sup> campaign.....	9
Table 3.2. Experimental techniques and isotopic concentrations (in %g/g <sup>238</sup> U) for 2 <sup>nd</sup> campaign.....	11
Table 3.3. Half-lives of isotopes used in data adjustment.....	12
Table 3.4. Isotopic concentrations – combined data (in %g/g <sup>238</sup> U) .....	13
Table 3.5. Isotopic concentrations – combined data (in g/g U <sub>initial</sub> ) .....	15
Table 4.1. Fuel rods and assemblies loading locations .....	20
Table 4.2. Assembly design data .....	21
Table 4.3. Adjacent assembly data.....	22
Table 4.4. Irradiation history data.....	22
Table 4.5. Fuel rod burnup data .....	22
Table 4.6. Cycle power data for each sample .....	22
Table 4.7. Moderator temperature and density data.....	23
Table 4.8. Boron concentration in moderator .....	24
Table 5.1. Cycle power data based on measured sample burnups .....	31
Table 6.1. C/E-1 (%) results .....	35



## ACKNOWLEDGMENTS

This work was performed under contract with the U.S. Nuclear Regulatory Commission (NRC) under Project N6540, *Neutronics for Reactor and Spent Nuclear Fuel*. The authors would like to thank staff of the NRC Office of Nuclear Regulatory Research and the NRC Division of Spent Fuel and Transportation for their review and helpful comments and Mourad Aissa of the Office of Nuclear Regulatory Research for guidance and support. Review of the manuscript by Steve Bowman and Georgeta Radulescu at Oak Ridge National Laboratory and the careful formatting of this document by Debbie Weaver are appreciated and acknowledged.



## ACRONYMS AND ABBREVIATIONS

ANL	Argonne National Laboratory
ATM	Advanced Testing Materials
ARIANE	<u>A</u> ctinides <u>R</u> esearch <u>I</u> n <u>A</u> <u>N</u> uclear <u>E</u> lement
BOC	beginning of cycle
C/E	calculated-to-experimental
CEA	Commissariat à l'Énergie Atomique
CSN	Consejo de Seguridad Nuclear
DOE	U.S. Department of Energy
EFPD	effective full power days
ENRESA	Empresa Nacional de Residuo Radioactivo, S. A.
ENUSA	Empresa Nacional del Uranio, S. A.
EOC	end of cycle
GE-VNC	General Electric – Vallecitos Nuclear Center
GKN II	Gemeinschaftskernkraftwerk Unit II
HPLC	high pressure liquid chromatography
ICP-MS	inductively coupled plasma mass spectrometry
IDA	isotope dilution analysis
ID-MS	isotope dilution mass spectrometry
ITU	Institute for Transuranium Elements
JAERI	Japanese Atomic Energy Research Institute
KRI	Khoplin Radium Institute
LA	luminescent analysis
LWR	light water reactor
MALIBU	<u>MOX</u> and <u>UOX</u> <u>LWR</u> <u>Fuels</u> <u>Irradiated</u> to <u>High</u> <u>Burnup</u>
MOX	mixed oxide
MS	mass spectrometry
MTU	metric ton uranium ( $10^6$ grams)
NRC	U.S. Nuclear Regulatory Commission
ORNL	Oak Ridge National Laboratory
PNNL	Pacific Northwest National Laboratory
ppm	parts per million
PSI	Paul Scherrer Institute
PWR	pressurized water reactor
REBUS	<u>R</u> eactivity <u>T</u> ests for a <u>D</u> irect <u>E</u> valuation of the <u>B</u> urnup <u>C</u> redit on <u>S</u> electe <u>D</u> <u>I</u> rradiated <u>LWR</u> <u>Fuel</u> <u>B</u> undles
SCALE	Standardized Computer Analyses for Licensing Evaluations
SCK-CEN	Studiecentrum voor Kernenergie – Centre d'Étude de l'Énergie Nucléaire
TIMS	thermal ionization mass spectrometry
TMI	Three Mile Island
UO <sub>2</sub>	uranium dioxide
YMP	Yucca Mountain Project





# 1 INTRODUCTION

The current trend toward extended irradiation cycles and higher fuel enrichments approaching 5 wt %  $^{235}\text{U}$  has led to an increase of the burnup for discharged nuclear fuel assemblies in the United States, which now routinely exceeds 60 GWd/metric ton uranium (MTU). Accurate analysis and evaluation of the uncertainties in the predicted isotopic composition for high-burnup spent nuclear fuel require rigorous computational tools and experimental data against which these tools can be benchmarked. However, the majority of isotopic assay measurements available to date involve spent fuel with burnups of less than 40 GWd/MTU and initial enrichments below 4 wt %  $^{235}\text{U}$ , limiting the ability to validate computer code predictions and accurately quantify the uncertainties of isotopic analyses for modern fuels in the high-burnup domain.

Quantifying and evaluating the uncertainty in spent fuel compositions is important for understanding and reducing the uncertainties associated with predicting the high-burnup fuel characteristics for spent fuel transportation and storage applications involving decay heat, radiation sources, and criticality safety evaluations with burnup credit, as well as for other reactor safety studies and accident consequence analyses.

This report documents the analyses performed by Oak Ridge National Laboratory (ORNL) of experimental data acquired from a Spanish high-burnup fuel program coordinated by the Spanish safety council for nuclear activities Consejo de Seguridad Nuclear (CSN), the Spanish fuel vendor Empresa Nacional del Uranio, S. A. (ENUSA), and Empresa Nacional de Residuo Radioactivo (ENRESA), the organization responsible for waste management in Spain. The assay measurements documented in this report include six spent fuel samples selected from three fuel rods with a 4.5 wt %  $^{235}\text{U}$  initial enrichment that were irradiated in the Vandellós II pressurized water reactor (PWR) operated in Spain. The samples cover a burnup range from 42 to 78 GWd/MTU. Measurement cross-check data were available for three of the six samples.

This report is one of several recent NUREG/CR reports documenting the validation of the Standardized Computer Analyses for Licensing Evaluations (SCALE) code system against radiochemical assay measurements data. The experimental data included in the reports were compiled from domestic and international programs. The isotopic assay measurements include data for a total of 51 spent fuel samples selected from fuel rods enriched from 2.6 to 4.7 wt %  $^{235}\text{U}$  and irradiated in six different PWRs operated in Germany, Japan, Spain, Switzerland, and the United States. The samples cover a large burnup range—from 14 to 78 GWd/MTU. A summary of the experimental programs and measured fuel characteristics is provided in Table 1.1. For consistency of the comparison, the validation studies against the measurement data shown in Table 1.1 were all carried out using SCALE 5.1 codes and nuclear data.

A brief description of the Spanish experimental program is given in Section 2 of this report. The main radiochemical methods employed, the measurement results, and the associated experimental uncertainties are provided in Section 3. Information on the assembly design data and irradiation history is presented in Section 4, and details on the computational models developed and simulation methodology used are shown in Section 5. A comparison of the experimental data with the results obtained from code simulations is presented in Section 6.

**Table 1.1. Summary of spent fuel measurements**

Reactor (country)	Measurement facility	Experimental program name	Assembly design	Enrichment (wt % <sup>235</sup> U)	No. of samples	Measurement methods	Burnup(s) <sup>a</sup> (GWd/MTU)
TMI-1 <sup>b</sup> (USA)	ANL (USA)	YMP	15 × 15	4.013	11	ICP-MS, α-spec, γ-spec	44.8 – 55.7
TMI-1 <sup>b</sup> (USA)	GE-VNC (USA)	YMP	15 × 15	4.657	8	TIMS, α-spec, γ-spec	22.8 – 29.9
Calvert Cliffs <sup>b</sup> (USA)	PNNL, KRI (USA, Russia)	ATM	14 × 14 CE	3.038	3	ID-MS, LA, α-spec, γ-spec	27.4, 37.1, 44.3
Takahama 3 <sup>b</sup> (Japan)	JAERI (Japan)	JAERI	17 × 17	2.63, 4.11	16	ID-MS, α-spec, γ-spec	14.3 – 47.3
Gösgen <sup>c</sup> (Switzerland)	SCK-CEN, ITU (Belgium, Germany)	ARIANE	15 × 15	3.5, 4.1	3	TIMS, ICP-MS, α-spec, β-spec, γ-spec	29.1, 52.5, 59.7
GKN II <sup>c</sup> (Germany)	SCK-CEN (Belgium)	REBUS	18 × 18	3.8	1	TIMS, ICP-MS α-spec, γ-spec	54.0
Gösgen <sup>d</sup> (Switzerland)	SCK-CEN, CEA, PSI (Belgium, France, Switzerland)	MALIBU	15 × 15	4.3	3	TIMS, ICP-MS, α-spec, γ-spec	46.0, 50.8, 70.3
Vandellós II <sup>e</sup> (Spain)	Studsvik (Sweden)	CSN/ENUSA	17 × 17	4.5	6	ICP-MS, γ-spec	42.5 – 78.3

<sup>a</sup> Correspond to operator-based values, as reported, except for data for MALIBU and CSN/ENUSA programs samples, which correspond to measured data for burnup indicators.

<sup>b</sup> Documented in G. Ilas, I. C. Gauld, F. C. Difilippo, and M. B. Emmett, *Analysis of Experimental Data for High Burnup PWR Spent Fuel Isotopic Validation—Calvert Cliffs, Takahama, and Three Mile Island Reactors*, NUREG/CR-6968 (ORNL/TM-2008/071), prepared for the U.S. Nuclear Regulatory Commission by Oak Ridge National Laboratory, Oak Ridge, Tennessee (2009).

<sup>c</sup> Documented in G. Ilas, I. C. Gauld, and B. D. Murphy, *Analysis of Experimental Data for High Burnup PWR Spent Fuel Isotopic Validation—ARIANE and REBUS Programs (UO<sub>2</sub> Fuel)*, NUREG/CR-6969 (ORNL/TM-2008/072), prepared for the U.S. Nuclear Regulatory Commission by Oak Ridge National Laboratory, Oak Ridge, Tennessee (2009).

<sup>d</sup> Details about the MALIBU program can be found in *MALIBU Program – Radiochemical Analysis of MOX and UOX LWR Fuels Irradiated to High Burnup*, Belgonucleaire Technical Proposal, MA 2001/02, Belgonucleaire, Brussels, Belgium (September 2001).

<sup>e</sup> Documented in current report.

## 2 EXPERIMENTAL PROGRAM

Assay data have been acquired and evaluated by ORNL, under support of the U.S. Nuclear Regulatory Commission (NRC), for high-burnup samples selected from three fuel rods irradiated in the Vandellós II PWR operated in Spain. This experimental program (Refs. 1–2) was coordinated by the Spanish safety council for nuclear activities, CSN, in collaboration with Spanish fuel vendor ENUSA and ENRESA, the organization responsible for waste management in Spain. The fuel isotopic measurements were performed at the laboratory of Studsvik Nuclear AB located in Nykoping, Sweden.

The Vandellós II samples were selected from three fuel rods identified as WZR0058, WZtR165, and WZtR160, which were taken from two fuel assemblies. Each of these three rods had an initial enrichment of 4.5 wt %  $^{235}\text{U}$ . The rods were irradiated in the reactor for five consecutive cycles, from cycle 7 to cycle 11. During the first four of the five irradiation cycles, rods WZR0058 and WZtR165 were located in the same fuel assembly, EC45, whereas rod WZtR160 was located in assembly EC46. For their last cycle, these three rods were removed from their original assemblies and inserted into different positions of rebuilt assembly EF05. The irradiation histories of rods WZtR160, WZR0058, and WZtR165 were similar and resulted in calculated final rod-average burnup of 66.5, 68.5, and 70.0 MWd/MTU, respectively. Details on the irradiation history are provided in Section 4.

The experimental program was carried out in two measurement campaigns:

- Phase 1, performed in 2002–2003 (Refs. 3–5), included measurements of seven samples from rods WZR0058 and WZtR165.
- Phase 2, performed in 2007 (Ref. 6), included reanalysis of two fuel sample solutions from the first campaign and measurements for two new samples from rods WZR0058 and WZtR160.

One sample was selected for analysis from each of the fuel rods WZtR165 and WZtR160, whereas seven fuel segments were selected from rod WZR0058. The locations of the samples with respect to the bottom of the active fuel region and the sample burnups are shown in Table 2.1. The locations of the samples selected from rod WZR0058 are illustrated in Figure 2.1. Three of the samples from rod WZR0058, measured in the first campaign and identified as E58-773, E58-793, and E58-796, were cut within a 23 mm section of the fuel rod in a relatively uniform high-burnup region of the rod. These samples all had the same burnup based on the gamma scan of the rod and are considered sister samples for analysis purposes, as discussed further in this section. These samples provide a measure of the experimental accuracy for all phases of the experimental procedures, including independent cutting, dissolution, separations, and radiochemical analysis.

**Table 2.1. Vandellós II fuel samples**

Rod ID	WZR0058							WZtR165	WZtR160
Sample ID	E58-88	E58-148	E58-263	E58-257	E58-773	E58-793	E58-796	165-2a	160-800
Axial location <sup>a</sup> (mm)	88	148	263	257	773	793	796	797	1060
Campaign	I   II	I	I	II	I	I   II	I	I	II
Combined sample ID	E58-88	E58-148	E58-260		E58-700			165-2a	160-800
Burnup <sup>b</sup> (GWd/MTU)	42.5	54.8	64.6		77.0			78.3	70.9

<sup>a</sup> With respect to the bottom of the active fuel region.

<sup>b</sup> Burnup based on measured data for burnup-indicator fission products  $^{148}\text{Nd}$  and  $^{137}\text{Cs}$ , as discussed in Section 5 of this report.

A second phase of the project was carried out with support of ORNL and the NRC to provide additional cross-check measurements and to better evaluate and reduce the uncertainties in the data obtained from the first phase. In the second phase, instrumentation with increased accuracy was used to repeat the measurements in some of the samples measured in the first campaign to resolve discrepancies observed for some isotopes and include some metallic isotopes not present in the first set of measurements. In addition to the reanalysis of two fuel sample solutions from the first campaign, a new fuel sample from rod WZR0058 was measured in the second campaign; this sample, identified as E58-257, was selected from a position adjacent to one (i.e., E68-263) of the first-campaign samples to provide confirmatory analysis of the measurement procedures, including cutting and fuel dissolution. Also, a new high-burnup (>70 GWd/t) sample from rod WZtR160 was examined.

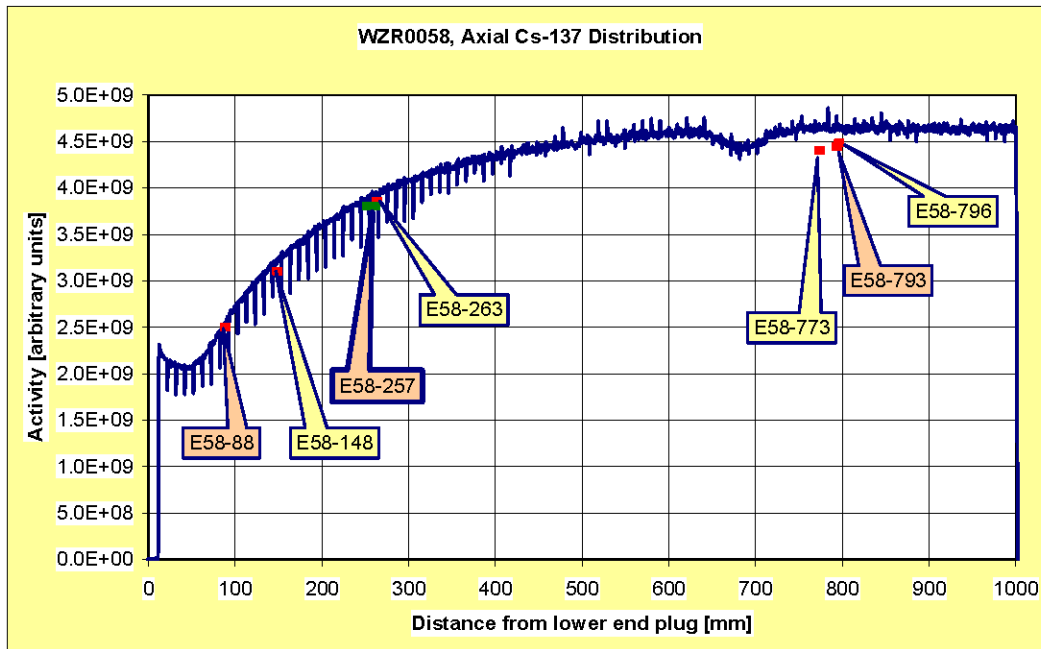


Figure 2.1. Locations of samples from rod WZR0058 (taken from Ref. 4).

### 3 ISOTOPIC MEASUREMENTS

The measurements were carried out by Studsvik in two experimental campaigns: Phase 1 measurements performed in 2002–2003 and Phase 2 measurements performed in 2007. The experiments in 2002–2003 were carried out for the samples identified as E58-88, E58-148, E58-263, E58-773, E58-793, E58-796, and 165-2a. Updated reports describing the 2003 experiments were issued later to address some inconsistencies observed in fuel handling and correlate the measured data to the actual rod identities. As part of the second experimental campaign at Studsvik, new measurements were performed to increase the number of available samples and confirm the accuracy of the previous measurements using improved instruments with increased accuracy. Reanalyses of samples E58-88 and E58-793 were carried out in the second campaign using solutions available from the 2003 measurement campaign. Two new samples were measured in 2007: one sample identified as E58-257, cut from rod WZR0058, and one sample identified as 160-800, cut from rod WZtR160.

High-performance liquid chromatography (HPLC) combined with an inductively coupled plasma mass spectrometer (ICP-MS) and ICP-MS without chemical separations were used at Studsvik Nuclear AB for the analysis of about 45 individual isotopes in a total of 9 samples. Fuel inventories of six additional fission product radionuclides with suitably long half-lives and gamma lines were determined based on gamma scans of the fuel rod.

The following main experimental techniques have been applied for measurements performed at Studsvik in Sweden:

- ICP-MS with isotope dilution analysis (IDA)
  - actinides: U, Pu, Am
  - lanthanides: Ce, Nd, Sm, Eu, Gd
  - metallics:  $^{95,97,98,100}\text{Mo}$
- ICP-MS with external calibration
  - metallics:  $^{99}\text{Tc}$ ,  $^{103}\text{Rh}$
  - actinides:  $^{237}\text{Np}$ ,  $^{244,246}\text{Cm}$
  - lanthanides:  $^{139}\text{La}$
  - fission products:  $^{133}\text{Cs}$ ,  $^{135}\text{Cs}$
- $\gamma$ -spectrometry
  - $^{103,106}\text{Ru}$ ,  $^{134,137}\text{Cs}$ ,  $^{144}\text{Ce}$ ,  $^{154}\text{Eu}$

Only the main techniques are summarized above. Some nuclides required multiple techniques to eliminate interferences. The measurements in the second campaign included more nuclides than measured in the first campaign:  $^{103}\text{Rh}$ ,  $^{139}\text{La}$ ,  $^{99}\text{Tc}$ , and  $^{95,97,98,100}\text{Mo}$ . The  $^{135}\text{Cs}$  isotope was not measured in the second campaign.

The measurement data as reported for the first campaign are shown in Table 3.1. The isotopic data were reported as weight percent relative to measured  $^{238}\text{U}$ . Data for most of the measured nuclides were reported at the time of measurement. Data from the  $\gamma$ -spectrometry were reported at discharge time. Data for isotopes measured by ICP-MS with external calibration correspond to a decay time of 1110 days, and data for isotopes measured by ICP-MS with IDA correspond to 1101 days decay time. For the three samples E58-773, E58-793, and E58-796 selected from a 23 mm length fuel segment the high-burnup region of rod WZR0058, which had effectively the same burnup, the reported data for these samples were compared to check measurement consistency. It was found that for 42 of the 44 measured isotopes, the measured concentrations were compatible at the 95% confidence level (i.e., the data agree within  $2\sigma$ ).

The data for the other two measured isotopes,  $^{243}\text{Am}$  and  $^{154}\text{Eu}$ , agreed within  $3\sigma$ . Therefore, these samples can be considered sister samples based on the similarity of the measurement data.

The data for the second measurement campaign, as reported, are shown in Table 3.2. The data include isotopic concentrations for two new samples, identified as 160-800 and E58-257, and isotopic concentrations measured in old solutions for samples E58-88 and E58-793 that were available from the first measurement campaign. The data from the  $\gamma$ -spectrometry were reported at discharge time. The second-campaign data for isotopes measured by ICP-MS with external calibration correspond to a decay time of 2298 d, and the data for isotopes measured by ICP-MS with IDA correspond to a 2334 d decay time. Some of the measurements from this second campaign were carried out with new, better-precision instruments than those used in the first campaign. The measured isotopic concentrations and the corresponding uncertainties were reported as weight percent relative to the measured content of  $^{238}\text{U}$ .

An evaluation of the experimental data from the two separate measurement campaigns was performed as part of the work for the current report. Second-campaign results for sample E58-88, which was measured using a sample solution from the first campaign, were combined with results available from the first campaign after an evaluation of the data for consistency. In addition, first-campaign measurement data for samples E58-773 and E58-796 were combined with the two separate measurements of sample E58-793 to form a single dataset identified as sample E58-700. Second-campaign measurements on sample E58-257 were also combined with the first-campaign results for sample E58-263. Sample E58-257 was cut from a position adjacent to that of sample E58-263, and the samples had the same burnup based on operator data. The size of sample E58-257 (10 mm) was larger than most of the other samples (2 mm). The maximum estimated burnup difference based on the  $^{137}\text{Cs}$  gamma scan data for these two samples was estimated to be less than 1%, which was less than the uncertainty on the burnup determination using destructive analysis data.

As part of the data evaluation procedure, measurement results for most second-campaign data were first back-calculated to the time of the first-campaign measurement dates to provide a consistent basis for comparing and combining the measurement data from both campaigns. The adjustment of the data from the second campaign accounted for the decay of the measured nuclides and the contributions from decay precursors. Measurements for  $^{144}\text{Nd}$  from the second campaign could not be adjusted for all samples because the precursor  $^{144}\text{Ce}$  was not measured in them all. Similarly,  $^{147}\text{Sm}$  data from the second campaign were not used because the precursor  $^{147}\text{Pm}$  was not measured in any of the samples, and therefore properly accounting for the decay time was not possible.

The half-lives used to adjust data to account for the different measurement times are listed in Table 3.3. These data are based on ENDF/B-VI nuclear data and are the same values as used in the code simulations.

The combination of the data (Ref. 7) was done as shown in Eq. (3.1), where  $x_i$  and  $\sigma_i$  ( $i=1,n$ ) are, respectively, the reported measured isotopic content and reported corresponding uncertainty (at 95% confidence level) for a given isotope, and  $\bar{x}$  and  $\sigma$  are, respectively, the combined measured isotopic content and corresponding uncertainty for that isotope.

$$\bar{x} = \frac{\sum_{i=1}^n x_i}{\sum_{i=1}^n \frac{1}{\sigma_i^2}} \quad \text{and} \quad \sigma^2 = \frac{1}{\sum_{i=1}^n \frac{1}{\sigma_i^2}} \quad (3.1)$$

The experimental data were compared at the 95% confidence level, corresponding to two standard deviations in the measurement uncertainty reported by the laboratory. Multiple measurements for a

sample that agreed within this level were combined according to Eq. (3.1) using the measurement uncertainty to weight the different measurements. For nuclides that did not agree within the uncertainties, additional evaluations of the data were performed, as discussed below. The combined data are shown in Table 3.4. To facilitate a consistent comparison, the uncertainty data shown for all samples in Table 3.4 correspond to a 95% confidence level.

Uranium measurements from the second campaign were not recommended or used in this study. The IDA results for  $^{235}\text{U}$  and  $^{236}\text{U}$  were systematically higher in the second campaign compared to the first and higher than ICP-MS with external calibration results (Ref. 6). This change was later traced by the laboratory to an instrumentation error in the second campaign.

Neodymium IDA results from the first measurement campaign for samples E58-88 and E58-263 were removed from the dataset. Large systematic differences were observed between Phase 1 and Phase 2 results for several neodymium isotopes for these two samples. In addition, the sample burnup based on first-phase  $^{148}\text{Nd}$  results were not consistent with the sample burnup determined from  $^{137}\text{Cs}$  gamma scanning. For these two samples, only neodymium data from the second measurement campaign were used. The  $^{142}\text{Nd}$  result for sample 165-2a was removed from the dataset, as it was significantly out of trend (lower by 25%) compared to corresponding results from all other similar burnup samples.

Second-campaign  $^{241}\text{Am}$  measurements for samples E58-88 and E58-793 were not included in the final dataset because the results were two times larger than the first-campaign results for the same two samples and larger than the second-campaign results for the two new samples. The results were also inconsistent with the  $^{241}\text{Am}$  concentration that would be produced from the decay of  $^{241}\text{Pu}$ , indicating measurement problems. The removed measurements corresponded to the two reanalyzed solutions, indicating the problem could have been related to instability over time of these solutions.

The  $^{243}\text{Am}$  results for sample E58-793, measured in both campaigns, did not agree within the 95% confidence level with the results for similar samples E58-796 and E58-773. The E58-793 results appeared to be out of trend; however, the difference was judged to be insufficient for removing the data for sample E58-793. Rather, the results for all four measurements from the two campaigns for the sample identified as E58-700 were combined, and the uncertainty was increased by a factor of two.

The  $^{142}\text{Ce}$  and  $^{149}\text{Sm}$  results for samples E58-257 and E58-263 were found to be inconsistent at the 95% confidence range. Likewise, the second-campaign  $^{160}\text{Gd}$  results for sample E58-793 were inconsistent compared to results for sample E58-796. The  $^{154}\text{Sm}$  results from the second campaign for sample E58-793 were also found to be inconsistent with the first-campaign results for the three samples E58-793, E58-796, and E58-773. In most of these cases, though, the differences were only slightly larger than the 95% confidence range. Consequently, the results for these samples were combined and the associated uncertainty similarly increased by a factor of two.

Second-campaign results for  $^{155}\text{Gd}$  were observed to be erratic and biased by more than 50% compared to the first-campaign results. Because the concentration of  $^{155}\text{Gd}$  is determined almost entirely from the decay of  $^{155}\text{Eu}$ , the expected  $^{155}\text{Gd}$  can be analytically calculated. Based on this calculation, the Phase 2  $^{155}\text{Gd}$  data were determined to be incorrect and removed from the final dataset.

Europium data from the second measurement campaign were not used. Results for  $^{153}\text{Eu}$ , the most abundant europium isotope, exhibited a 20% discrepancy between Phases 1 and 2. The spike solution used in the Phase 1 measurements was reanalyzed and the initial results adjusted accordingly by Studsvik. However, no basis for performing a similar adjustment of the Phase 2 data was identified (Ref. 6). The results for  $^{151}\text{Eu}$  were not used from either campaign due to erratic behavior of the data, likely due to very low concentrations that resulted in larger uncertainties than actually reported.

The  $^{133}\text{Cs}$  data for the two new samples E58-257 and 160-800 measured in the second campaign were not considered due to a reported loss of cesium from the solutions for these two samples (Ref. 6). The  $^{103}\text{Rh}$  data for sample E58-257 were removed due to suspected incomplete recovery of the metallic nuclide in solution. Similarly, the  $^{99}\text{Tc}$  data for samples E58-257 and E58-793 were removed due to recovery problems (Ref. 6). The molybdenum data were not considered as it was discovered that these measurements were contaminated by natural molybdenum (Ref. 6).

For comparison to measured data obtained from other experimental programs, the experimental data shown in Table 3.4 were also expressed in units of g/g  $U_{\text{initial}}$ , as shown in Table 3.5, using the initial uranium content in the sample as a basis. The concentration in g/g  $U_{\text{initial}}$  of nuclide  $i$  was determined as (Ref. 8)

$$\frac{m_i}{\sum_k m_{U_k} + \sum_l m_{Pu_l} + \sum_m m_{Am_m} + \sum_n m_{Cm_n} + 238 \frac{m_{^{148}\text{Nd}}}{148\bar{Y}}} \quad (3.2)$$

where  $m_i$  is the mass of isotope  $i$  reported in %g/g  $^{238}\text{U}$  measured. The denominator in Eq. (3.2) is the derived value for the initial uranium content, calculated as a sum of the measured heavy metal isotopes (uranium, plutonium, americium, and curium) masses in the sample and the heavy metal mass loss due to burnup. The reduction in heavy metal mass due to burnup is approximated by  $238 \frac{m_{^{148}\text{Nd}}}{148\bar{Y}}$ , where  $\bar{Y}$  is a weighted cumulative atom fission yield of  $^{148}\text{Nd}$ . A value  $\bar{Y} = 0.0176$  is recommended for PWR  $\text{UO}_2$  fuel (Ref. 8). Note that  $m_{U_{238}} = 100$  in Eq. (3.2) because all measurements were reported in percentage relative to measured  $^{238}\text{U}$  in the samples. No error propagation was carried out on the ratio in Eq. (3.2) as any additional error associated with the unit conversion is extremely small relative to the reported measurement uncertainties.



**Table 3.1. Experimental techniques and isotopic concentrations (in %g/g<sup>238</sup>U) for 1<sup>st</sup> campaign**

Sample ID		E58-88		E58-148		E58-263		E58-773		E58-793		E58-796		165-2a	
Burnup <sup>a</sup>	(GWd/t)	42.5		54.8		64.6		77.0		77.0		77.0		78.3	
Nuclide <sup>b</sup>	Method <sup>c</sup>	Mass <sup>d</sup> %g/g <sup>238</sup> U	2 $\sigma$ <sup>d</sup> %g/g <sup>238</sup> U	Mass %g/g <sup>238</sup> U	2 $\sigma$ %g/g <sup>238</sup> U	Mass %g/g <sup>238</sup> U	2 $\sigma$ %g/g <sup>238</sup> U	Mass %g/g <sup>238</sup> U	2 $\sigma$ %g/g <sup>238</sup> U	Mass %g/g <sup>238</sup> U	2 $\sigma$ %g/g <sup>238</sup> U	Mass %g/g <sup>238</sup> U	2 $\sigma$ %g/g <sup>238</sup> U	Mass %g/g <sup>238</sup> U	2 $\sigma$ %g/g <sup>238</sup> U
U-234	ICP-MS IDA	0.0245	0.0044	0.0232	0.0034	0.0161	0.0064	0.0136	0.0036	0.0150	0.0066	0.0152	0.0038	0.0140	0.0038
U-235	ICP-MS IDA	1.328	0.148	0.921	0.064	0.525	0.072	0.321	0.032	0.312	0.054	0.320	0.030	0.294	0.026
U-236	ICP-MS IDA	0.568	0.056	0.687	0.050	0.677	0.090	0.645	0.058	0.684	0.094	0.671	0.050	0.681	0.050
Pu-238	ICP-MS IDA	0.0281	0.0020	0.0402	0.0054	0.0651	0.007	0.0884	0.0084	0.0977	0.0136	0.0859	0.010	0.0971	0.0096
Pu-239	ICP-MS IDA	0.652	0.032	0.642	0.044	0.640	0.064	0.676	0.046	0.724	0.084	0.679	0.048	0.741	0.044
Pu-240	ICP-MS IDA	0.250	0.012	0.293	0.020	0.327	0.032	0.372	0.026	0.395	0.052	0.385	0.028	0.404	0.026
Pu-241	ICP-MS IDA	0.140	0.008	0.160	0.012	0.182	0.018	0.199	0.014	0.216	0.030	0.205	0.018	0.221	0.014
Pu-242	ICP-MS IDA	0.0574	0.0032	0.0920	0.0066	0.1370	0.0138	0.1864	0.0136	0.1994	0.0276	0.1853	0.0144	0.2095	0.0130
Np-237	ICP-MS ext	0.073	0.012	0.100	0.016	0.130	0.022	0.127	0.020	0.117	0.018	0.122	0.020	0.140	0.022
Am-241	ICP-MS IDA	0.026	0.002	0.029	0.002	0.032	0.004	0.036	0.002	0.031	0.004	0.033	0.002	0.037	0.002
Am-243	ICP-MS IDA	0.0093	0.0008	0.0245	0.003	0.0418	0.007	0.0634	0.0052	0.0510	0.0058	0.0649	0.0054	0.0766	0.004
Cm-244	ICP-MS ext	0.0019	0.0004	0.0060	0.0012	0.0151	0.003	0.0234	0.0046	0.0221	0.0044	0.0227	0.0046	0.0291	0.0058
Cm-246	ICP-MS ext	0.000018	0.000008	0.000062	0.000024	0.000250	0.00008	0.000570	0.00018	0.000530	0.00018	0.000540	0.00018	0.000730	0.00024
Nd-142	ICP-MS IDA	0.0026	0.0002	0.0038	0.0006	0.0073	0.0004	0.0104	0.0008	0.0099	0.0008	0.0098	0.0012	0.0072	0.0004
Nd-143	ICP-MS IDA	0.119	0.006	0.126	0.006	0.143	0.006	0.147	0.010	0.140	0.012	0.133	0.008	0.132	0.008
Nd-144	ICP-MS IDA	0.191	0.008	0.238	0.012	0.307	0.014	0.392	0.024	0.382	0.034	0.370	0.018	0.373	0.020
Nd-145	ICP-MS IDA	0.0991	0.0048	0.1118	0.0056	0.1386	0.0062	0.1567	0.0098	0.1491	0.013	0.1430	0.0072	0.1413	0.0076
Nd-146	ICP-MS IDA	0.1019	0.0044	0.1263	0.0056	0.1698	0.0068	0.2094	0.0124	0.2041	0.0176	0.1920	0.0094	0.1928	0.0096
Nd-148	ICP-MS IDA	0.0561	0.0028	0.0660	0.0036	0.0894	0.0038	0.0995	0.0064	0.0998	0.009	0.0947	0.0048	0.1026	0.0084
Nd-150	ICP-MS IDA	0.0991	0.0048	0.1118	0.0056	0.1386	0.0062	0.1567	0.0098	0.1491	0.013	0.1430	0.0072	0.1413	0.0076
Cs-133	ICP-MS ext	0.162	0.026	0.183	0.028	0.228	0.036	0.237	0.038	0.219	0.034	0.221	0.034	0.219	0.034
Cs-134	$\gamma$ -spec	0.017	0.004	0.024	0.006	0.034	0.01	0.045	0.012	0.045	0.012	0.045	0.012	0.047	0.002
Cs-135	ICP-MS ext	0.089	0.014	0.103	0.016	0.118	0.02	0.111	0.018	0.101	0.016	0.103	0.016	0.114	0.020
Cs-137	$\gamma$ -spec	0.171	0.022	0.211	0.024	0.254	0.028	0.300	0.034	0.300	0.034	0.300	0.034	0.299	0.018
Ce-140	ICP-MS IDA	0.165	0.008	0.212	0.008	0.270	0.01	0.324	0.014	0.301	0.014	0.300	0.020	0.320	0.018
Ce-142	ICP-MS IDA	0.156	0.008	0.201	0.006	0.251	0.01	0.299	0.012	0.280	0.012	0.279	0.018	0.294	0.016
Ce-144	$\gamma$ -spec	0.021	0.0058	0.0245	0.0068	0.0288	0.008	0.0325	0.0090	0.0328	0.0090	0.0328	0.0090	0.033	0.004

**Table 3.1. Experimental techniques and isotopic concentrations (in %g/g<sup>238</sup>U) for 1<sup>st</sup> campaign (cont.)**

Sample ID		E58-88		E58-148		E58-263		E58-773		E58-793		E58-796		165-2a	
Burnup <sup>a</sup>	(GWd/t)	42.5		54.8		64.6		77.0		77.0		77.0		78.3	
Nuclide <sup>b</sup>	Method <sup>c</sup>	Mass <sup>d</sup> %/g <sup>238</sup> U	2σ <sup>d</sup> %/g <sup>238</sup> U	Mass %/g <sup>238</sup> U	2σ %/g <sup>238</sup> U	Mass %/g <sup>238</sup> U	2σ %/g <sup>238</sup> U	Mass %/g <sup>238</sup> U	2σ %/g <sup>238</sup> U	Mass %/g <sup>238</sup> U	2σ %/g <sup>238</sup> U	Mass %/g <sup>238</sup> U	2σ %/g <sup>238</sup> U	Mass %/g <sup>238</sup> U	2σ %/g <sup>238</sup> U
Sm-147	ICP-MS IDA	0.0284	0.0016	0.0297	0.0014	0.0282	0.0026	0.0282	0.0026	0.0298	0.0028	0.0286	0.0016	0.0319	0.0020
Sm-148	ICP-MS IDA	0.0204	0.0010	0.0300	0.0014	0.0373	0.0034	0.0506	0.0046	0.0543	0.0050	0.0498	0.0024	0.0565	0.0034
Sm-149	ICP-MS IDA	0.00036	0.00006	0.00039	0.00006	0.00032	0.00004	0.00038	0.00006	0.00040	0.00006	0.00042	0.00008	0.00039	0.0001
Sm-150	ICP-MS IDA	0.0353	0.0020	0.0472	0.0022	0.0529	0.0048	0.0675	0.0060	0.0709	0.0064	0.0649	0.0032	0.0659	0.0040
Sm-151	ICP-MS IDA	0.00149	0.00016	0.00015	0.00012	0.00154	0.00014	0.00192	0.0002	0.00203	0.00022	0.00194	0.0001	0.00192	0.0002
Sm-152	ICP-MS IDA	0.0132	0.0060	0.0155	0.0006	0.0164	0.0014	0.0193	0.0016	0.0199	0.0018	0.0195	0.0010	0.0204	0.0010
Sm-154	ICP-MS IDA	0.00426	0.00032	0.00563	0.0003	0.00678	0.00062	0.00872	0.00082	0.00911	0.00084	0.00917	0.00056	0.01185	0.00100
Eu-151	ICP-MS IDA	0.000054	0.000004	0.000100	0.000012	0.000073	0.000072	0.000063	0.000012	0.000079	0.000008	0.000066	0.000016	0.000072	0.000006
Eu-153	ICP-MS IDA	0.0169	0.0010	0.0224	0.0012	0.0273	0.0024	0.0317	0.002	0.0326	0.0028	0.0299	0.0014	0.0323	0.0016
Eu-154	ICP-MS IDA	0.00236	0.00028	0.00338	0.0002	0.00398	0.00052	0.00433	0.00048	0.00495	0.00066	0.00389	0.00028	0.00560	0.0006
Eu-155	ICP-MS IDA	0.00062	0.00004	0.00098	0.0001	0.00118	0.00012	0.00147	0.00018	0.00148	0.00018	0.00123	0.00008	0.00133	0.00016
Gd-154	ICP-MS IDA	0.00101	0.00010	0.00154	0.00014	0.00170	0.00020	0.00236	0.00016	0.00236	0.00028	0.00224	0.00014	0.00281	0.00048
Gd-155	ICP-MS IDA	3.0E-04	5.0E-05	4.9E-04	8.0E-05	5.5E-04	5.2E-05	7.8E-04	6.8E-05	7.5E-04	8.0E-05	6.8E-04	4.0E-05	6.1E-04	5.6E-05
Gd-156	ICP-MS IDA	0.00988	0.00056	0.01918	0.00176	0.02925	0.00268	0.04849	0.0033	0.04963	0.00444	0.04720	0.0023	0.04963	0.00456
Gd-158	ICP-MS IDA	0.0017	0.0002	0.0030	0.0004	0.0042	0.0004	0.0072	0.0006	0.0072	0.0008	0.0068	0.0004	0.0074	0.0010
Gd-160	ICP-MS IDA	0.00014	0.00002	0.00018	0.00006	0.00024	0.00002	0.00039	0.00012	0.00031	0.00012	0.00028	0.00002	0.00039	0.00004
Ru-103	γ-spec													0.0071	0.0022
Ru-106	γ-spec	0.015	0.004	0.020	0.006	0.026	0.006	0.032	0.008	0.032	0.008	0.032	0.008	0.033	0.002

<sup>a</sup> Burnup based on measured data for burnup indicators fission products <sup>148</sup>Nd and <sup>137</sup>Cs, as discussed in Section 5 of this report.

<sup>b</sup> The measured isotopic data correspond to discharge time for isotopes measured by γ-spectrometry; data for isotopes measured by ICP-MS with external calibration are at 1110 d decay time; data for isotopes measured by IDA are at 1101 d decay time.

<sup>c</sup> Main technique is mentioned; some nuclides required multiple techniques to eliminate interferences.

<sup>d</sup> Shown as weight percent relative to measured <sup>238</sup>U as reported in H. U. Zwicky and J. Low, *Fuel Pellet Isotopic Analyses of Vandellós 2 Rods WZr165 and WZR0058: Complementary Report*, STUDEVIK/N(H)-04/135 Rev. 1 (2008).

**Table 3.2. Experimental techniques and isotopic concentrations (in %g/g<sup>238</sup>U) for 2<sup>nd</sup> campaign**

Sample ID		E58-88(new)		E58-793(new)		E58-257		160-800	
Burnup <sup>a</sup> (GWd/t)		42.5		77.0		64.6		70.9	
Nuclide <sup>b</sup>	Method <sup>c</sup>	Mass <sup>d</sup>	2 $\sigma$ <sup>d</sup>	Mass	2 $\sigma$	Mass	2 $\sigma$	Mass	2 $\sigma$
		%g/g <sup>238</sup> U	%g/g <sup>238</sup> U	%g/g <sup>238</sup> U	%g/g <sup>238</sup> U	%g/g <sup>238</sup> U	%g/g <sup>238</sup> U	%g/g <sup>238</sup> U	%g/g <sup>238</sup> U
U-234	ICP-MS IDA	0.0247	0.0032	0.0192	0.0028	0.0219	0.0026	0.02	0.0024
U-235	ICP-MS IDA	1.386	0.046	0.342	0.016	0.572	0.022	0.397	0.016
U-236	ICP-MS IDA	0.679	0.024	0.776	0.028	0.772	0.026	0.789	0.028
Pu-238	ICP-MS IDA	0.0277	0.0022	0.0869	0.003	0.0688	0.0072	0.0802	0.0026
Pu-239	ICP-MS IDA	0.646	0.026	0.666	0.02	0.664	0.028	0.658	0.02
Pu-240	ICP-MS IDA	0.249	0.012	0.373	0.014	0.347	0.02	0.379	0.012
Pu-241	ICP-MS IDA	0.117	0.008	0.169	0.006	0.162	0.016	0.169	0.006
Pu-242	ICP-MS IDA	0.058	0.004	0.190	0.008	0.143	0.016	0.183	0.006
Np-237	ICP-MS ext	0.063	0.01	0.113	0.018	0.099	0.016	0.112	0.018
Am-241	ICP-MS IDA	0.075	0.004	0.093	0.004	0.064	0.006	0.065	0.004
Am-243	ICP-MS IDA	0.012	0.004	0.053	0.002	0.037	0.004	0.050	0.004
Cm-244	ICP-MS ext	0.0017	0.0004	0.021	0.004	0.011	0.002	0.018	0.004
Cm-246	ICP-MS ext	2.E-05	4.E-06	7.E-04	2.E+04	2.E-04	6.E-05	5.E-04	1.E-04
Nd-142	ICP-MS IDA	0.0023	0.0002	0.0093	0.0004	0.0061	0.0004	0.008	0.0008
Nd-143	ICP-MS IDA	0.114	0.004	0.140	0.004	0.134	0.006	0.132	0.004
Nd-144	ICP-MS IDA	0.183	0.006	0.375	0.012	0.305	0.012	0.338	0.012
Nd-145	ICP-MS IDA	0.093	0.004	0.145	0.006	0.129	0.006	0.134	0.004
Nd-146	ICP-MS IDA	0.096	0.002	0.194	0.006	0.157	0.004	0.175	0.006
Nd-148	ICP-MS IDA	0.050	0.002	0.094	0.004	0.077	0.004	0.084	0.004
Nd-150	ICP-MS IDA	0.0243	0.0008	0.048	0.0028	0.0393	0.0024	0.0433	0.003
Cs-133	ICP-MS ext	0.145	0.024	0.226	0.036				
Cs-134	$\gamma$ -spec	0.017	0.002	0.045	0.012	0.034	0.002	0.040	0.002
Cs-137	$\gamma$ -spec	0.171	0.014	0.300	0.034	0.254	0.016	0.285	0.018
Ce-140	ICP-MS IDA	0.173	0.006	0.314	0.014	0.255	0.018	0.304	0.022
Ce-142	ICP-MS IDA	0.158	0.006	0.279	0.01	0.228	0.010	0.268	0.018
Ce-144	$\gamma$ -spec	0.020	0.002	0.0328	0.009	0.029	0.004		
Sm-147	ICP-MS IDA	0.033	0.004	0.032	0.002	0.034	0.002	0.035	0.002
Sm-148	ICP-MS IDA	0.0195	0.0018	0.0502	0.0024	0.0388	0.0024	0.0482	0.004
Sm-149	ICP-MS IDA	0.00035	0.00006	0.00036	0.00006	0.00043	0.00004	0.00041	0.0002
Sm-150	ICP-MS IDA	0.0342	0.0032	0.0670	0.0032	0.0561	0.0034	0.0633	0.0054
Sm-151	ICP-MS IDA	0.00152	0.00014	0.00189	0.00014	0.00176	0.00016	0.00183	0.00018
Sm-152	ICP-MS IDA	0.0129	0.0004	0.0189	0.0008	0.0173	0.0080	0.0191	0.0140
Sm-154	ICP-MS IDA	0.00466	0.00058	0.01105	0.00062	0.00787	0.00206	0.01029	0.00086
Eu-151	ICP-MS IDA	0.000064	0.000014	0.000072	0.000036	0.000068	0.000020	0.000085	0.000008
Eu-153	ICP-MS IDA	0.0137	0.0012	0.0244	0.0008	0.0220	0.0020	0.0247	0.0020
Eu-154	ICP-MS IDA	0.00172	0.00016	0.00350	0.00016	0.00307	0.00028	0.00346	0.00030
Eu-155	ICP-MS IDA	0.00044	0.00010	0.00092	0.00004	0.00076	0.00010	0.00090	0.00008

**Table 3.2. Experimental techniques and isotopic concentrations (in %g/g<sup>238</sup>U) for 2<sup>nd</sup> campaign (cont.)**

Sample ID		E58-88(new)		E58-793(new)		E58-257		160-800	
Burnup <sup>a</sup> (GWd/t)		42.5		77.0		64.6		70.9	
Nuclide <sup>b</sup>	Method <sup>c</sup>	Mass <sup>d</sup>	2 $\sigma$ <sup>d</sup>	Mass	2 $\sigma$	Mass	2 $\sigma$	Mass	2 $\sigma$
		%g/g <sup>238</sup> U	%g/g <sup>238</sup> U	%g/g <sup>238</sup> U	%g/g <sup>238</sup> U	%g/g <sup>238</sup> U	%g/g <sup>238</sup> U	%g/g <sup>238</sup> U	%g/g <sup>238</sup> U
Gd-154	ICP-MS IDA	0.00141	0.00004	0.00313	0.00022	0.00262	0.00018	0.00318	0.00026
Gd-155	ICP-MS IDA	0.00049	0.00009	0.00083	0.000112	0.00093	0.00008	0.0022	0.000072
Gd-156	ICP-MS IDA	0.0095	0.0004	0.0467	0.0020	0.0293	0.0012	0.0434	0.0014
Gd-158	ICP-MS IDA	0.0017	0.00008	0.00692	0.00032	0.00433	0.00022	0.00632	0.00038
Gd-160	ICP-MS IDA	0.00014	0.00002	0.00037	0.00002	<0.0004		0.00033	0.00002
Rh-103	ICP-MS ext					0.0448	0.0080	0.0818	0.0160
Ru-106	$\gamma$ -spec	0.015	0.002	0.032	0.008	0.026	0.002		
La-139	ICP-MS ext	0.161	0.026	0.286	0.046	0.23	0.036	0.259	0.042
Tc-99	ICP-MS ext	0.103	0.016	0.115	0.018	0.134	0.022	0.163	0.026
Mo-95	ICP-MS IDA					0.051	0.004	0.116	0.032
Mo-97	ICP-MS IDA					0.056	0.004	0.134	0.008
Mo-98	ICP-MS IDA					0.072	0.006	0.159	0.044
Mo-100	ICP-MS IDA					0.068	0.008	0.172	0.05

<sup>a</sup> Burnup based on measured data for burnup indicators fission products <sup>148</sup>Nd and <sup>137</sup>Cs, as discussed in Section 5 of this report.

<sup>b</sup> The measured isotopic data correspond to discharge time for isotopes measured by  $\gamma$ -spectrometry; data for isotopes measured by ICP-MS with external calibration are at 2298 d decay time; data for isotopes measured by IDA are at 2334 d decay time.

<sup>c</sup> Main technique is mentioned; some nuclides required multiple techniques to eliminate interferences.

<sup>d</sup> Shown as weight percent relative to measured <sup>238</sup>U.

**Table 3.3. Half-lives of isotopes used in data adjustment**

Nuclide	Half-life (years)	Nuclide	Half-life (years)
Am-241	432.54	Eu-154	8.592
Pu-241	14.35	Eu-155	4.68
Ce-144	0.78	Pu-238	87.71
Cm-244	18.1	Ru-106	1.017
Cs-137	30	Sm-151	90

**Table 3.4. Isotopic concentrations – combined data (in %/g<sup>238</sup>U)**

Sample ID Burnup <sup>a</sup>	E58-88			E58-148			E58-260			E58-700			165-2a			160-800		
	42.5			54.8			64.6			77.0			78.3			70.9		
Nuclide <sup>b</sup>	Mass <sup>c</sup> %/g <sup>238</sup> U	Uncert <sup>d</sup> %/g <sup>238</sup> U	Uncert <sup>e</sup> (%)	Mass %/g <sup>238</sup> U	Uncert %/g <sup>238</sup> U	Uncert (%)	Mass %/g <sup>238</sup> U	Uncert %/g <sup>238</sup> U	Uncert (%)	Mass %/g <sup>238</sup> U	Uncert %/g <sup>238</sup> U	Uncert (%)	Mass %/g <sup>238</sup> U	Uncert %/g <sup>238</sup> U	Uncert (%)	Mass %/g <sup>238</sup> U	Uncert %/g <sup>238</sup> U	Uncert (%)
U-234	2.453E-02	4.323E-03	17.6	2.318E-02	3.381E-03	14.6	1.612E-02	6.478E-03	40.2	1.446E-02	2.449E-03	16.9	1.400E-02	3.838E-03	27.4	1.770E-02	2.139E-03	12.1
U-235	1.328E+00	1.484E-01	11.2	9.211E-01	6.324E-02	6.9	5.251E-01	7.138E-02	13.6	3.192E-01	2.023E-02	6.3	2.939E-01	2.690E-02	9.2	3.970E-01	1.568E-02	3.9
U-236	5.676E-01	5.606E-02	9.9	6.868E-01	5.003E-02	7.3	6.773E-01	8.950E-02	13.2	6.629E-01	3.541E-02	5.3	6.809E-01	5.022E-02	7.4	7.891E-01	2.752E-02	3.5
Pu-238	2.826E-02	1.469E-03	5.2	4.016E-02	5.339E-03	13.3	6.774E-02	5.111E-03	7.5	8.928E-02	2.697E-03	3.0	9.711E-02	9.504E-03	9.8	8.257E-02	2.598E-03	3.1
Pu-239	6.481E-01	1.969E-02	3.0	6.419E-01	4.441E-02	6.9	6.599E-01	2.617E-02	4.0	6.715E-01	1.672E-02	2.5	7.410E-01	4.457E-02	6.0	6.580E-01	1.902E-02	2.9
Pu-240	2.494E-01	8.354E-03	3.4	2.927E-01	2.049E-02	7.0	3.402E-01	1.695E-02	5.0	3.737E-01	1.050E-02	2.8	4.043E-01	2.591E-02	6.4	3.762E-01	1.094E-02	2.9
Pu-241	1.387E-01	5.427E-03	3.9	1.603E-01	1.148E-02	7.2	1.869E-01	1.305E-02	7.0	2.005E-01	5.969E-03	3.0	2.211E-01	1.424E-02	6.4	2.008E-01	6.125E-03	3.1
Pu-242	5.776E-02	2.388E-03	4.1	9.201E-02	6.622E-03	7.2	1.396E-01	1.026E-02	7.3	1.888E-01	6.114E-03	3.2	2.095E-01	1.295E-02	6.2	1.831E-01	5.357E-03	2.9
Np-237	6.676E-02	7.575E-03	11.3	9.987E-02	1.598E-02	16.0	1.100E-01	1.256E-02	11.4	1.194E-01	9.562E-03	8.0	1.404E-01	2.246E-02	16.0	1.121E-01	1.794E-02	16.0
Am-241	2.603E-02	1.934E-03	7.4	2.880E-02	1.885E-03	6.5	3.297E-02	2.149E-03	6.5	3.296E-02	1.369E-03	4.2	3.707E-02	1.921E-03	5.2	3.251E-02	1.789E-03	5.5
Am-243	9.493E-03	7.679E-04	8.1	2.453E-02	2.935E-03	12.0	3.733E-02	2.767E-03	7.4	5.566E-02	3.735E-03	6.7	7.660E-02	4.014E-03	5.2	4.982E-02	3.923E-03	7.9
Cm-244	1.908E-03	2.699E-04	14.1	5.961E-03	1.192E-03	20.0	1.323E-02	1.883E-03	14.2	2.300E-02	2.301E-03	10.0	2.907E-02	5.814E-03	20.0	2.091E-02	4.182E-03	20.0
Cm-246	1.847E-05	3.918E-06	21.2	6.226E-05	1.868E-05	30.0	2.416E-04	5.129E-05	21.2	5.750E-04	8.691E-05	15.1	7.267E-04	2.180E-04	30.0	5.488E-04	1.646E-04	30.0
Nd-142	2.310E-03	1.024E-04	4.4	3.834E-03	5.508E-04	14.4	6.144E-03	4.212E-04	6.9	9.510E-03	3.090E-04	3.2				8.038E-03	7.118E-04	8.9
Nd-143	1.145E-01	4.083E-03	3.6	1.259E-01	6.582E-03	5.2	1.343E-01	5.954E-03	4.4	1.395E-01	3.690E-03	2.6	1.318E-01	7.078E-03	5.4	1.321E-01	4.271E-03	3.2
Nd-145	9.289E-02	3.972E-03	4.3	1.118E-01	5.658E-03	5.1	1.288E-01	5.616E-03	4.4	1.468E-01	4.047E-03	2.8	1.413E-01	7.653E-03	5.4	1.339E-01	4.787E-03	3.6
Nd-146	9.552E-02	2.777E-03	2.9	1.263E-01	5.574E-03	4.4	1.567E-01	4.573E-03	2.9	1.961E-01	4.355E-03	2.2	1.928E-01	9.642E-03	5.0	1.749E-01	5.182E-03	3.0
Nd-148	5.048E-02	1.944E-03	3.9	6.604E-02	3.526E-03	5.3	7.670E-02	3.391E-03	4.4	9.576E-02	2.502E-03	2.6	1.026E-01	8.438E-03	8.2	8.440E-02	4.846E-03	5.7
Nd-150	2.432E-02	8.933E-04	3.7	2.997E-02	1.700E-03	5.7	3.933E-02	2.383E-03	6.1	4.511E-02	1.430E-03	3.2	5.266E-02	3.235E-03	6.1	4.327E-02	2.915E-03	6.7
Cs-133	1.526E-01	1.729E-02	11.3	1.826E-01	2.922E-02	16.0	2.277E-01	3.644E-02	16.0	2.254E-01	1.804E-02	8.0	2.191E-01	3.506E-02	16.0			
Cs-134	1.680E-02	1.990E-03	11.8	2.438E-02	1.999E-03	8.2	3.410E-02	2.342E-03	6.9	4.484E-02	2.067E-03	4.6	4.702E-02	3.283E-03	7.0	3.974E-02	2.641E-03	6.6
Cs-135	8.907E-02	1.425E-02	16.0	1.035E-01	1.656E-02	16.0	1.179E-01	1.886E-02	16.0	1.050E-01	9.710E-03	9.2	1.141E-01	1.826E-02	16.0			
Cs-137	1.708E-01	1.347E-02	7.9	2.102E-01	1.430E-02	6.8	2.538E-01	1.572E-02	6.2	2.990E-01	1.323E-02	4.4	3.094E-01	2.066E-02	6.7	2.850E-01	1.752E-02	6.1
Ce-140	1.698E-01	5.096E-03	3.0	2.121E-01	7.684E-03	3.6	2.659E-01	9.217E-03	3.5	3.117E-01	7.199E-03	2.3	3.201E-01	1.850E-02	5.8	3.037E-01	2.101E-02	6.9
Ce-142	1.572E-01	4.355E-03	2.8	2.012E-01	6.099E-03	3.0	2.406E-01	1.480E-02	6.2	2.852E-01	6.259E-03	2.2	2.938E-01	1.691E-02	5.8	2.677E-01	1.846E-02	6.9
Ce-144	2.040E-02	2.950E-03	14.5	2.445E-02	3.166E-03	13.0	2.874E-02	3.775E-03	13.1	3.260E-02	2.999E-03	9.2	3.440E-02	1.340E-02	39.0			

**Table 3.4. Isotopic concentrations – combined data (in %g/g<sup>238</sup>U) (cont.)**

Sample ID	E58-88			E58-148			E58-260			E58-700			165-2a			160-800		
	42.5			54.8			64.6			77.0			78.3			70.9		
Burnup <sup>a</sup>	Mass <sup>c</sup> %g/g <sup>238</sup> U	Uncert <sup>d</sup> %g/g <sup>238</sup> U	Uncert <sup>e</sup> (%)	Mass %g/g <sup>238</sup> U	Uncert %g/g <sup>238</sup> U	Uncert (%)	Mass %g/g <sup>238</sup> U	Uncert %g/g <sup>238</sup> U	Uncert (%)	Mass %g/g <sup>238</sup> U	Uncert %g/g <sup>238</sup> U	Uncert (%)	Mass %g/g <sup>238</sup> U	Uncert %g/g <sup>238</sup> U	Uncert (%)	Mass %g/g <sup>238</sup> U	Uncert %g/g <sup>238</sup> U	Uncert (%)
Sm-147	2.836E-02	1.542E-03	5.4	2.974E-02	1.429E-03	4.8	2.817E-02	2.576E-03	9.1	2.875E-02	1.235E-03	4.3	3.187E-02	1.971E-03	6.2			
Sm-148	2.018E-02	8.855E-04	4.4	2.996E-02	1.406E-03	4.7	3.832E-02	1.930E-03	5.0	5.052E-02	1.551E-03	3.1	5.649E-02	3.456E-03	6.1	4.816E-02	3.927E-03	8.2
Sm-149	3.579E-04	4.078E-05	11.4	3.947E-04	5.199E-05	13.2	3.853E-04	5.244E-05	13.6	3.874E-04	3.236E-05	8.4	3.856E-04	9.766E-05	25.3	4.105E-04	1.952E-04	47.6
Sm-150	3.500E-02	1.672E-03	4.8	4.717E-02	2.154E-03	4.6	5.504E-02	2.765E-03	5.0	6.662E-02	2.030E-03	3.0	6.593E-02	3.998E-03	6.1	6.634E-02	5.418E-03	8.2
Sm-151	1.529E-03	1.046E-04	6.8	1.545E-03	1.122E-04	7.3	1.650E-03	1.083E-04	6.6	1.948E-03	7.050E-05	3.6	1.921E-03	2.070E-04	10.8	1.886E-03	1.848E-04	9.8
Sm-152	1.306E-02	3.865E-04	3.0	1.545E-02	6.887E-04	4.5	1.705E-02	7.381E-04	4.3	1.924E-02	5.603E-04	2.9	2.035E-02	9.877E-04	4.9	1.914E-02	1.413E-03	7.4
Sm-154	4.358E-03	2.822E-04	6.5	5.634E-03	3.018E-04	5.4	6.868E-03	5.953E-04	8.7	9.648E-03	3.381E-04	3.5	1.185E-02	1.002E-03	8.5	1.029E-02	8.605E-04	8.4
Eu-153	1.685E-02	9.788E-04	5.8	2.240E-02	1.115E-03	5.0	2.726E-02	2.406E-03	8.8	3.082E-02	1.099E-03	3.6	3.234E-02	1.543E-03	4.8			
Eu-154	2.363E-03	2.800E-04	11.8	3.380E-03	2.099E-04	6.2	3.976E-03	5.223E-04	13.1	4.121E-03	2.270E-04	5.5	5.601E-03	5.931E-04	10.6			
Eu-155	6.157E-04	4.174E-05	6.8	9.792E-04	9.275E-05	9.5	1.184E-03	1.134E-04	9.6	1.303E-03	6.920E-05	5.3	1.329E-03	1.528E-04	11.5			
Gd-154	8.867E-04	2.909E-05	3.3	1.535E-03	1.417E-04	9.2	1.594E-03	9.117E-05	5.7	2.211E-03	8.379E-05	3.8	2.813E-03	4.729E-04	16.8	1.986E-03	1.675E-04	8.4
Gd-155	2.992E-04	5.065E-05	16.9	4.865E-04	8.034E-05	16.5	5.481E-04	5.228E-05	9.5	7.149E-04	3.156E-05	4.4	6.051E-04	5.691E-05	9.4			
Gd-156	9.580E-03	2.667E-04	2.8	1.918E-02	1.750E-03	9.1	2.932E-02	1.113E-03	3.8	4.737E-02	1.293E-03	2.7	4.963E-02	4.567E-03	9.2	4.337E-02	1.355E-03	3.1
Gd-158	1.698E-03	6.307E-05	3.7	3.012E-03	3.112E-04	10.3	4.309E-03	1.863E-04	4.3	6.968E-03	2.036E-04	2.9	7.385E-03	9.081E-04	12.3	6.323E-03	3.718E-04	
Gd-160	1.388E-04	1.805E-05	13.0	1.838E-04	5.857E-05	31.9	2.401E-04	4.777E-05	19.9	3.243E-04	1.428E-05	4.4	3.905E-04	4.892E-05	12.5	3.310E-04	1.341E-05	
Ru-103													7.117E-03	1.064E-03	14.9			
Ru-106	1.492E-02	1.556E-03	10.4	1.990E-02	1.709E-03	8.6	2.598E-02	1.968E-03	7.6	3.217E-02	1.763E-03	5.5	3.286E-02	2.709E-03	8.2			
La-139	1.612E-01	2.579E-02	16.0				2.295E-01	3.672E-02	16.0	2.859E-01	4.574E-02	16.0				2.592E-01	4.147E-02	16.0
Rh-103																8.180E-02	1.636E-02	20.0
Tc-99	1.034E-01	1.654E-02	16.0													1.634E-01	2.615E-02	16.0

<sup>a</sup> Burnup based on measured data for burnup indicators fission products <sup>148</sup>Nd and <sup>137</sup>Cs, as discussed in Section 5 of this report.

<sup>b</sup> The measured isotopic data correspond to discharge time for isotopes measured by  $\gamma$ -spectrometry; data for isotopes measured by ICP-MS with external calibration are at 1110 d decay time; data for isotopes measured by IDA are at 1101 d decay time.

<sup>c</sup> Shown as weight percent relative to measured <sup>238</sup>U.

<sup>d</sup> Measurement uncertainty at 95% confidence level.

<sup>e</sup> Relative measurement uncertainty.

**Table 3.5. Isotopic concentrations – combined data (in g/g U<sub>initial</sub>)**

Sample ID	E58-88			E58-148			E58-260			E58-700			165-2a			160-800		
Burnup <sup>d</sup>	42.5			54.8			64.6			77.0			78.3			70.9		
Nuclide <sup>b</sup>	Mass <sup>c</sup> %g/g <sup>238</sup> U	Uncert <sup>e</sup> %g/g <sup>238</sup> U	Uncert <sup>f</sup> (%)	Mass %g/g <sup>238</sup> U	Uncert %g/g <sup>238</sup> U	Uncert (%)	Mass %g/g <sup>238</sup> U	Uncert %g/g <sup>238</sup> U	Uncert (%)	Mass %g/g <sup>238</sup> U	Uncert %g/g <sup>238</sup> U	Uncert (%)	Mass %g/g <sup>238</sup> U	Uncert %g/g <sup>238</sup> U	Uncert (%)	Mass %g/g <sup>238</sup> U	Uncert %g/g <sup>238</sup> U	Uncert (%)
U-234	2.276E-04	4.012E-05	17.6	2.528E+00	3.687E-01	14.6	1.468E-04	5.899E-05	40.2	1.297E-04	2.196E-05	16.9	1.246E-04	3.417E-05	27.4			
U-235	1.232E-02	1.377E-03	11.2	1.004E+02	6.897E+00	6.9	4.782E-03	6.500E-04	13.6	2.863E-03	1.814E-04	6.3	2.617E-03	2.395E-04	9.2			
U-236	5.267E-03	5.203E-04	9.9	7.490E+01	5.456E+00	7.3	6.168E-03	8.150E-04	13.2	5.945E-03	3.175E-04	5.3	6.062E-03	4.471E-04	7.4			
Pu-238	2.623E-04	1.363E-05	5.2	4.379E+00	5.823E-01	13.3	6.168E-04	4.654E-05	7.5	8.007E-04	2.419E-05	3.0	8.646E-04	8.461E-05	9.8	7.464E-04	2.348E-05	3.1
Pu-239	6.014E-03	1.828E-04	3.0	7.000E+01	4.843E+00	6.9	6.009E-03	2.383E-04	4.0	6.022E-03	1.499E-04	2.5	6.597E-03	3.968E-04	6.0	5.948E-03	1.719E-04	2.9
Pu-240	2.314E-03	7.753E-05	3.4	3.192E+01	2.235E+00	7.0	3.098E-03	1.544E-04	5.0	3.351E-03	9.416E-05	2.8	3.599E-03	2.306E-04	6.4	3.400E-03	9.886E-05	2.9
Pu-241	1.287E-03	5.036E-05	3.9	1.748E+01	1.252E+00	7.2	1.702E-03	1.189E-04	7.0	1.798E-03	5.353E-05	3.0	1.968E-03	1.268E-04	6.4	1.815E-03	5.536E-05	3.1
Pu-242	2.276E-04	4.012E-05	17.6	2.528E+00	3.687E-01	14.6	1.468E-04	5.899E-05	40.2	1.297E-04	2.196E-05	16.9	1.246E-04	3.417E-05	27.4			
Np-237	6.195E-04	7.029E-05	11.3	1.089E+01	1.743E+00	16.0	1.001E-03	1.144E-04	11.4	1.071E-03	8.576E-05	8.0	1.250E-03	1.999E-04	16.0	1.014E-03	1.622E-04	16.0
Am-241	2.415E-04	1.795E-05	7.4	3.141E+00	2.056E-01	6.5	3.003E-04	1.957E-05	6.5	2.956E-04	1.228E-05	4.2	3.300E-04	1.710E-05	5.2	2.938E-04	1.617E-05	5.5
Am-243	8.810E-05	7.126E-06	8.1	2.675E+00	3.201E-01	12.0	3.400E-04	2.519E-05	7.4	4.992E-04	3.349E-05	6.7	6.820E-04	3.574E-05	5.2	4.503E-04	3.546E-05	7.9
Cm-244	1.771E-05	2.505E-06	14.1	6.500E-01	1.300E-01	20.0	1.205E-04	1.715E-05	14.2	2.063E-04	2.064E-05	10.0	2.588E-04	5.176E-05	20.0	1.890E-04	3.780E-05	20.0
Cm-246	1.714E-07	3.636E-08	21.2	6.789E-03	2.037E-03	30.0	2.200E-06	4.671E-07	21.2	5.157E-06	7.794E-07	15.1	6.469E-06	1.941E-06	30.0	4.961E-06	1.488E-06	30.0
Nd-142	2.144E-05	9.501E-07	4.4	4.181E-01	6.007E-02	14.4	5.595E-05	3.836E-06	6.9	8.529E-05	2.772E-06	3.2				7.265E-05	6.434E-06	8.9
Nd-143	1.062E-03	3.789E-05	3.6	1.373E+01	7.178E-01	5.2	1.223E-03	5.422E-05	4.4	1.251E-03	3.309E-05	2.6	1.173E-03	6.301E-05	5.4	1.194E-03	3.860E-05	3.2
Nd-145	8.620E-04	3.686E-05	4.3	1.219E+01	6.170E-01	5.1	1.173E-03	5.114E-05	4.4	1.316E-03	3.630E-05	2.8	1.258E-03	6.814E-05	5.4	1.210E-03	4.327E-05	3.6
Nd-146	8.864E-04	2.577E-05	2.9	1.377E+01	6.078E-01	4.4	1.427E-03	4.164E-05	2.9	1.759E-03	3.906E-05	2.2	1.716E-03	8.584E-05	5.0	1.581E-03	4.684E-05	3.0
Nd-148	4.684E-04	1.804E-05	3.9	7.202E+00	3.845E-01	5.3	6.985E-04	3.088E-05	4.4	8.588E-04	2.244E-05	2.6	9.137E-04	7.513E-05	8.2	7.629E-04	4.380E-05	5.7
Nd-150	2.257E-04	8.289E-06	3.7	3.268E+00	1.854E-01	5.7	3.581E-04	2.170E-05	6.1	4.046E-04	1.283E-05	3.2	4.688E-04	2.880E-05	6.1	3.911E-04	2.635E-05	6.7
Cs-133	1.416E-03	1.605E-04	11.3	1.991E+01	3.186E+00	16.0	2.074E-03	3.318E-04	16.0	2.022E-03	1.618E-04	8.0	1.951E-03	3.121E-04	16.0			
Cs-134	1.559E-04	1.846E-05	11.8	2.658E+00	2.180E-01	8.2	3.105E-04	2.133E-05	6.9	4.022E-04	1.854E-05	4.6	4.186E-04	2.923E-05	7.0	3.592E-04	2.387E-05	6.6
Cs-135	8.266E-04	1.323E-04	16.0	1.129E+01	1.806E+00	16.0	1.074E-03	1.718E-04	16.0	9.420E-04	8.708E-05	9.2	1.016E-03	1.625E-04	16.0			
Cs-137	1.585E-03	1.250E-04	7.9	2.292E+01	1.560E+00	6.8	2.312E-03	1.431E-04	6.2	2.681E-03	1.186E-04	4.4	2.754E-03	1.839E-04	6.7	2.576E-03	1.584E-04	6.1
Ce-140	1.576E-03	4.729E-05	3.0	2.313E+01	8.379E-01	3.6	2.422E-03	8.393E-05	3.5	2.796E-03	6.456E-05	2.3	2.850E-03	1.647E-04	5.8	2.746E-03	1.899E-04	6.9
Ce-142	1.459E-03	4.041E-05	2.8	2.194E+01	6.651E-01	3.0	2.191E-03	1.348E-04	6.2	2.558E-03	5.614E-05	2.2	2.616E-03	1.506E-04	5.8	2.420E-03	1.669E-04	6.9
Ce-144	1.893E-04	2.738E-05	14.5	2.666E+00	3.453E-01	13.0	2.617E-04	3.437E-05	13.1	2.924E-04	2.690E-05	9.2	3.063E-04	1.193E-04	39.0			

**Table 3.5. Isotopic concentrations – combined data (in g/g U<sub>initial</sub>) (cont.)**

Sample ID Burnup <sup>a</sup>	E58-88			E58-148			E58-260			E58-700			165-2a			160-800		
	42.5			54.8			64.6			77.0			78.3			70.9		
Nuclide <sup>b</sup>	Mass <sup>c</sup> %/g <sup>238</sup> U	Uncert <sup>d</sup> %/g <sup>238</sup> U	Uncert <sup>e</sup> (%)	Mass %/g <sup>238</sup> U	Uncert %/g <sup>238</sup> U	Uncert (%)	Mass %/g <sup>238</sup> U	Uncert %/g <sup>238</sup> U	Uncert (%)	Mass %/g <sup>238</sup> U	Uncert %/g <sup>238</sup> U	Uncert (%)	Mass %/g <sup>238</sup> U	Uncert %/g <sup>238</sup> U	Uncert (%)	Mass %/g <sup>238</sup> U	Uncert %/g <sup>238</sup> U	Uncert (%)
Sm-147	2.632E-04	1.431E-05	5.4	3.244E+00	1.558E-01	4.8	2.565E-04	2.346E-05	9.1	2.579E-04	1.108E-05	4.3	2.837E-04	1.755E-05	6.2			
Sm-148	1.873E-04	8.217E-06	4.4	3.267E+00	1.534E-01	4.7	3.490E-04	1.757E-05	5.0	4.531E-04	1.391E-05	3.1	5.029E-04	3.077E-05	6.1	4.353E-04	3.550E-05	8.2
Sm-149	3.321E-06	3.785E-07	11.4	4.304E-02	5.669E-03	13.2	3.509E-06	4.776E-07	13.6	3.474E-06	2.902E-07	8.4	3.433E-06	8.695E-07	25.3	3.710E-06	1.765E-06	47.6
Sm-150	3.248E-04	1.551E-05	4.8	5.144E+00	2.349E-01	4.6	5.012E-04	2.518E-05	5.0	5.975E-04	1.821E-05	3.0	5.869E-04	3.560E-05	6.1	5.996E-04	4.897E-05	8.2
Sm-151	1.419E-05	9.710E-07	6.8	1.684E-01	1.224E-02	7.3	1.503E-05	9.861E-07	6.6	1.747E-05	6.323E-07	3.6	1.710E-05	1.843E-06	10.8	1.704E-05	1.670E-06	9.8
Sm-152	1.212E-04	3.587E-06	3.0	1.685E+00	7.510E-02	4.5	1.553E-04	6.722E-06	4.3	1.725E-04	5.025E-06	2.9	1.812E-04	8.793E-06	4.9	1.730E-04	1.277E-05	7.4
Sm-154	4.044E-05	2.619E-06	6.5	6.144E-01	3.291E-02	5.4	6.254E-05	5.421E-06	8.7	8.653E-05	3.033E-06	3.5	1.055E-04	8.924E-06	8.5	9.299E-05	7.778E-06	8.4
Eu-153	1.564E-04	9.083E-06	5.8	2.443E+00	1.216E-01	5.0	2.483E-04	2.191E-05	8.8	2.764E-04	9.856E-06	3.6	2.880E-04	1.373E-05	4.8			
Eu-154	2.192E-05	2.598E-06	11.8	3.686E-01	2.289E-02	6.2	3.620E-05	4.756E-06	13.1	3.695E-05	2.036E-06	5.5	4.986E-05	5.280E-06	10.6			
Eu-155	5.714E-06	3.873E-07	6.8	1.068E-01	1.011E-02	9.5	1.078E-05	1.032E-06	9.6	1.169E-05	6.206E-07	5.3	1.183E-05	1.361E-06	11.5			
Gd-154	8.228E-06	2.700E-07	3.3	1.674E-01	1.545E-02	9.2	1.452E-05	8.302E-07	5.7	1.983E-05	7.514E-07	3.8	2.505E-05	4.210E-06	16.8	1.795E-05	1.514E-06	8.4
Gd-155	2.777E-06	4.700E-07	16.9	5.305E-02	8.761E-03	16.5	4.991E-06	4.761E-07	9.5	6.411E-06	2.831E-07	4.4	5.388E-06	5.067E-07	9.4			
Gd-156	8.890E-05	2.475E-06	2.8	2.092E+00	1.909E-01	9.1	2.670E-04	1.014E-05	3.8	4.248E-04	1.159E-05	2.7	4.418E-04	4.066E-05	9.2	3.920E-04	1.224E-05	3.1
Gd-158	1.576E-05	5.853E-07	3.7	3.285E-01	3.393E-02	10.3	3.924E-05	1.696E-06	4.3	6.249E-05	1.826E-06	2.9	6.575E-05	8.085E-06	12.3	5.715E-05	3.360E-06	5.9
Gd-160	1.288E-06	1.675E-07	13.0	2.004E-02	6.388E-03	31.9	2.186E-06	4.350E-07	19.9	2.909E-06	1.281E-07	4.4	3.477E-06	4.355E-07	12.5	2.992E-06	1.212E-07	4.1
Ru-103													6.336E-05	9.470E-06	14.9			
Ru-106	1.385E-04	1.444E-05	10.4	2.170E+00	1.863E-01	8.6	2.366E-04	1.792E-05	7.6	2.885E-04	1.581E-05	5.5	2.925E-04	2.412E-05	8.2			
La-139	1.496E-03	2.394E-04	16.0				2.090E-03	3.344E-04	16.0	2.564E-03	4.102E-04	16.0				2.343E-03	3.749E-04	16.0
Rh-103																7.394E-04	1.479E-04	20.0
Tc-99	9.591E-04	1.535E-04	16.0													1.477E-03	2.363E-04	16.0

<sup>a</sup> Burnup based on measured data for burnup indicators fission products <sup>148</sup>Nd and <sup>137</sup>Cs, as discussed in Section 5 of this report.

<sup>b</sup> The measured isotopic data correspond to discharge time for isotopes measured by  $\gamma$ -spectrometry; data for isotopes measured by ICP-MS with external calibration are at 1110 d decay time; data for isotopes measured by IDA are at 1101 d decay time.

<sup>c</sup> Shown as g per g of initial uranium.

<sup>d</sup> Measurement uncertainty at 95% confidence level.

<sup>e</sup> Relative measurement uncertainty.



## 4 ASSEMBLY DESIGN AND IRRADIATION HISTORY DATA

This section presents information on the fuel assembly geometry, irradiation history, and sample burnup necessary for developing a computational model to calculate the isotopic composition of the samples under consideration. For the cases in which information was unavailable, assumptions are stated for derived data used in calculations.

The analyzed samples were selected from three fuel rods, identified as WZR0058, WZtR165, and WZtR160, that were irradiated in the Vandellós II reactor for five consecutive cycles, from cycle 7 through cycle 11. The initial enrichment of these fuel rods was 4.4982 wt%  $^{235}\text{U}$ . Rods WZR0058 and WZtR165 were included in the same fuel assembly in each of the five irradiation cycles. During cycles 7 through 10, rods WZR0058 and WZtR165 were part of assembly EC45; whereas, during the same cycles, fuel rod WZtR160 was included in assembly EC46. For the last irradiation cycle, cycle 11, the three rods were removed from original assemblies EC45 and EC46 and inserted into the rebuilt assembly EF05. Assembly EF05 had an estimated burnup of 26.5 GWd/MTU at the beginning of cycle (BOC) for cycle 11 (BOC-11); the initial enrichment of the fuel rods in assembly EF05, other than the three measured rods mentioned, was 4.240 wt%  $^{235}\text{U}$ .

The layout of the Vandellós II fuel assemblies, with a  $17 \times 17$  configuration, is illustrated in Figure 4.1, which shows the locations of the fuel rods from which the samples were selected. Each fuel assembly included 264 fuel rods and 25 guide tubes. No absorber rods were present in assemblies EC45, EC46, or EF05 in any of the irradiation cycles.

The loading positions of the fuel rods in the assembly and of the assemblies in the core are listed in Table 4.1. The locations of the assemblies EC45 and EC46 in the core during irradiation are also illustrated in Figure 4.2. Assembly design data are shown in Table 4.2. During cycles 7 through 10, all three measured rods were located at the periphery of the fuel assembly: rod WZR0058 at the east side of assembly EC45, rod WZtR165 at the west side of assembly EC45, and rod WZtR160 at the east side of assembly EC46. For modeling purposes the information for assemblies located east and west of EC45, as well as the assembly neighboring EC46 to the east, is required to accurately account for the influences of the neighbor assembly rods residing adjacent to measured rods. Data on these adjacent assemblies—location in core, initial fuel enrichment, and burnup at BOC—for each of the irradiation cycles 7 through 10 are provided in Table 4.3. As noted, assembly EC46 was located at the edge of the core during cycle 10.

Operating history data, including irradiation cycle start and end dates, cycle duration and down days, and cycle burnup (Ref. 9) for each of the three rods WZR0058, WZtR165, and WZtR160 are shown in Table 4.4. Sample burnups based on operating data are available (Ref. 9) for some samples selected from rod WZR0058 and for the sample selected from rod WZtR165. Sample burnup based on operation data for the sample from rod WZtR160 was not available; the burnup value used in the initial simulations for this sample was a value estimated by Studsvik using measured actinide and fission product concentrations and CASMO burnup calculations (Ref. 6).

The fuel rod burnups based on operator data are presented in Table 4.5. The sample burnups and powers based on operator data are included in Table 4.6. As further discussed in Section 5 of this report, the sample burnups were later calculated based on the measured data for the burnup indicators fission products  $^{148}\text{Nd}$  and  $^{137}\text{Cs}$ , and the power data shown in Table 4.6 were renormalized accordingly.

The power values for each sample and in each irradiation cycle shown in Table 4.6 were calculated based on the burnups and the available operating history data (as shown in Tables 4.4 and 4.5) for the fuel rods

from which the samples were selected. It was assumed that the sample cycle burnup had the same distribution as the cycle burnup of the fuel rod from which the sample was selected. The power  $P_i^s$  in cycle  $i$  for sample  $s$  was calculated as:

$$P_i^s = \frac{1}{\Delta t_i} B_s^i = \frac{1}{\Delta t_i} \left( B^s \frac{B_i^{rod,s}}{\sum_{i=7}^{11} B_i^{rod,s}} \right) \quad i = 7, \dots, 11 \quad (4.1)$$

$B_s^i$  in Eq. (4.1) stands for sample cycle burnup in cycle  $i$ ,  $\Delta t_i$  is the duration of cycle  $i$ , and  $B_i^{rod,s}$  represents the cycle burnup in cycle  $i$  of the fuel rod from which sample  $s$  was selected.

Temperature and density data of the water moderator at the sample level (with respect to the axial location along the fuel rod), as listed in Table 4.7, were available (Ref. 9) for most of the samples except sample 160-800. For this sample the data corresponding to sample E58-796, located at a similar axial level, were used instead. The concentration of soluble boron in the moderator as a function of time was available from Ref. 9 and is illustrated in Figure 4.3. As shown, the variation of boron was linear during an irradiation cycle, with the exception of the first 10 to 15 days of the cycle. For the time points between day 10 for cycles 7 through 10 (day 15 for cycle 11) and the last day of the cycle, a linear fit was performed on the available data and used in the calculations. The variation of the boron concentration for each irradiation cycle is presented in Table 4.8, which includes boron concentration data for the first 10 or 15 days and the last day of the cycle. The data in Table 4.8 that correspond to day 10 and the last day of the cycle completely define the line that expresses the linear variation with time of the boron concentration on this time range.

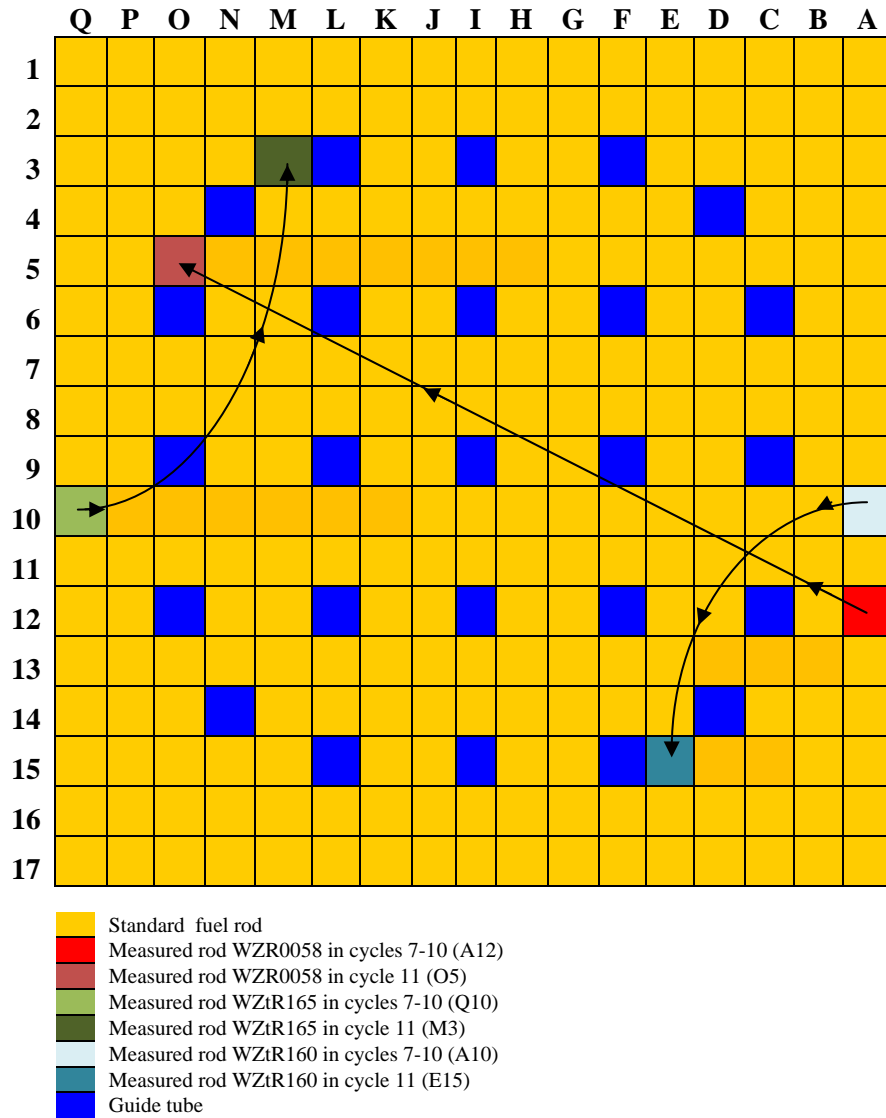


**Figure 4.1. Assembly layout for Vandellós II samples.**

**Table 4.1. Fuel rods and assemblies loading locations**

Cycle #	Fuel rod WZR0058			Fuel rod WZtR165			Fuel rod WZtR160		
	Assembly ID	Rod location in assembly	Assembly location in core	Assembly ID	Rod location in assembly	Assembly location in core	Assembly ID	Rod location in assembly	Assembly location in core
7	EC45	A12	M-04	EC45	Q10	M-04	EC46	A10	D-04
8	EC45	A12	D-12	EC45	Q10	D-12	EC46	A10	M-12
9	EC45	A12	F-10	EC45	Q10	F-10	EC46	A10	K-10
10	EC45	A12	H-15	EC45	Q10	H-15	EC46	A10	A-08
11	EF05	O5	H-11	EF05	M3	H-11	EF05	E15	H-11

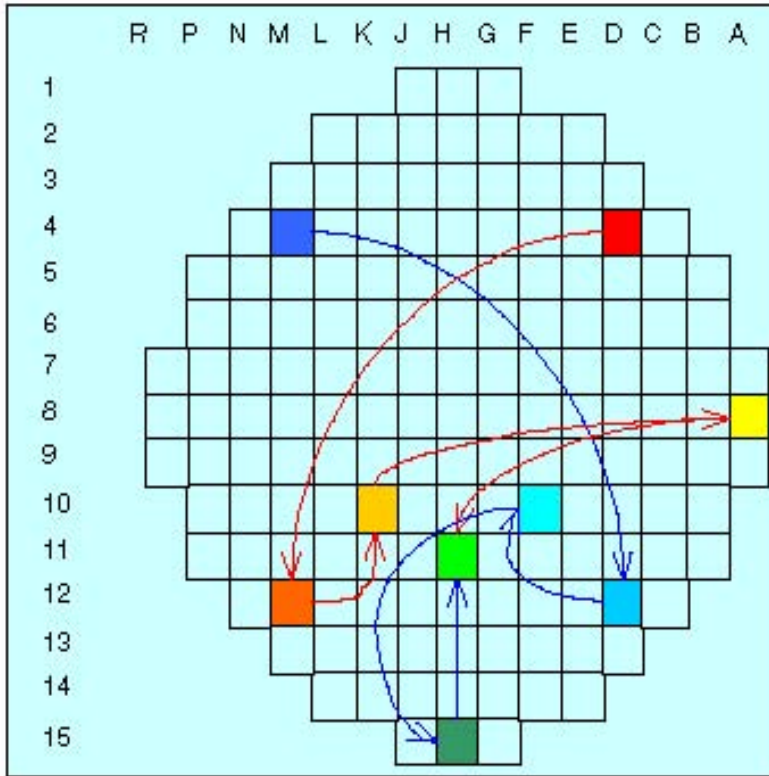


**Figure 4.2. Vandellós II core layout.**

**Table 4.2. Assembly design data**

<b>Parameter</b>	<b>Data</b>
<b>Assembly and reactor data</b>	
Reactor	Vandellós II
Operating pressure (psia)	2250
Lattice geometry	17 × 17
Rod pitch (cm)	1.26
Number of fuel rods	264
Number of guide/instrument tubes	25
Assembly pitch (cm)	21.504
Active fuel rod length (cm)	365.76
Sample location <sup>a</sup> (cm)	See Table 2.1
<b>Fuel rod data</b>	
Fuel material type	UO <sub>2</sub>
Fuel pellet density (%TD <sup>b</sup> )	96.016
Fuel pellet diameter (cm)	0.8191
Fuel temperature (K)	928
U isotopic composition (wt %)	
<sup>234</sup> U	0.0410
<sup>235</sup> U	4.4982
<sup>236</sup> U	0.0030
<sup>238</sup> U	95.4578
Clad temperature (K)	607
Clad inner diameter (cm)	0.8356
Clad outer diameter (cm)	0.950
Clad material density (g/cm <sup>3</sup> )	6.5
Clad material	Zirlo
Clad material composition (wt %)	
Zr	97.9
Sn	1.0
Fe	0.1
Nb	1.0
<b>Moderator data</b>	
Inlet temperature (K)	565
Outlet temperature (K)	601
Temperature at sample level (K)	See Table 4.7
Density at sample level (g/cm <sup>3</sup> )	See Table 4.7
Soluble boron content (ppm)	See Table 4.8
<b>Guide tube data</b>	
Guide tube material	Zirlo
Inner diameter (cm)	1.125
Outer diameter (cm)	1.205

<sup>a</sup> Relative to the bottom of the active fuel region.

<sup>b</sup> TD = theoretical density (10.96 g/cm<sup>3</sup>).

**Table 4.3. Adjacent assembly data**

Rod	WZR0058			WZtR165			WZtR160		
Assembly	EC45			EC45			EC46		
Adjacent assembly	East of EC45			West of EC45			East of EC46		
Cycle #	Location in core	Enrichment (wt% <sup>235</sup> U)	BOC burnup (GWd/t)	Location in core	Enrichment (wt% <sup>235</sup> U)	BOC burnup (GWd/t)	Location in core	Enrichment (wt% <sup>235</sup> U)	BOC burnup (GWd/t)
7	L4	3.60	22.125	N4	3.60	32.204	C4	3.60	32.204
8	C12	3.60	31.333	E12	3.60	14.032	L12	3.60	14.032
9	E10	4.23	0	G10	3.60	13.648	J10	3.60	13.648
10	G15	3.60	34.678	J15	3.60	34.678	NA <sup>a</sup>	NA	NA

<sup>a</sup> During cycle 10 assembly EC46 was located at the edge of the core.

**Table 4.4. Irradiation history data**

Cycle #	Start date	End date	Irradiation (days)	Down (days)
7	06/19/94	06/12/95	358	33
8	07/15/95	06/09/96	330	35
9	07/14/96	08/25/97	407	31
10	09/25/97	03/14/99	535	50
11	05/03/99	09/10/00	496	

**Table 4.5. Fuel rod burnup data**

Cycle #	Rod WZR0058		Rod WZtR165		Rod WZtR160	
	Cycle burnup <sup>a</sup> (MWd/MTU)	Fraction of total burnup	Cycle burnup (MWd/MTU)	Fraction of total burnup	Cycle burnup (MWd/MTU)	Fraction of total burnup
7	17,475	0.255	13,083	0.187	13,083	0.197
8	8,938	0.130	14,467	0.207	14,467	0.218
9	17,675	0.258	16,899	0.242	16,877	0.254
10	6,025	0.088	6,663	0.095	3,152	0.047
11	18,387	0.268	18,851	0.269	18,921	0.285

<sup>a</sup> As provided in ENUSA COM-006998, Rev. 1, 4/4/2008, from A. Romano.

**Table 4.6. Cycle power data for each sample**

Sample ID	Sample burnup <sup>a</sup> (GWd/MTU)	Sample cycle power (MW/MTU)				
		Cycle 7	Cycle 8	Cycle 9	Cycle 10	Cycle 11
E58-88	43.524	31.015	17.209	27.593	7.156	23.554
E58-148	51.332	36.579	20.297	32.543	8.439	27.780
E58-260	63.008	44.899	24.913	39.946	10.359	34.098
E58-700	74.566	53.135	29.483	47.273	12.259	40.353
165-2a	76.323	39.867	47.825	45.295	13.586	41.461
160-800	72.800	40.007	47.993	45.395	6.450	41.761

<sup>a</sup> Based on operator data.

**Table 4.7. Moderator temperature and density data**

Sample ID	Data	Cycles 7 through 9	Cycle 10	Cycle 11
E58-88	Temperature (K)	565.4	565.4	563.7
	Density (g/cm <sup>3</sup> )	0.7421	0.7425	0.7456
E58-148	Temperature (K)	566	565.4	564.3
	Density (g/cm <sup>3</sup> )	0.7411	0.7423	0.7446
E58-263	Temperature (K)	567.1	565.4	565.4
	Density (g/cm <sup>3</sup> )	0.7387	0.7418	0.7421
E58-773	Temperature (K)	573.2	567.1	572.1
	Density (g/cm <sup>3</sup> )	0.7263	0.7392	0.729
E58-793	Temperature (K)	573.7	567.1	572.1
	Density (g/cm <sup>3</sup> )	0.7258	0.7391	0.7285
E58-796	Temperature (K)	573.7	567.1	572.1
	Density (g/cm <sup>3</sup> )	0.7258	0.7391	0.7285
165-2a	Temperature (K)	574.3	569.3	573.2
	Density (g/cm <sup>3</sup> )	0.7242	0.7348	0.7268

**Boron history (Vandellos 2; C7-C11)**

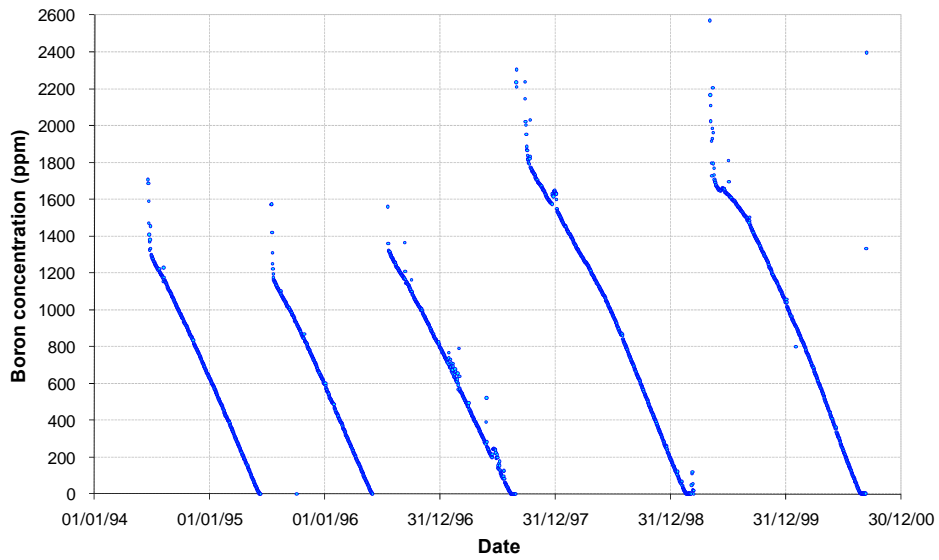


**Figure 4.3. Boron concentration vs. irradiation time (from Ref. 9).**

**Table 4.8. Boron concentration in moderator**

Cycle 7			Cycle 8			Cycle 9			Cycle 10			Cycle 11		
Time <sup>a</sup> (days)	Boron (ppm)	Ratio <sup>b</sup>	Time <sup>a</sup> (days)	Boron (ppm)	Ratio	Time <sup>a</sup> (days)	Boron (ppm)	Ratio	Time <sup>a</sup> (days)	Boron (ppm)	Ratio	Time <sup>a</sup> (days)	Boron (ppm)	Ratio
0	1707	1.000	0	1572	1.000	0	1559	1.000	2237	0	1.000	0	2570	1.000
1	1686	0.988	1	1574	1.001	1	1359	0.872	2145	1	0.959	2	2166	0.843
2	1590	0.931	2	1420	0.903	2	1321	0.847	2022	2	0.904	3	2109	0.821
3	1469	0.860	3	1310	0.833	3	1320	0.847	2002	3	0.895	4	2023	0.787
4	1408	0.825	4	1250	0.795	4	1319	0.846	1951	4	0.872	5	1915	0.745
5	1368	0.802	5	1221	0.777	5	1315	0.843	1886	5	0.843	6	1796	0.699
6	1325	0.776	6	1193	0.759	6	1311	0.841	1871	6	0.836	7	1727	0.672
7	1381	0.809	7	1173	0.746	7	1304	0.836	1865	7	0.834	8	1929	0.750
8	1454	0.851	8	1162	0.739	8	1300	0.834	1837	8	0.821	9	1984	0.772
9	1334	0.781	9	1155	0.735	9	1297	0.832	1819	9	0.813	10	2204	0.858
10	1326	0.777	10	1185	0.754	10	1329	0.852	1886	10	0.843	11	1960	0.763
358	1	0.000	330	2	0.001	407	1	0.000	5	535	0.002	12	1794	0.698
												13	1769	0.688
												14	1732	0.674
												15	1859	0.723
												496	5	0.002

<sup>a</sup>Time since BOC.

<sup>b</sup>Ratio of boron concentration relative to boron concentration at BOC.



## 5 COMPUTATIONAL ANALYSIS

### 5.1 COMPUTATIONAL METHODS

The computational analysis of the measurements was carried out using the two-dimensional (2-D) depletion sequence TRITON in the SCALE computer code system (Ref. 10). For a consistent comparison of the calculated results against all measurement data in Table 1.1, the same methods and nuclear data were used in calculations, as available in version 5.1 of SCALE. TRITON couples the 2-D arbitrary polygonal mesh transport code NEWT with the depletion and decay code ORIGEN-S to perform the burnup simulation. At each depletion step, the transport flux solution from NEWT is used to generate cross sections for the ORIGEN-S calculation. The isotopic composition data resulting from ORIGEN-S are employed in the subsequent transport calculation to obtain cross sections for the next depletion step in an iterative manner throughout the irradiation history.

TRITON has the capability of individually simulating the depletion of multiple mixtures (e.g., fuel rods) in a fuel assembly model. This is a very useful and powerful feature in a nuclide inventory analysis as it allows a more accurate representation of the local flux distribution and neutronic environment of the specific measured fuel rod in the assembly. The flux normalization in a TRITON calculation can be performed using either the power in a specified mixture, the total power corresponding to multiple mixtures, or the assembly power. The first option permits the burnup (power) in the measured sample to be input, usually inferred from measurement data for burnup indicators (such as  $^{148}\text{Nd}$  or  $^{137}\text{Cs}$ ), rather than an assembly average value.

Individual TRITON models, to be presented in this section, were developed for each of the measured samples. All TRITON calculations employed the SCALE 44-group ENDF/B-V cross-section library and the NITAWL resonance cross-section processor. Default values were used for the convergence parameters in the NEWT transport calculation. At each depletion step, all 232 isotopes for which cross-section data are available in the SCALE 44-group library used with NEWT were applied in updating cross sections for the ORIGEN-S fuel depletion calculation based on the flux solution from the transport calculation with NEWT. Selected TRITON input files are provided in Appendix A.

### 5.2 MODELS

The analysis of the fuel samples was carried out by developing individual models for each of the considered samples. Given the location of the fuel rod from which each sample was selected, at the periphery of the fuel assembly during irradiation cycles 7 through 10, the assembly adjacent to the assembly hosting that fuel rod was also included in the model. As shown in previous studies (Ref. 11), for fuel rods located at the edge of the assembly, a more accurate representation of the rod environment in the simulation model is desirable, as it has a significant effect on the calculated isotopic composition in the rod. During cycle 11, the measured fuel rods were located nearer the center of the fuel assembly; for this cycle the adjacent assembly was not included in the model because in this case the rod environment was mainly influenced by the configuration of the assembly in which the rod was located. The geometry, material, and burnup data used in the TRITON models are as listed in Tables 4.1–4.8. Individual depleting mixtures were specified for the measured rod and its adjacent nearest-neighbor fuel rods. All other fuel rods were treated as a single depletion material with uniform composition.

The simulation of the fuel irradiation for each sample took into account the change, from cycle to cycle, of the adjacent assembly data as well as the reconstitution of the assembly before cycle 11. As previously noted, fuel rods WZR0058, WZtR165, and WZtR160 were removed from the fuel assembly in which they were irradiated during cycles 7 through 10 and inserted in a rebuilt assembly for irradiation during

cycle 11. Taking advantage of the assembly symmetry, only one quarter of the assembly hosting the measured rod was included in the TRITON model. The illustrations of the TRITON models for each irradiation cycle for samples in fuel rod WZR0058 are shown in Figures 5.1–5.5. During cycle 10, assembly EC45, which hosted fuel rod WZR0058, was located at the edge of the core (see Figure 4.2 and Table 4.3); a layer of water was included in the model for this cycle, as illustrated in Figure 5.4. Note that during cycles 7 through 10, rod WZR0058 was located in the lower right quadrant of assembly EC45 (see Figure 4.1), while during cycle 11 it was located in the upper left quadrant of assembly EF05, as illustrated in Figures 5.1–5.5.

The fuel assemblies adjacent to assembly EC45 on the east side had different burnups at BOC-7 through BOC-10, as shown in Table 4.3. The influence of the neighboring assemblies during each cycle was accounted for in the computational model. The nominal composition of the adjacent fuel assembly in each cycle was calculated to correspond to the operator-reported burnup at the BOC. During the burnup simulation the isotopic contents of the neighbor assembly were allowed to deplete. For example, assembly C12 that neighbored assembly EC45 at BOC-8, had an assembly average burnup of 31.333 GWd/MTU. Assuming that the burnup distribution on the axial direction for assembly C12 was the same as the available burnup distribution on the axial direction for rod WZR0058, the burnup at the axial location  $z_s$  (corresponding to axial location  $z$  of sample  $s$  in rod WZR0058) in assembly C12,  $B_{C12}^{z_s}$ , was calculated as

$$B_{C12}^{z_s} = \overline{B_{C12}} \frac{B_{WZR0058}^s}{\overline{B_{WZR0058}}} \quad (5.1)$$

where  $\overline{B_{C12}}$  is the assembly average burnup at BOC-11 for assembly C12,  $\overline{B_{WZR0058}}$  is the average burnup of fuel rod WZR0058, and  $B_{WZR0058}^s$  is the burnup of sample  $s$  selected from rod WZR0058 at axial location  $z_s$ . Separate TRITON simulations of assembly C12 were performed to determine its fuel composition at BOC-8 corresponding to the burnup values calculated as in Eq. (5.1).

At the end of the TRITON simulation for each cycle from 7 through 10, the composition of all fuel mixtures in the assembly hosting the measured rod was extracted and used as input data in the TRITON model for the subsequent irradiation cycle. Therefore, there were five TRITON simulations (five models) for each of the samples considered. The variation of the boron concentration in the moderator was included in the TRITON models through the use of the TIMETABLE record in the input files. The composition at BOC-11 of the fuel in rebuilt assembly EF05, other than the fuel in measured fuel rods, was calculated based on the provided assembly burnup of 26.5 GWd/MTU at BOC-11 and initial enrichment of 4.240 wt%  $^{235}\text{U}$  in a manner similar to that discussed above for assembly C12 and expressed by Eq. (5.1).

An important parameter in the computational model is the value of the sample burnup used in the calculation. As the burnup estimated by the utility is generally not of sufficient accuracy to be used in benchmarks, the burnup based on the measured values of burnup indicators is widely used instead. The isotopes generally used as burnup indicators are fission products that are reliable measures of the integral number of fissions occurring in the fuel during irradiation. High-precision measurements of these nuclides are desirable to obtain a reliable measure of the sample burnup.

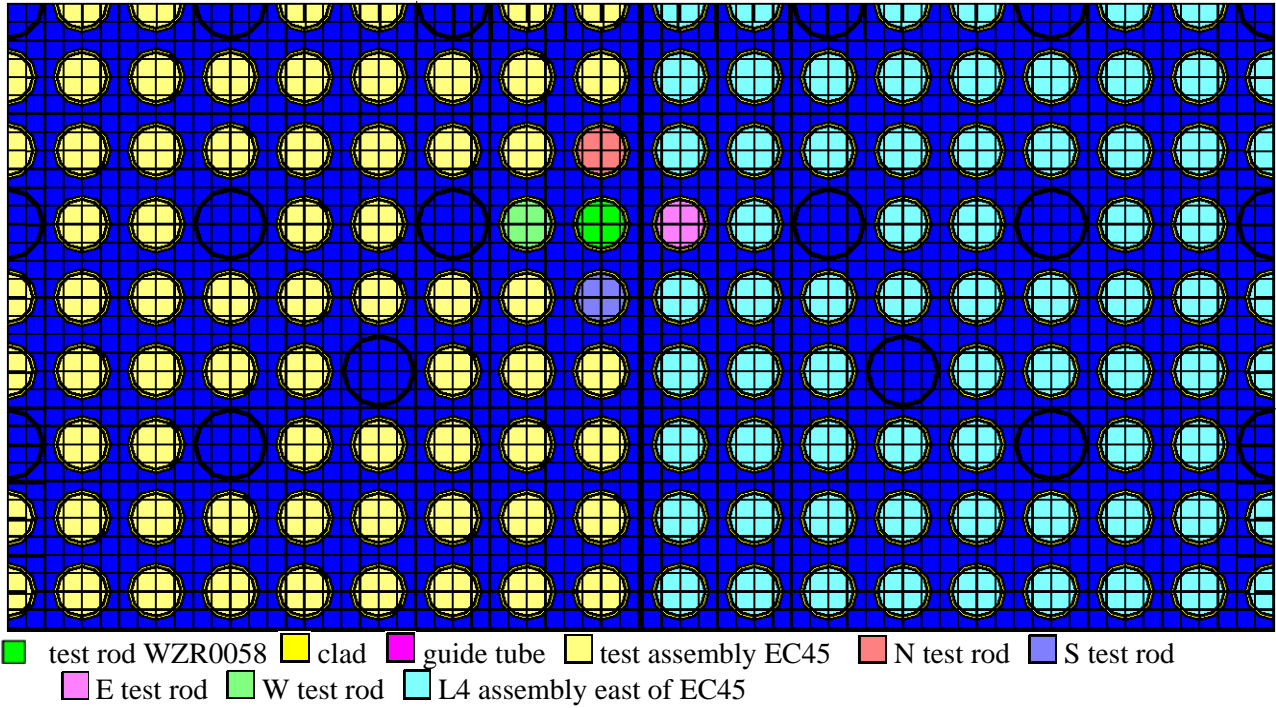


**Figure 5.1. TRITON model for rod WZR0058 – cycle 7.**

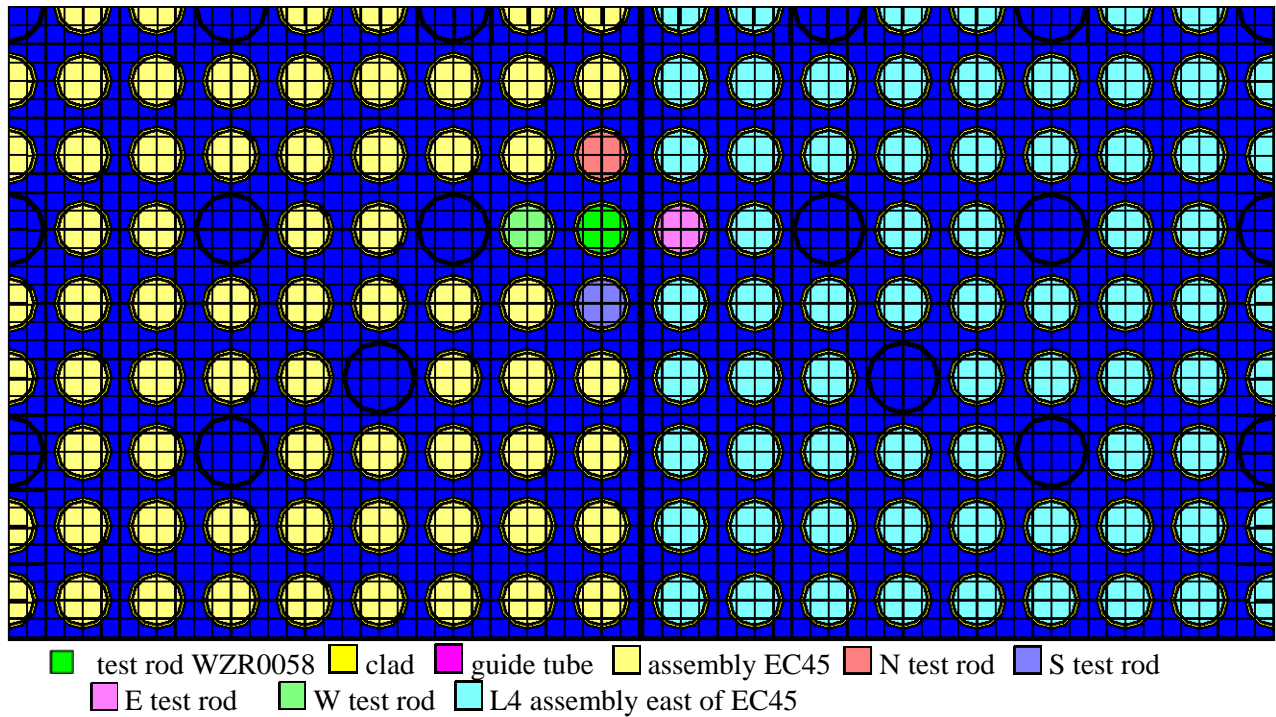
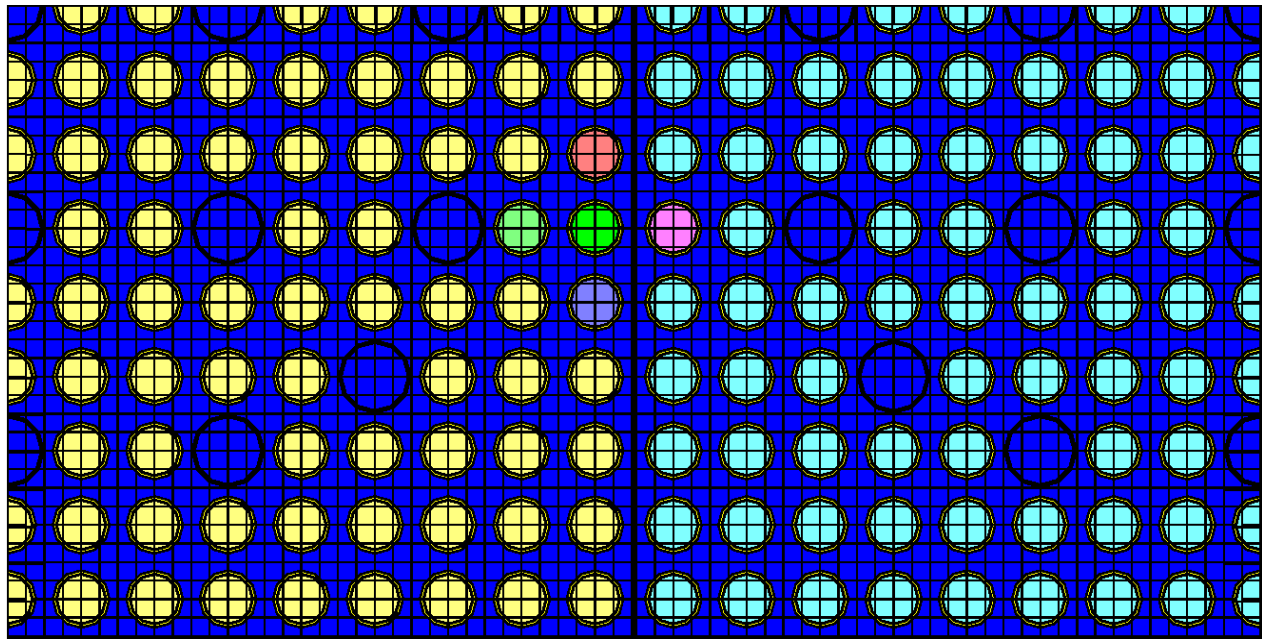


**Figure 5.2. TRITON model for rod WZR0058 – cycle 8.**



■ test rod WZR0058  
 ■ clad  
 ■ guide tube  
 ■ test assembly EC45  
 ■ N test rod  
 ■ S test rod  
■ E test rod  
 ■ W test rod  
 ■ E10 assembly east of EC45

**Figure 5.3. TRITON model for rod WZR0058 – cycle 9.**

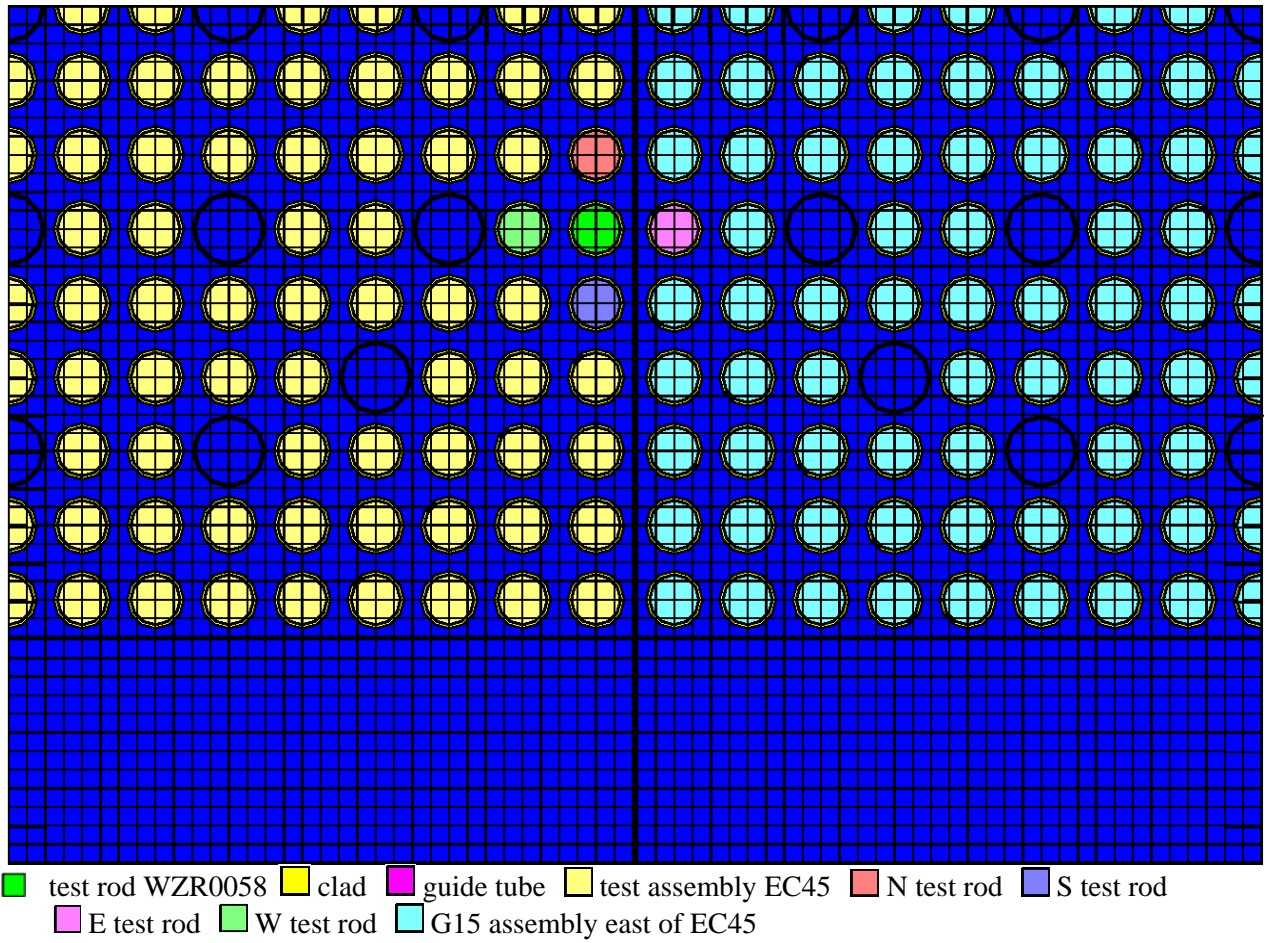


**Figure 5.4. TRITON model for rod WZR0058 – cycle 10.**

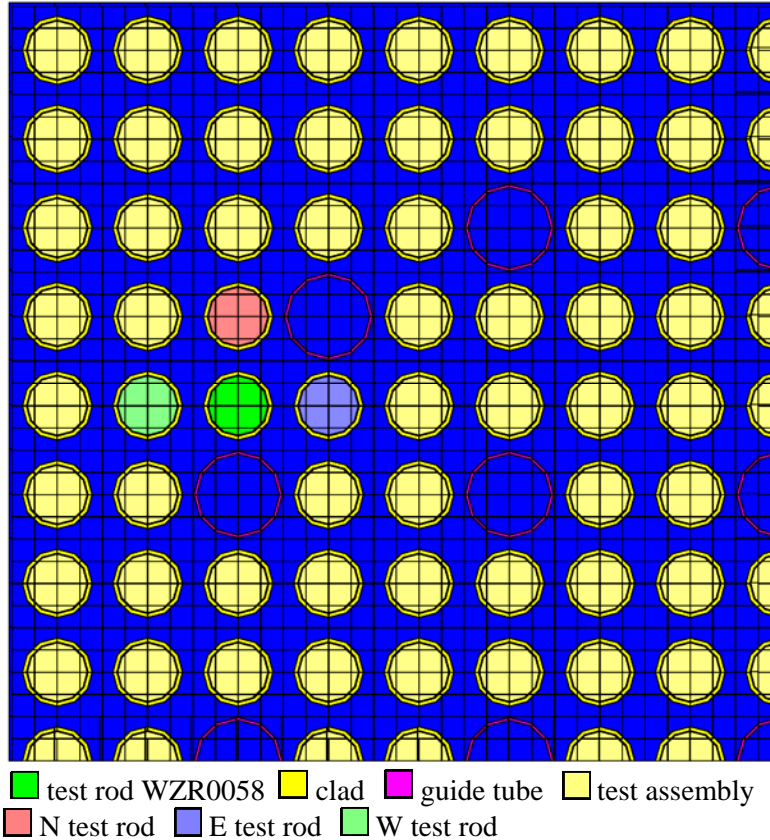


**Figure 5.5. TRITON model for rod WZR0058 – cycle 11.**

For the calculations in the current report, initial TRITON simulations were carried out for all samples using the burnup values provided in Table 4.6. Based on the results of these simulations, sample burnups were determined that reproduced the measured content of the burnup indicators fission products  $^{148}\text{Nd}$  and  $^{137}\text{Cs}$ . A weighted average of the sample burnup  $\bar{B}$  based on measured  $^{137}\text{Cs}$  and  $^{148}\text{Nd}$  content, with the measurement uncertainty used as a weighting function, was calculated as

$$\bar{B} = \frac{\sum_{i=1}^2 (B_i / \sigma_i^2)}{\sum_{i=1}^2 (1 / \sigma_i^2)} \quad (5.2)$$

where  $B_i$  is the burnup calculated based on the measured burnup-indicating isotope  $i$ , and  $\sigma_i$  is the measurement uncertainty for that isotope.

To assess the accuracy of measured data for the burnup indicators  $^{148}\text{Nd}$  and  $^{137}\text{Cs}$  for samples from rod WZR0058, the variation (see Figure 5.6) of the measured values for these two nuclides with the sample location along the length of fuel rod WZR0058 was investigated. Gamma scan measurement data for rod WZR0058 from measurements carried out in 2002 were available for  $^{137}\text{Cs}$ . The isotope  $^{148}\text{Nd}$  was measured in 2003 for samples E58-88, E58-148, E58-263, E58-773, E58-793, and E58-796, and in 2007 for samples E58-257 and E58-793. The error bars shown in Figure 5.6 correspond to one standard deviation of the measurement uncertainty.

As shown in Figure 5.6, the measured concentration for  $^{148}\text{Nd}$  in sample E58-263, which was measured in the first campaign, was significantly different from the value for sample E58-257, which was measured in the second campaign. These two samples were cut from fuel segments adjacent to each other along the length of rod WZR0058 (26.3 and 25.7 cm, respectively, from the bottom of the active fuel region) and were expected to have only slightly different burnups, as confirmed by the gamma scan. Moreover, as seen in Figure 5.6, the measured  $^{148}\text{Nd}$  in sample E58-263 was similar to the measured content in samples located in the high-burnup region of the fuel rod, located 79 cm from the bottom of the active fuel region, in the flat profile burnup region (see Figure 2.1). Given the observed discrepancy in the measured  $^{148}\text{Nd}$  data in the case of sample E58-263, the sample burnup for sample E58-260 (combined data for samples E58-263 and E58-257) was determined based on the measured content of  $^{137}\text{Cs}$  and  $^{148}\text{Nd}$  for E58-257 from the second campaign.

For the two samples, E58-88 and E58-700, for which measurement data were available from two campaigns, the  $^{148}\text{Nd}$  and  $^{137}\text{Cs}$  measured in the second campaign were used to calculate the sample burnup. This is due to the fact that the measurement methodologies for this later campaign were based on higher performance instruments (i.e., smaller measurement uncertainties) and improved measurement methods and standards. In addition, the burnups based on each of the measured fission products  $^{148}\text{Nd}$  and  $^{137}\text{Cs}$  in the second campaign were consistent. For sample 165-2a, measured in the first campaign only, the burnup was based on the measured  $^{137}\text{Cs}$ , as it was found that the burnup based on  $^{148}\text{Nd}$  was inconsistent with the  $^{137}\text{Cs}$  and was out of trend.

The derived sample burnups based on the measured  $^{148}\text{Nd}$  and  $^{137}\text{Cs}$  data are listed in Table 5.1. TRITON simulations based on these calculated sample burnups were carried out for the samples. The power values used in these simulations were slightly different than the data shown in Table 4.6, which were based on the operator burnup data. The power data corresponding to the measurement-based sample burnups were calculated by multiplying the power data shown in Table 4.6 by the ratio of the measurement-based sample burnup (see Table 5.1) and the initial estimate of sample burnup (see Table 4.6). The renormalized power data are presented in Table 5.1.

**Table 5.1. Cycle power data based on measured sample burnups**

Sample ID	Sample burnup (GWd/MTU)	Sample cycle power (MW/MTU)				
		Cycle 7	Cycle 8	Cycle 9	Cycle 10	Cycle 11
E58-88	42.489	30.277	16.800	26.937	6.985	22.994
E58-148	54.820	39.064	21.676	34.754	9.013	29.667
E58-260	64.624	46.051	25.552	40.971	10.625	34.973
E58-700	77.013	54.879	30.451	48.824	12.661	41.677
165-2a	78.291	40.895	49.058	46.464	13.937	42.530
160-800	70.921	38.974	46.754	44.223	6.283	40.683

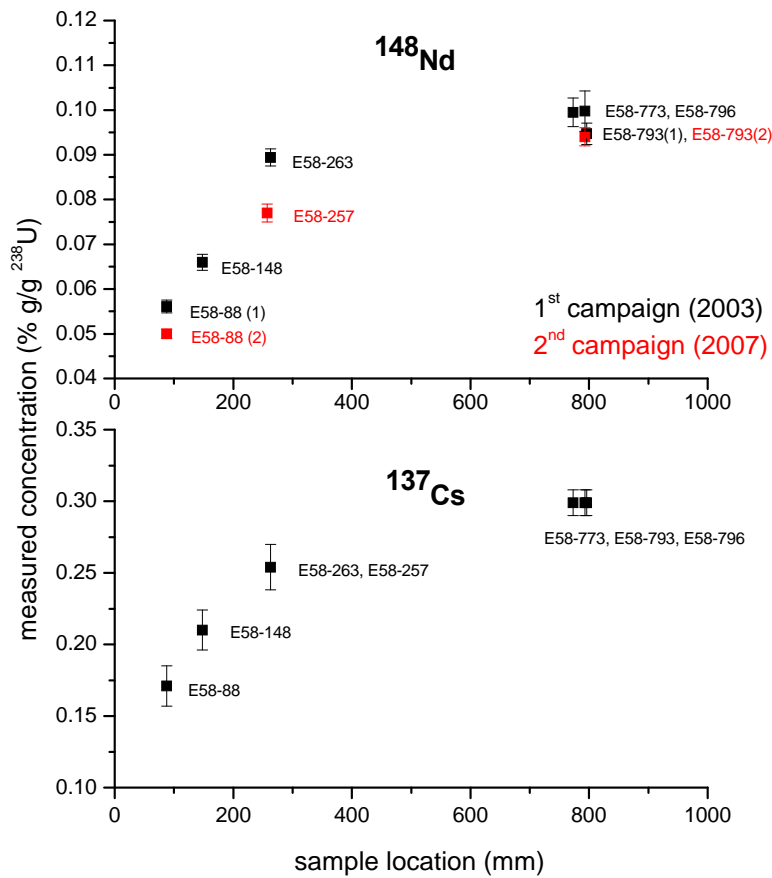


**Figure 5.6. Measured data for  $^{148}\text{Nd}$  and  $^{137}\text{Cs}$  vs. sample location for rod WZR0058.**

Sample TRITON input files are provided in Appendix A for simulations corresponding to nominal burnups (power data as provided in Table 4.6) during cycles 7 through 11 for sample E58-88. As observed in the input files, the power values used in the depletion records of the TRITON inputs for cycles 8 through 11 were slightly different than the power values shown in Table 5.1. This is because the power in TRITON is normalized to the heavy metal mass of the measured fuel rod at the BOC of each simulation cycle, whereas the power data shown in Table 5.1 is expressed using the heavy metal mass in the measured fuel rod for fresh fuel before the irradiation as a basis. Because each cycle is modeled as a separate case, the TRITON user should recognize the fact that at the beginning of each simulation cycle the heavy metal mass in the measured rod changes slightly due to depletion. The user should renormalize the power to account for this.



## 6 RESULTS AND DISCUSSION

The results of the comparison of the calculated nuclide concentrations with the measured data shown in Table 3.5 are listed in Table 6.1 and illustrated in Figures 6.1–6.44. The calculated nuclide concentrations correspond to the burnup values listed in Table 5.1. These burnup values were estimated based on measured data for the burnup indicators  $^{148}\text{Nd}$  and  $^{137}\text{Cs}$ , as discussed in Sections 4 and 5 of this report. The comparison data in Table 6.1 include the calculated-to-experimental (C/E) nuclide concentration ratios in percentage. The average value shown in the final column of Table 6.1 represents a simple mean over the six samples of the C/E-1 value. The error bars shown in Figures 6.1–6.44 for the C/E-1 quantity include only the uncertainty on the measured data (E) corresponding to a 95% confidence level, as listed in Table 3.5.

The data for uranium nuclides are illustrated in Figures 6.1–6.3. The isotope  $^{235}\text{U}$  was underestimated, on average by 5.5%. Note that the samples considered in this study are in the high burnup range, a region in which the variation of  $^{235}\text{U}$  content with burnup transitions from linear to exponential. This means that a small uncertainty in the sample burnup will significantly affect the calculated nuclide content. The isotopes  $^{234}\text{U}$  and  $^{236}\text{U}$  were calculated on average within about 10% and 4% of the measured data, respectively. The plutonium isotopes (see Figures 6.4–6.8) were all calculated on average within 6% of the measurement for all plutonium isotopes measured. The major actinide  $^{239}\text{Pu}$  is well estimated, within 6% of the measured data for each of the six samples, with an average deviation of 1.2%.

The comparisons of the isotopic concentrations for the minor actinides are illustrated in Figures 6.9–6.13. The two measured americium isotopes,  $^{241}\text{Am}$  and  $^{243}\text{Am}$ , are overestimated by an average of approximately 20–25%. The curium isotope  $^{244}\text{Cm}$  was highly overestimated, indicating possible issues with the measurements in this case. Note that the measurement errors for this isotope were large, between 20 and 45% at the 95% confidence level. The  $^{246}\text{Cm}$  nuclide was overestimated by an average of approximately 15%. The isotope  $^{237}\text{Np}$ , of importance for burnup credit, was underestimated on average by approximately 5%.

The cerium isotopes  $^{140}\text{Ce}$  and  $^{142}\text{Ce}$  (see Figures 6.14–6.15) were calculated on average between 1 and 2% of the measurement, respectively. The agreement was not as good for the other measured cerium nuclide  $^{144}\text{Ce}$  (i.e., 22% on average), as seen in Figure 6.16. Note that the latter nuclide was measured by gamma scanning, with measurement uncertainties in the range of 10–50%, as compared with the other cerium nuclides measured by IDA for which the experimental uncertainties were less than 6%.

The results for cesium isotopes are illustrated in Figures 6.38–6.41. The isotope  $^{133}\text{Cs}$ , of importance to burnup credit, is calculated on average within 6% of the measured value, within the range of the measurement error. The isotope  $^{137}\text{Cs}$  was calculated within 1.5% of the measurement. The isotopes  $^{134}\text{Cs}$  and  $^{135}\text{Cs}$  were consistently underestimated, on average by about 15% and 11%, respectively. The underestimation of  $^{134}\text{Cs}$  was consistent with data previously obtained with the 44-group ENDF/B-V SCALE cross-section library. As documented in Ref. 12, this is mainly due to deficiencies in the basic ENDF/B-V data, and improvements were observed when cross sections based on the most recent ENDF/B-VII evaluations were used.

The neodymium nuclides, except for  $^{142}\text{Nd}$ , were on average predicted within about 3% of the measurement, as illustrated in Figures 6.17–6.22.

The results for samarium nuclides are illustrated in Figures 6.23–6.29. The  $^{149}\text{Sm}$  isotope, an important fission product for burnup credit criticality calculations, was overestimated on average by 14.3%. The

$^{147}\text{Sm}$  and  $^{148}\text{Sm}$  nuclides were on average predicted within 2.2 and 3.6%, respectively, of the measurement, whereas  $^{151}\text{Sm}$  and  $^{152}\text{Sm}$  were consistently overestimated in the 30% range;  $^{150}\text{Sm}$  and  $^{154}\text{Sm}$  were overpredicted, on average by 4.8 and 8.5% compared to measurement. As shown previously (Ref. 12), the large differences for  $^{151}\text{Sm}$  and  $^{152}\text{Sm}$  were associated with cross-section data deficiencies, and significant improvements were seen when ENDF/B-VII cross sections were used.

The results for europium nuclides are shown in Figures 6.30–6.32. The nuclide  $^{153}\text{Eu}$ , important for burnup credit criticality calculations, was calculated on average within 3% of measurement. The  $^{154}\text{Eu}$  isotope, an important gamma emitter, was overestimated by an average of 17%. The  $^{155}\text{Eu}$  nuclide was underestimated by 22.4% on average.

The results for gadolinium nuclides are illustrated in Figures 6.33–6.37. The isotopes  $^{154}\text{Gd}$  and  $^{158}\text{Gd}$  were consistently overestimated in the 30% range. The isotopes  $^{156}\text{Gd}$  and  $^{160}\text{Gd}$  were calculated on average within about 3 and 5% of the measurement, respectively. The nuclide  $^{155}\text{Gd}$ , of importance to burnup credit, was underestimated by an average of approximately 8%.

Results for  $^{106}\text{Ru}$  are shown in Figure 6.42. This fission product was underestimated on average by approximately 6%. The burnup-indicator fission product  $^{139}\text{La}$  (see Figure 6.43) was consistently overestimated, on average by 8%. Note that this nuclide was measured by a method (ICP-MS with external calibration) with larger inherent measurement uncertainties (17%) than the ICP-MS with IDA method.

Two metallic fission products for which measurement data were available,  $^{99}\text{Tc}$  (see Figure 6.44) and  $^{103}\text{Rh}$ , both of importance to burnup credit criticality calculations, were overestimated by 5% and 8% on average, respectively.

**Table 6.1. C/E-1 (%) results**

<b>Sample ID Rod ID Burnup (GWd/MTU)</b>	<b>E58-88 WZR0058 42.5</b>	<b>E58-148 WZR0058 54.85</b>	<b>E58-260 WZR0058 64.65</b>	<b>E58-700 WZR0058 77.05</b>	<b>165-2a WZtR165 78.3</b>	<b>160-800 WZtR160 70.9</b>	<b>AVG<sup>a</sup></b>
U-234	3.9	-6.1	18.9	14.3	16.9		9.6
U-235	-4.2	-14.6	-1.9	-4.8	-1.9		-5.5
U-236	8.7	-1.3	3.0	5.6	3.3		3.9
U-238	-0.2	-0.1	-0.4	-0.2	0.4		-0.1
Pu-238	0.3	20.4	-3.4	-2.2	-7.6	-9.1	-0.3
Pu-239	0.9	4.4	2.3	2.9	-6.0	2.9	1.2
Pu-240	8.3	12.1	6.6	6.6	0.2	0.0	5.6
Pu-241	-0.9	5.6	-0.6	0.9	-7.2	-4.3	-1.1
Pu-242	8.8	17.8	6.2	5.7	-1.7	-4.2	5.4
Np-237	-1.8	-11.5	-5.4	0.7	-12.8	-0.2	-5.2
Am-241	23.8	29.9	19.0	23.5	10.8	19.7	21.1
Am-243	50.8	25.4	27.4	28.6	-2.8	20.6	25.0
Cm-244	106.9	103.0	79.1	99.6	68.3	62.7	86.6
Cm-246	-10.0	49.7	11.4	34.0	17.3	-14.5	14.6
Cs-133	3.1	6.1	-3.6	10.6	15.8		6.4
Cs-134	-25.1	-14.3	-15.8	-11.2	-11.8	-12.6	-15.1
Cs-135	-10.8	-15.1	-20.5	-2.2	-7.5		-11.2
Cs-137	-5.2	0.2	-1.6	0.8	-0.1	-3.1	-1.5
Ce-140	1.8	5.3	-0.9	1.5	1.2	-4.4	0.8
Ce-142	-0.4	-0.4	-2.4	-2.1	-2.8	-3.8	-2.0
Ce-144	19.0	23.6	21.0	24.7	21.9		22.0
Nd-142	25.3	34.0	21.9	17.2		16.5	23.0
Nd-143	-0.9	1.8	0.4	1.1	8.0	3.2	2.2
Nd-145	1.2	2.5	0.0	-1.0	4.5	2.6	1.6
Nd-146	2.4	3.9	1.9	1.4	6.0	2.7	3.0
Nd-148	0.4	-0.5	1.3	-2.3	-6.8	1.7	-1.0
Nd-150	-0.4	8.0	-0.5	6.7	-6.2	0.9	1.4
Sm-147	-2.1	-1.5	4.0	-0.6	-10.7		-2.2
Sm-148	3.8	2.5	0.7	-4.1	-12.3	-12.2	-3.6
Sm-149	-0.1	0.9	12.5	26.6	29.9	16.2	14.3
Sm-150	5.3	3.8	6.1	5.5	9.4	-1.6	4.8
Sm-151	23.8	36.9	38.8	32.7	37.1	30.2	33.3
Sm-152	26.7	30.9	34.2	35.4	30.7	28.5	31.1
Sm-154	6.4	17.9	22.8	13.7	-4.5	-5.2	8.5
Eu-153	-7.1	-3.3	-4.0	2.1	-0.5		-2.6
Eu-154	5.6	11.2	18.8	43.1	8.0		17.3
Eu-155	-24.8	-29.2	-26.0	-16.3	-15.6		-22.4

**Table 6.1 C/E-1 (%) results (cont.)**

<b>Sample ID Rod ID Burnup (GWd/MTU)</b>	<b>E58-88 WZR0058 42.489</b>	<b>E58-148 WZR0058 54.820</b>	<b>E58-263 WZR0058 64.624</b>	<b>E58-700 WZR0058 77.013</b>	<b>165-2a WZtR165 80.466</b>	<b>160-800 WZtR160 70.921</b>	<b>AVG<sup>a</sup></b>
Gd-154	41.3	24.4	51.8	37.7	10.5	35.5	33.5
Gd-155	-9.3	-17.1	-7.4	-11.8	6.9		-7.8
Gd-156	9.1	5.6	6.3	2.7	2.9	-8.6	3.0
Gd-158	27.4	29.6	39.0	40.7	40.0	25.4	33.7
Gd-160	-6.5	10.8	13.7	15.2	-0.8	-2.6	5.0
Ru-106	-17.3	-6.3	-6.5	-0.5	1.4		-5.8
La-139	5.6		11.4	6.3		8.1	7.8
Rh-103						8.0	8.0
Tc-99	6.9					2.9	4.9

<sup>a</sup> Simple mean (not weighted) of C/E-1 (%).

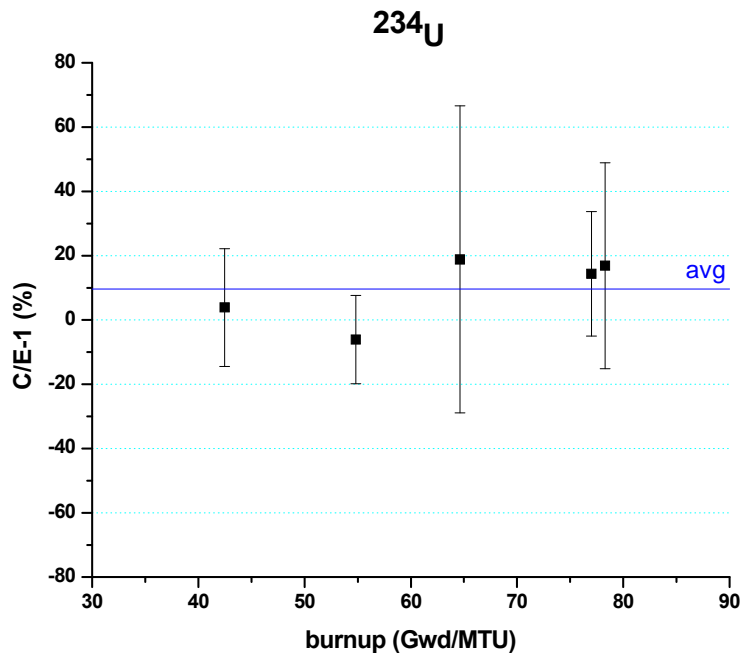


Figure 6.1. Calculation-to-measurement comparison for  $^{234}\text{U}$ .

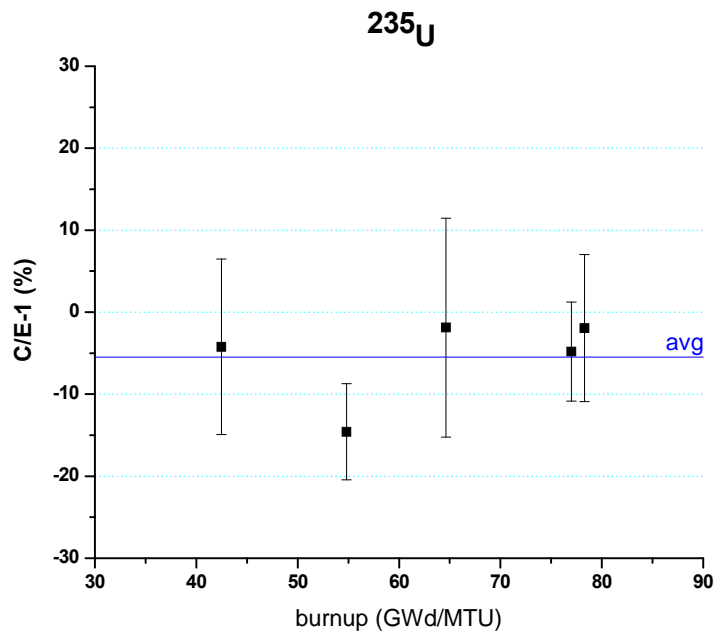


Figure 6.2. Calculation-to-measurement comparison for  $^{235}\text{U}$ .

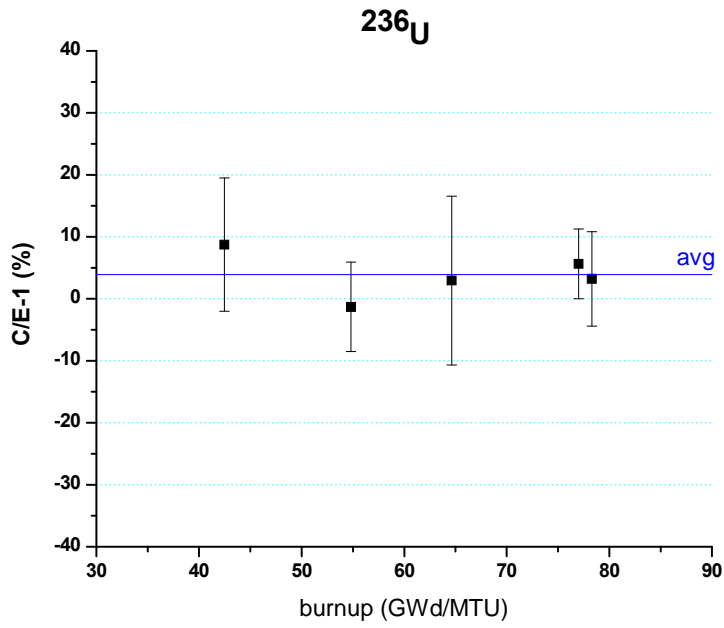


Figure 6.3. Calculation-to-measurement comparison for  $^{236}\text{U}$ .

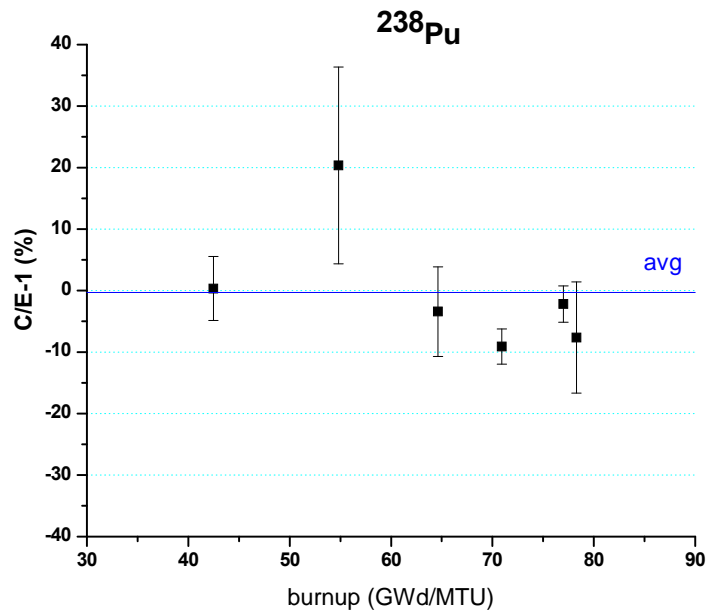


Figure 6.4. Calculation-to-measurement comparison for  $^{238}\text{Pu}$ .

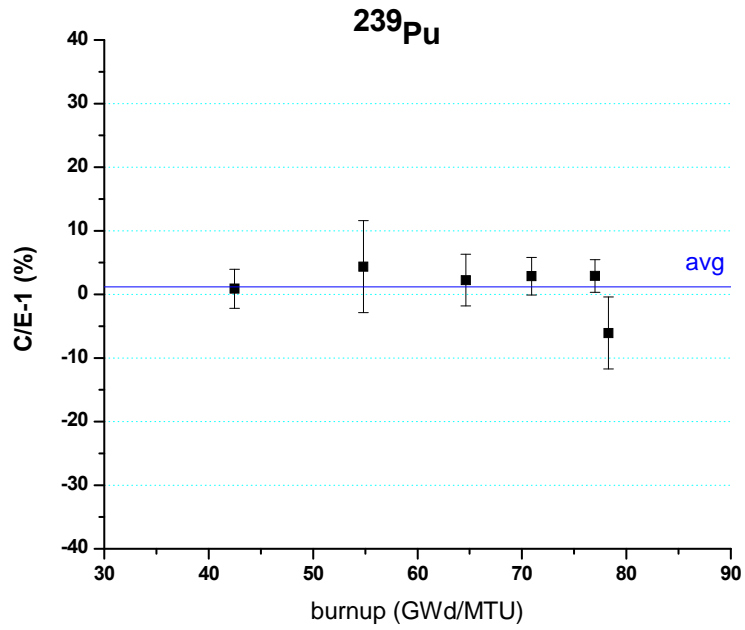


Figure 6.5. Calculation-to-measurement comparison for <sup>239</sup>Pu.

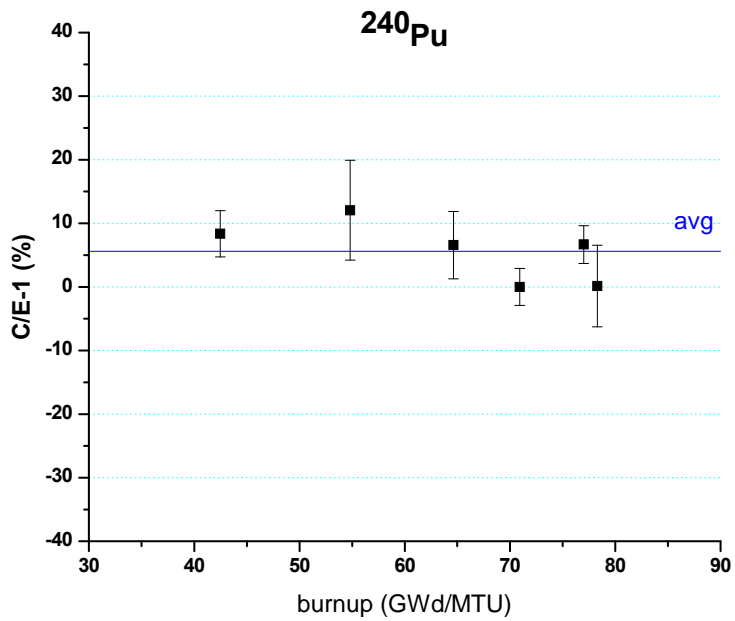
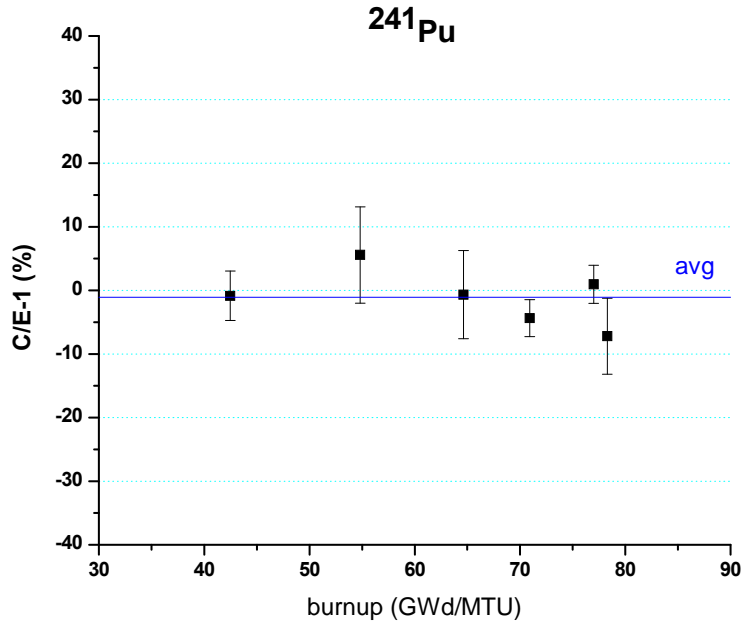
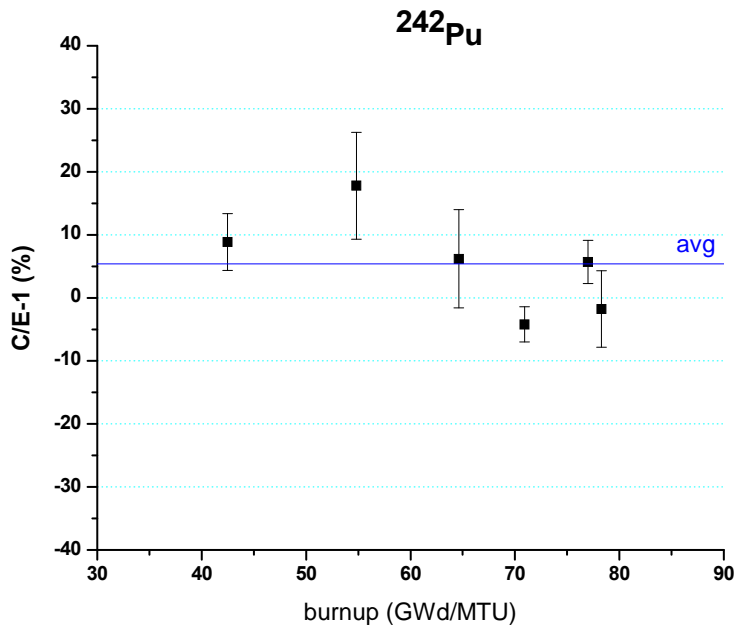


Figure 6.6. Calculation-to-measurement comparison for <sup>240</sup>Pu.



**Figure 6.7. Calculation-to-measurement comparison for  $^{241}\text{Pu}$ .**



**Figure 6.8. Calculation-to-measurement comparison for  $^{242}\text{Pu}$ .**



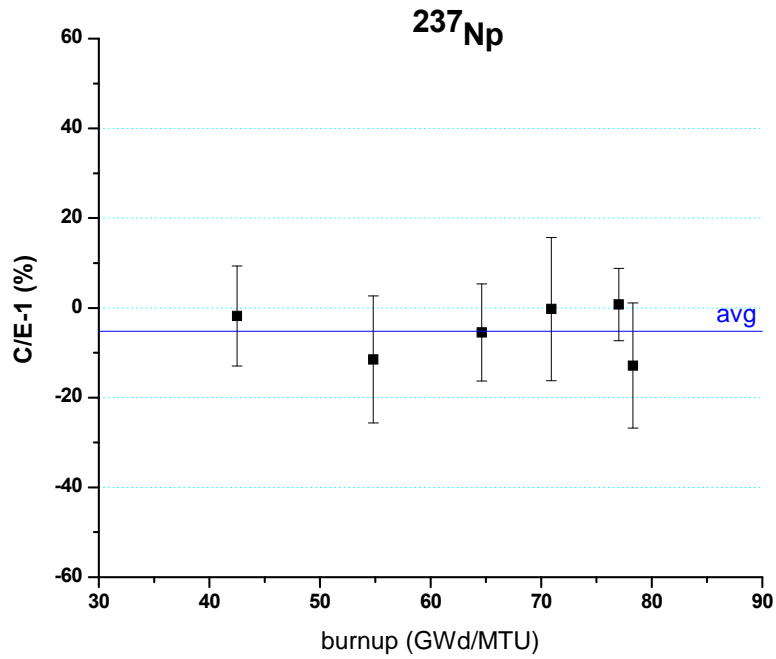


Figure 6.9. Calculation-to-measurement comparison for <sup>237</sup>Np.

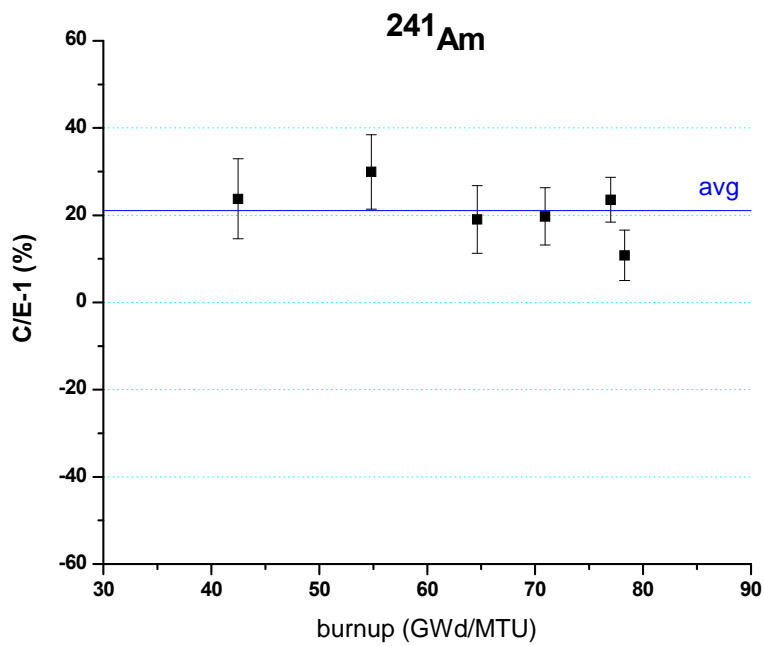
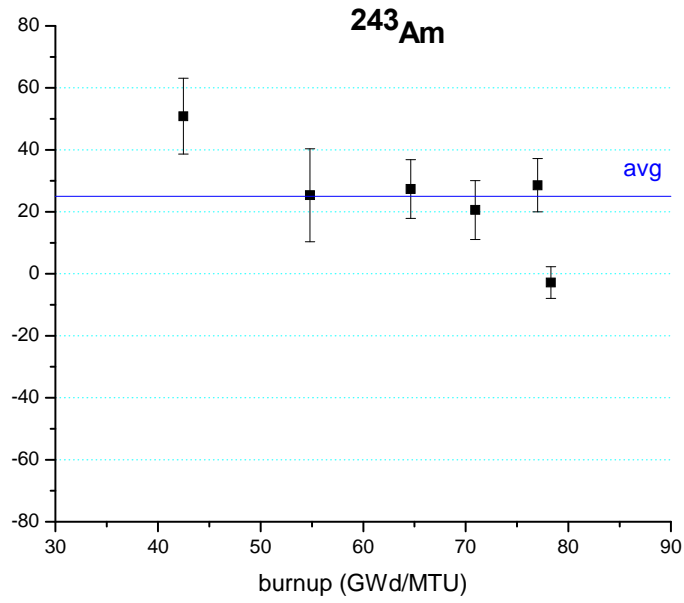
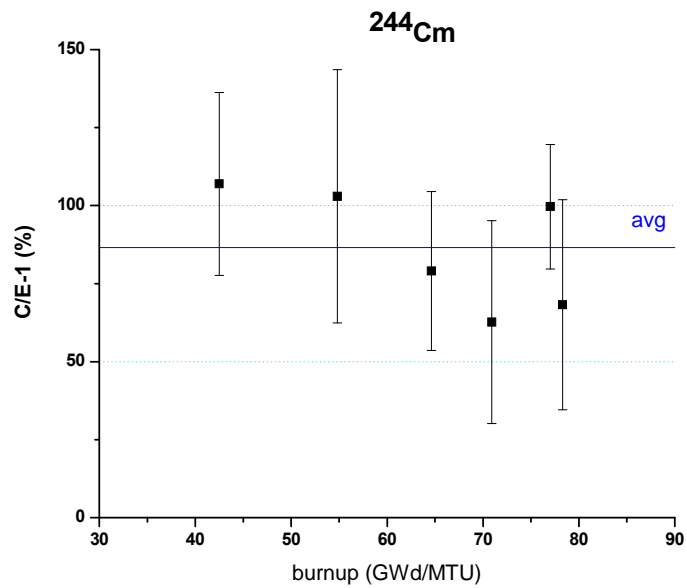


Figure 6.10. Calculation-to-measurement comparison for <sup>241</sup>Am.



**Figure 6.11. Calculation-to-measurement comparison for  $^{243}\text{Am}$ .**



**Figure 6.12. Calculation-to-measurement comparison for  $^{244}\text{Cm}$ .**

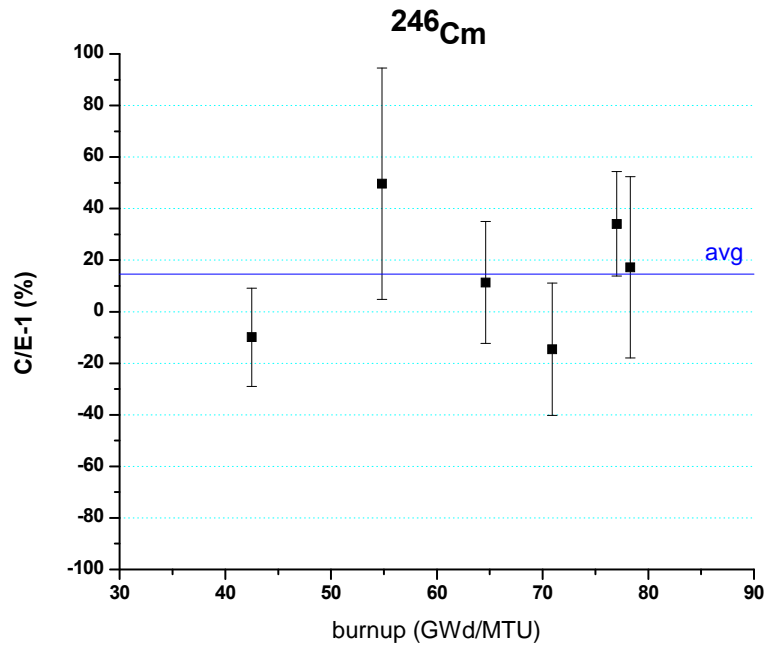


Figure 6.13. Calculation-to-measurement comparison for  $^{246}\text{Cm}$

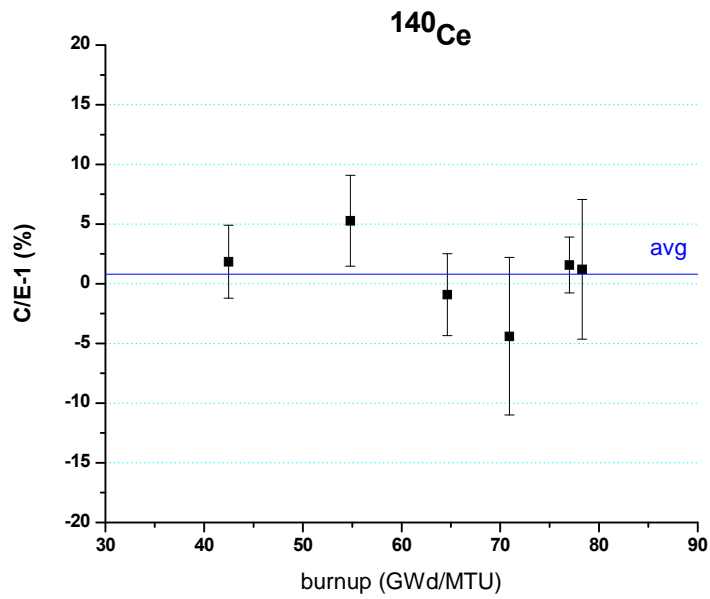


Figure 6.14. Calculation-to-measurement comparison for  $^{140}\text{Ce}$ .

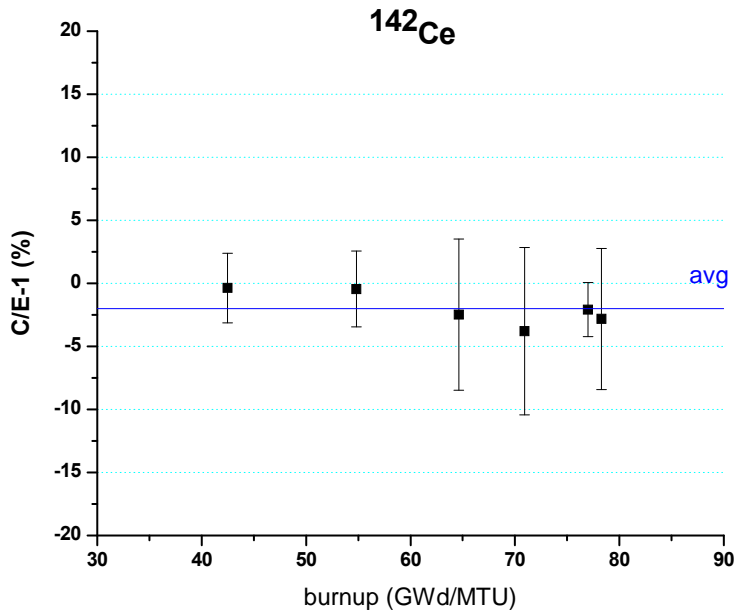


Figure 6.15. Calculation-to-measurement comparison for  $^{142}\text{Ce}$ .

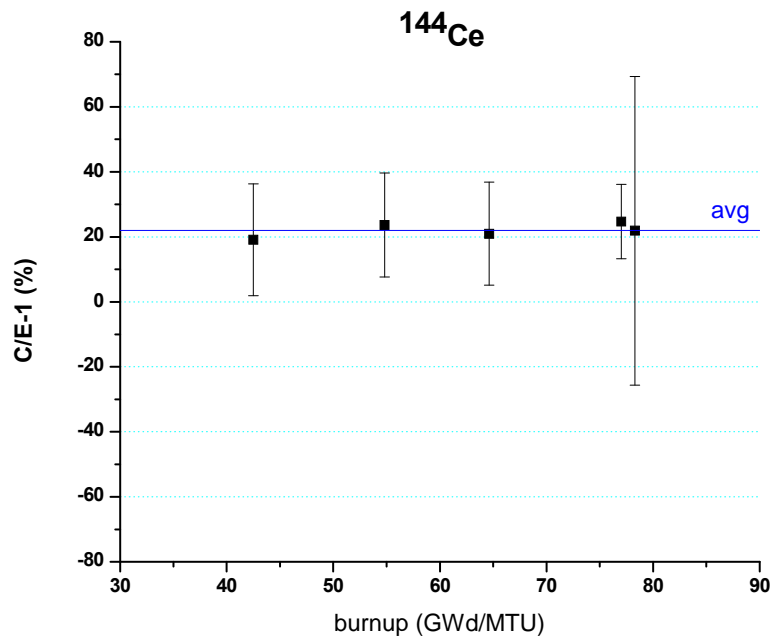


Figure 6.16. Calculation-to-measurement comparison for  $^{144}\text{Ce}$ .

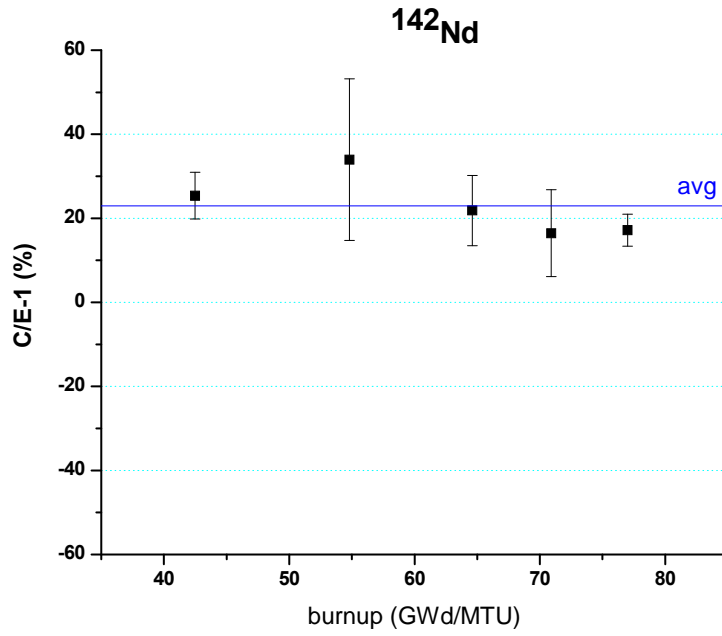


Figure 6.17. Calculation-to-measurement comparison for  $^{142}\text{Nd}$ .

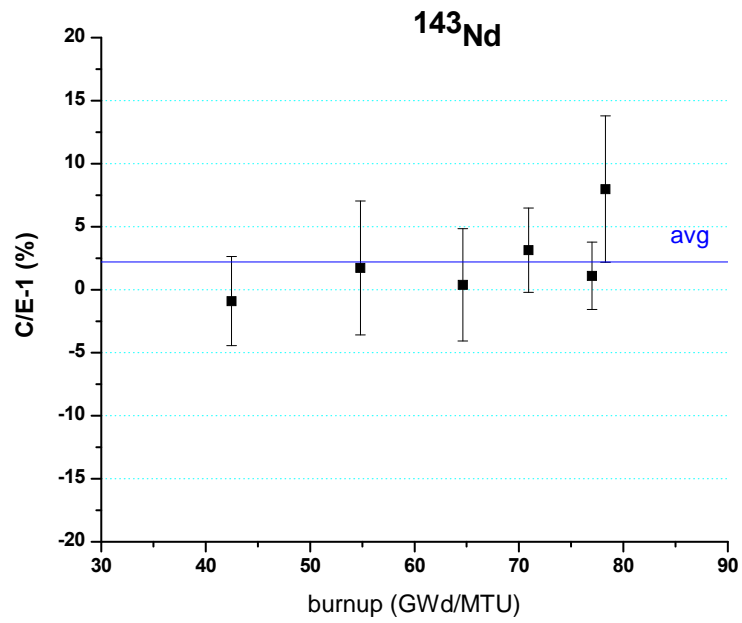
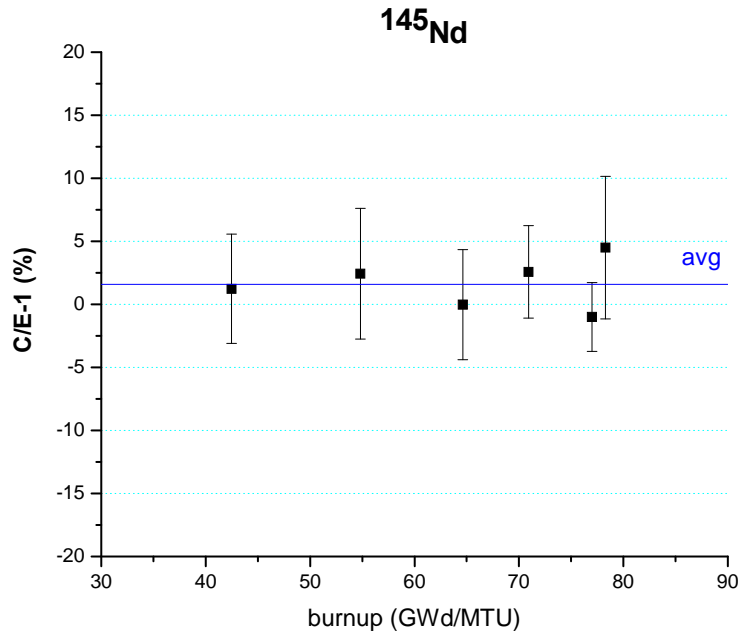
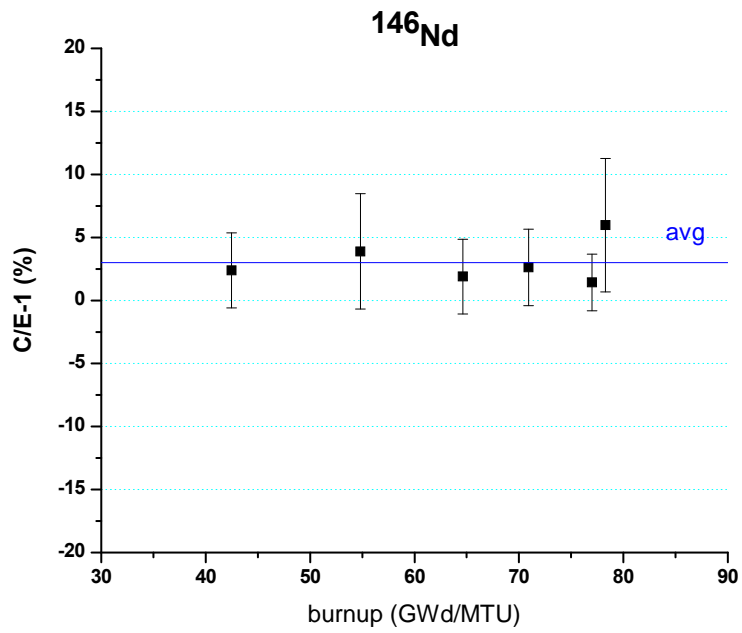


Figure 6.18. Calculation-to-measurement comparison for  $^{143}\text{Nd}$ .



**Figure 6.19. Calculation-to-measurement comparison for <sup>145</sup>Nd.**



**Figure 6.20. Calculation-to-measurement comparison for <sup>146</sup>Nd.**

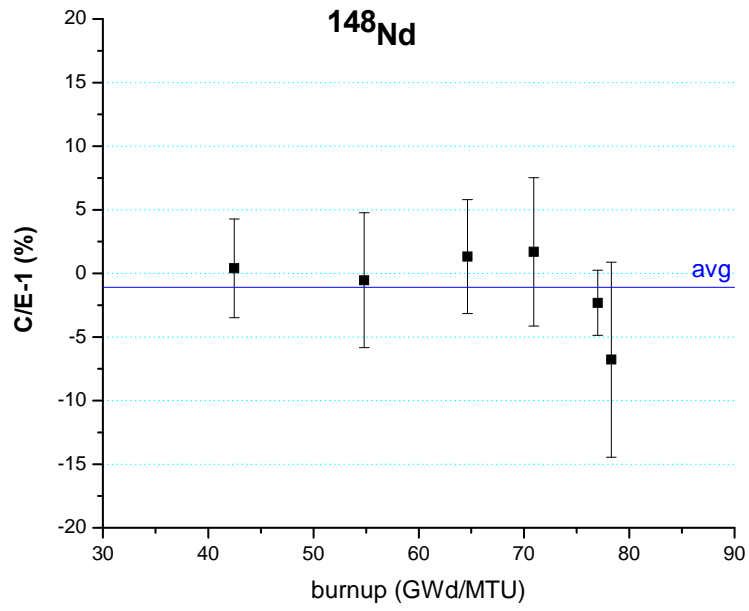


**Figure 6.21. Calculation-to-measurement comparison for <sup>148</sup>Nd.**

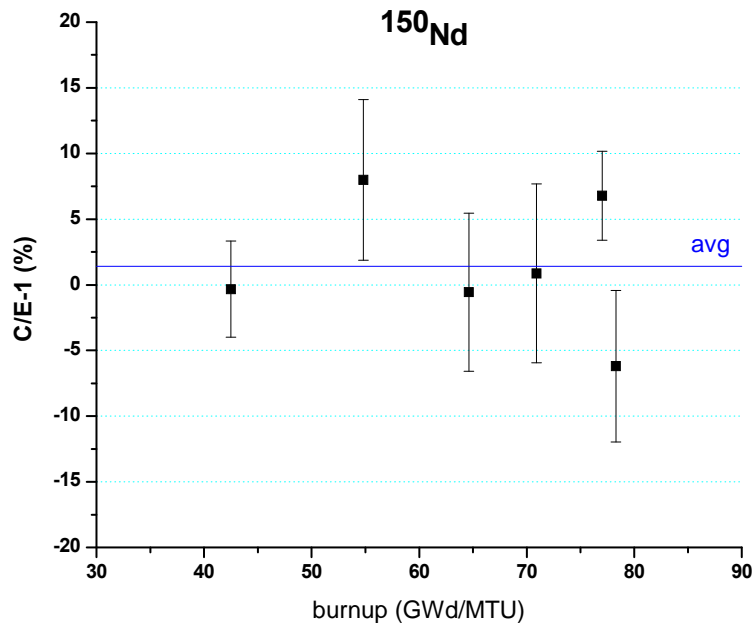


**Figure 6.22. Calculation-to-measurement comparison for <sup>150</sup>Nd.**

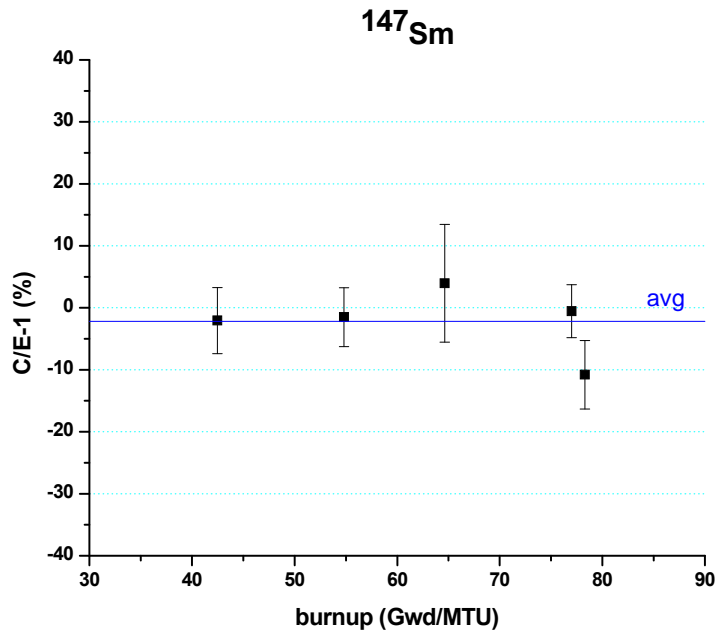


Figure 6.23. Calculation-to-measurement comparison for <sup>147</sup>Sm.

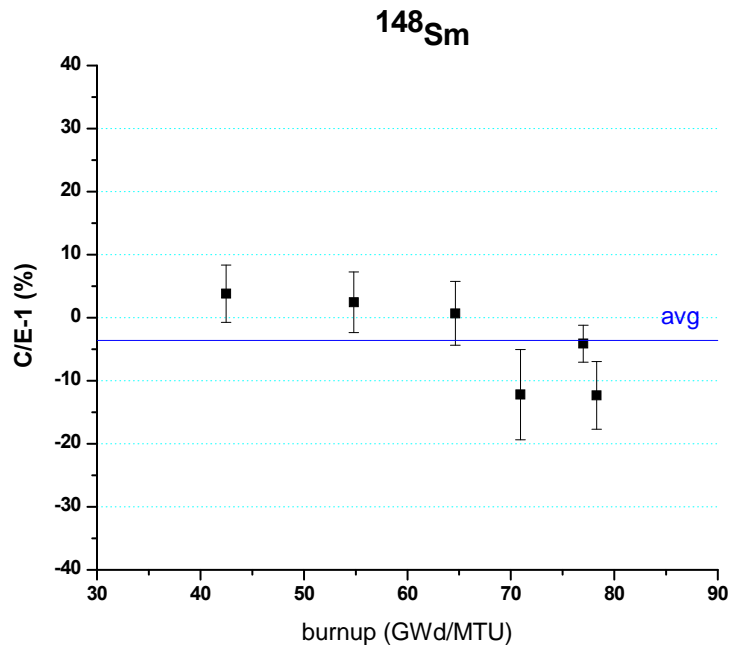


Figure 6.24. Calculation-to-measurement comparison for <sup>148</sup>Sm.



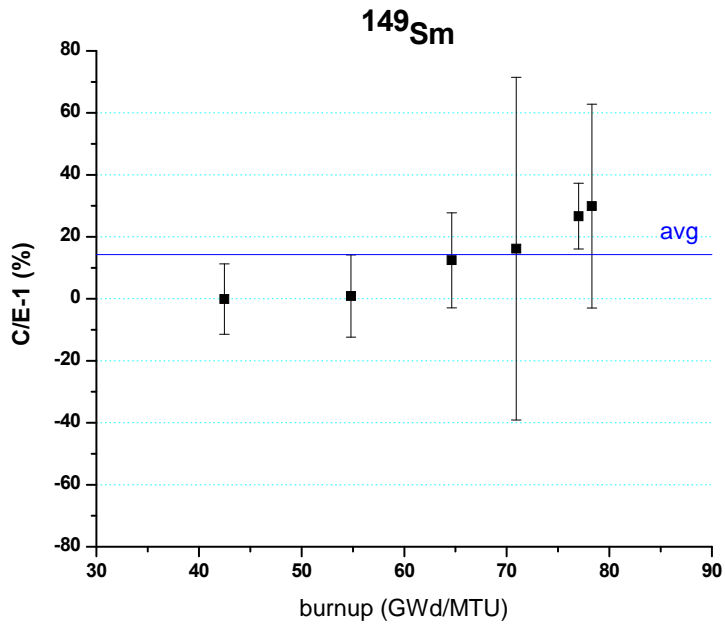


Figure 6.25. Calculation-to-measurement comparison for <sup>149</sup>Sm.

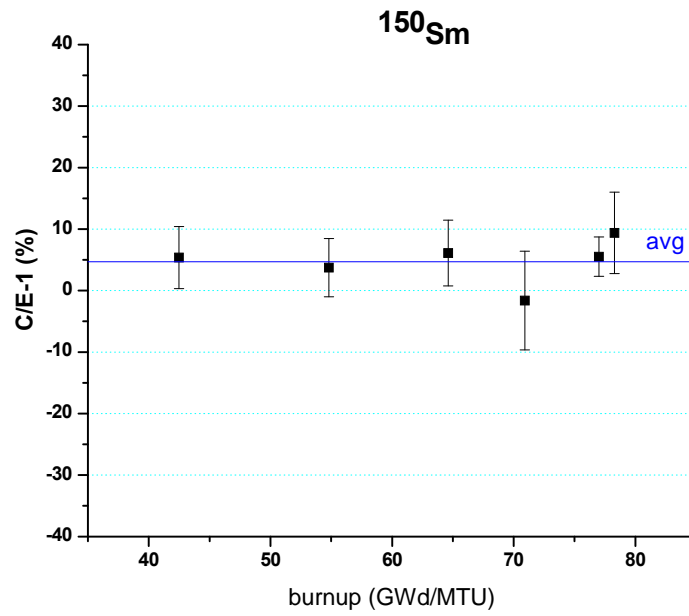


Figure 6.26. Calculation-to-measurement comparison for <sup>150</sup>Sm.

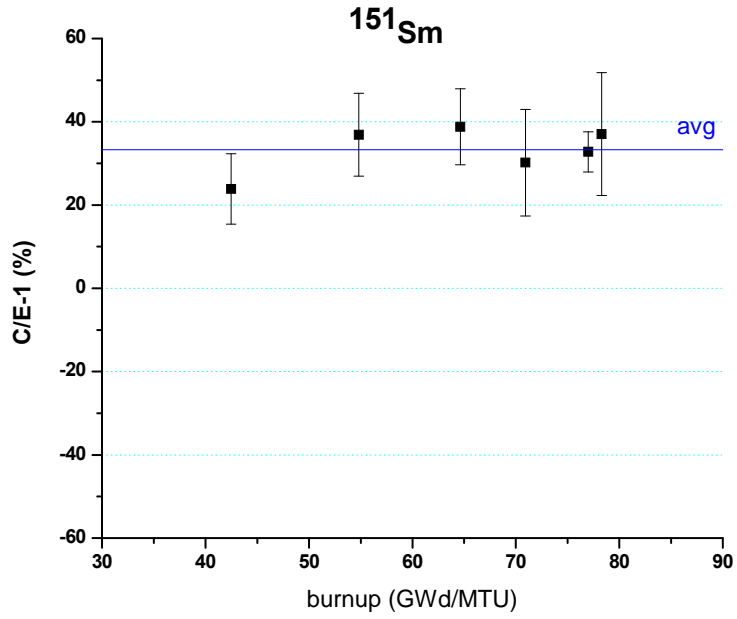


Figure 6.27. Calculation-to-measurement comparison for <sup>151</sup>Sm.

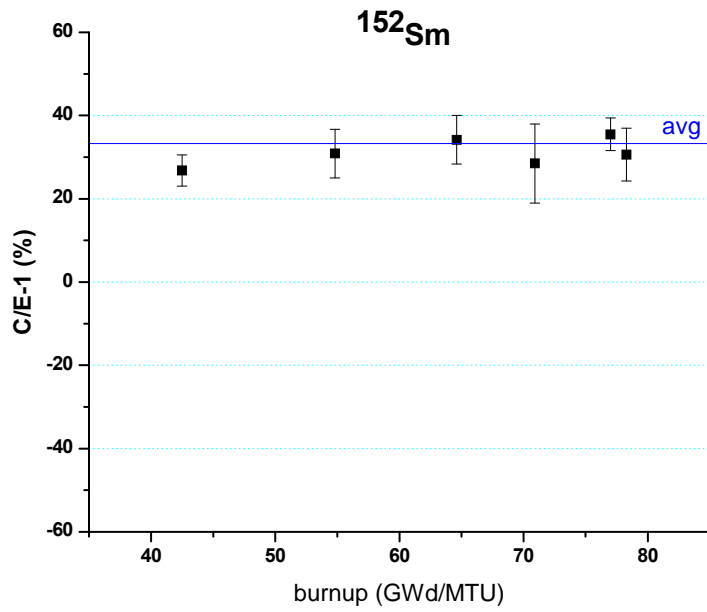


Figure 6.28. Calculation-to-measurement comparison for <sup>152</sup>Sm.

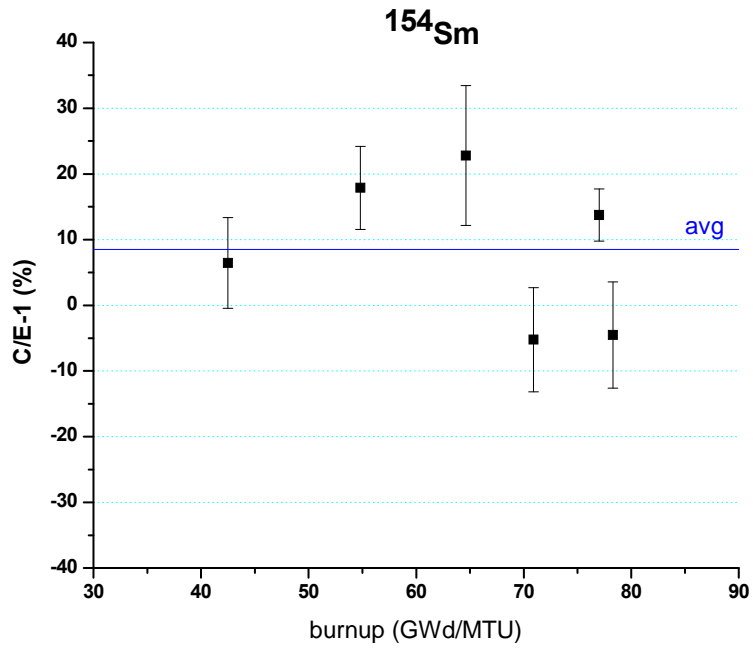


Figure 6.29. Calculation-to-measurement comparison for <sup>154</sup>Sm.

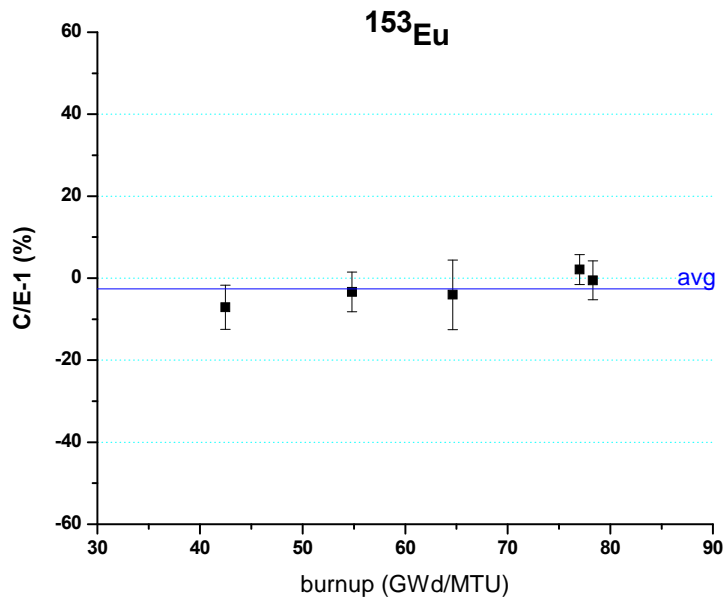


Figure 6.30. Calculation-to-measurement comparison for <sup>153</sup>Eu.

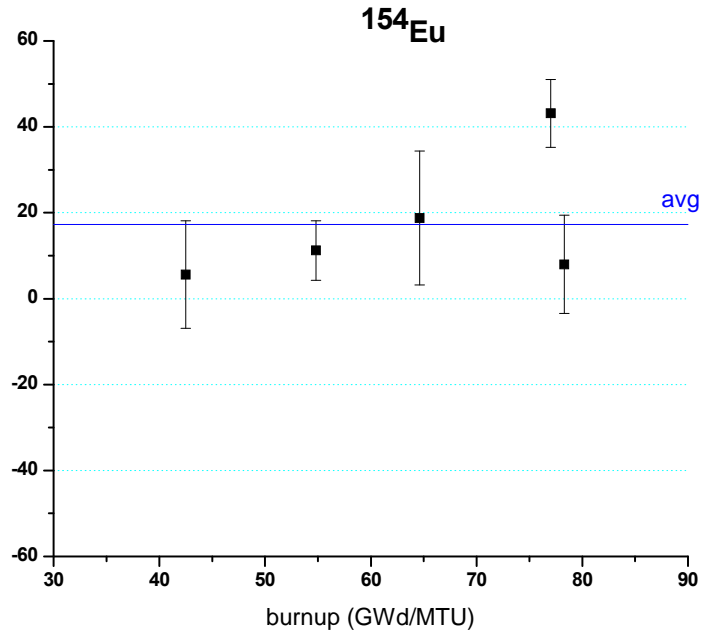


Figure 6.31. Calculation-to-measurement comparison for  $^{154}\text{Eu}$ .

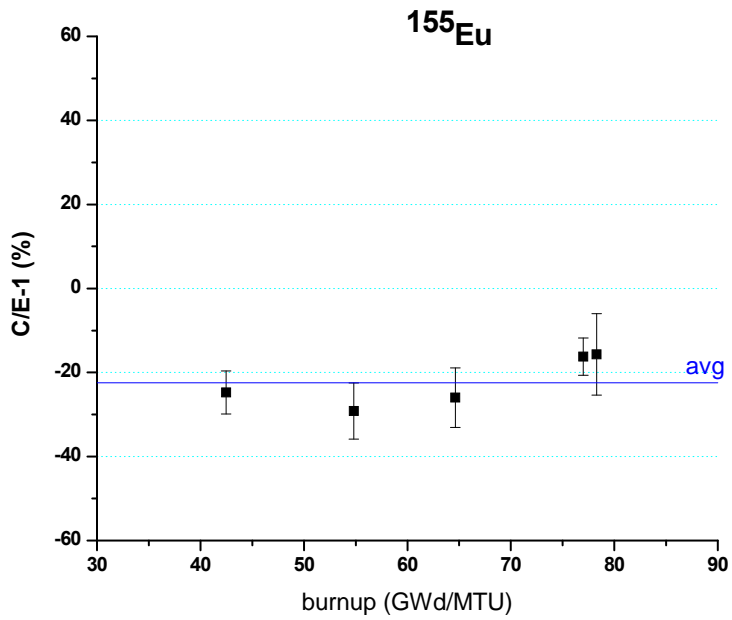


Figure 6.32. Calculation-to-measurement comparison for  $^{155}\text{Eu}$ .

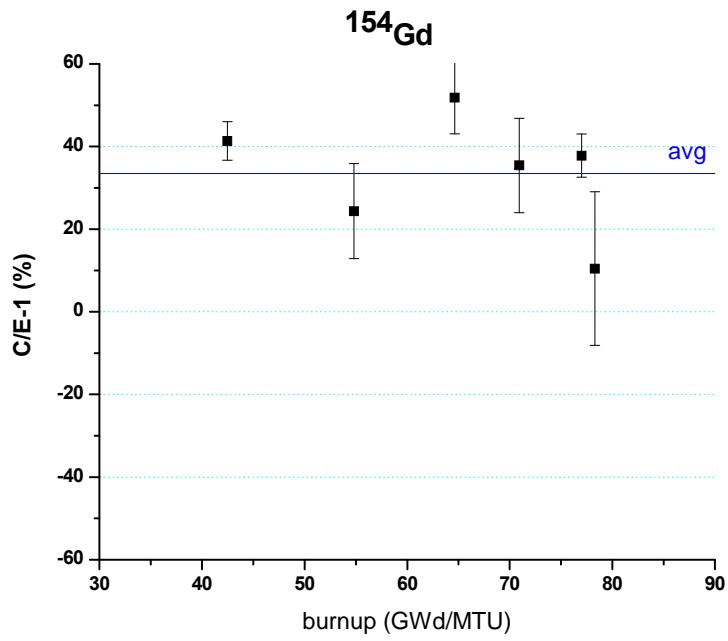


Figure 6.33. Calculation-to-measurement comparison for  $^{154}\text{Gd}$ .

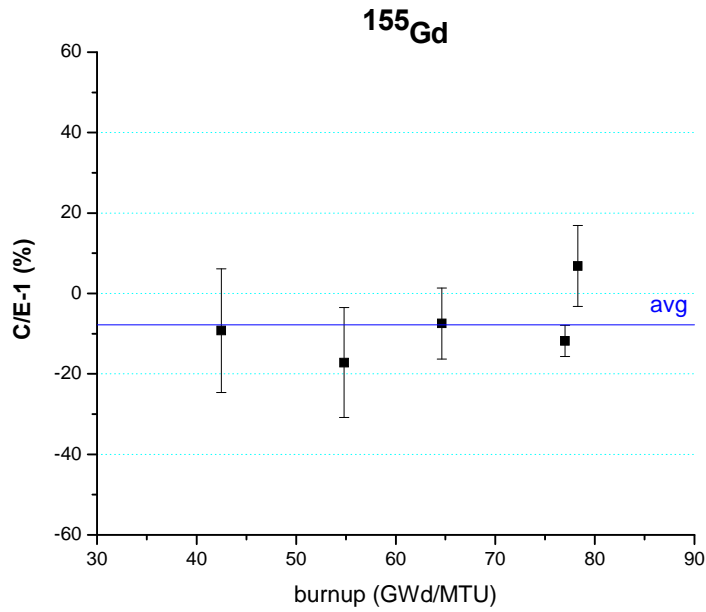


Figure 6.34. Calculation-to-measurement comparison for  $^{155}\text{Gd}$ .

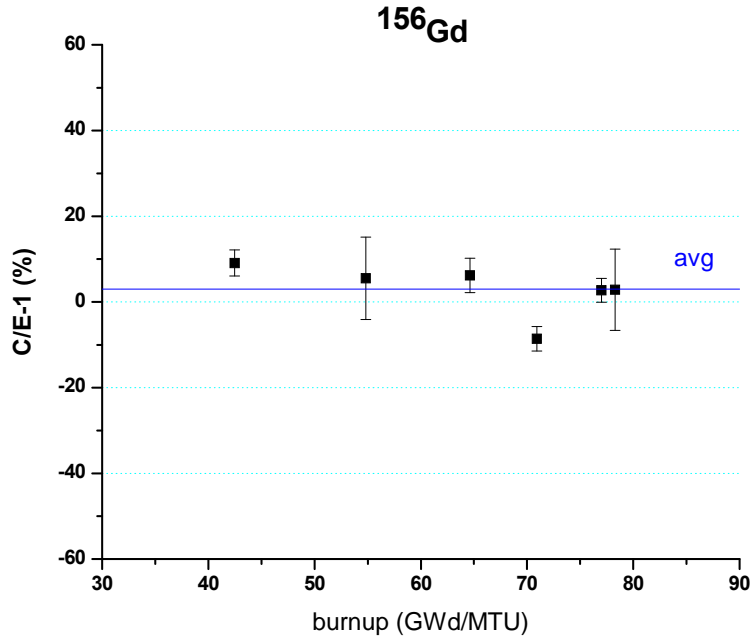


Figure 6.35. Calculation-to-measurement comparison for <sup>156</sup>Gd.

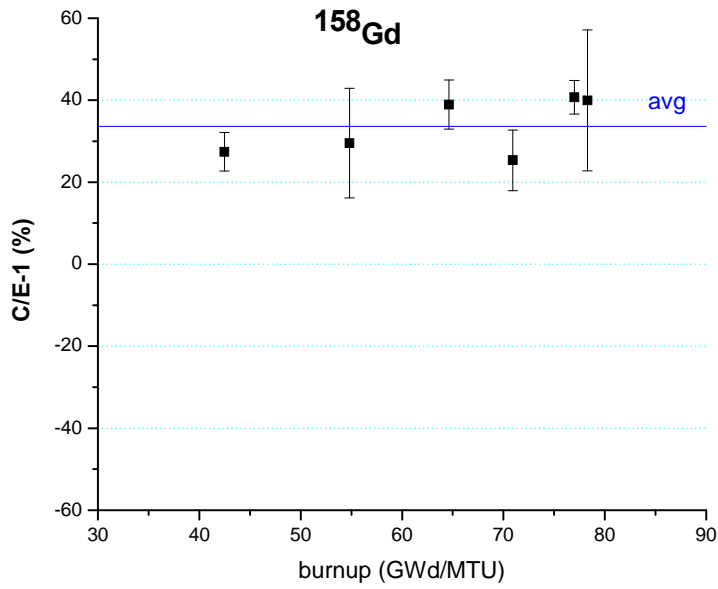


Figure 6.36. Calculation-to-measurement comparison for <sup>158</sup>Gd.

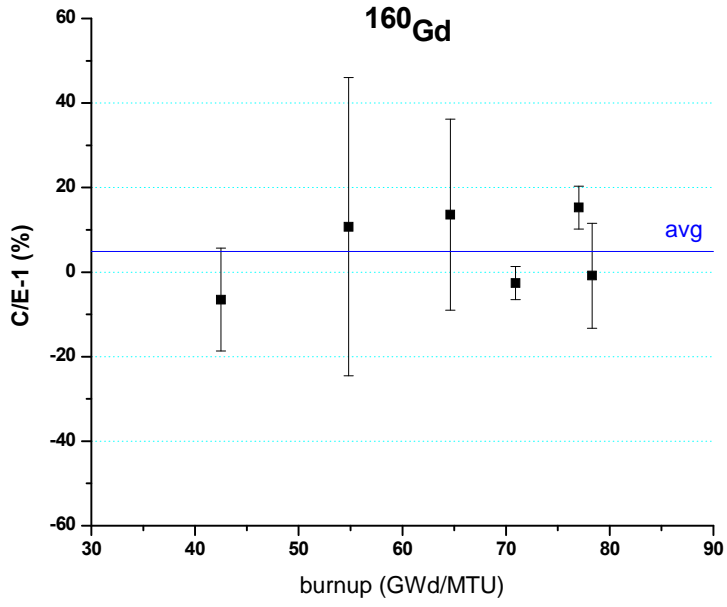


Figure 6.37. Calculation-to-measurement comparison for  $^{160}\text{Gd}$ .

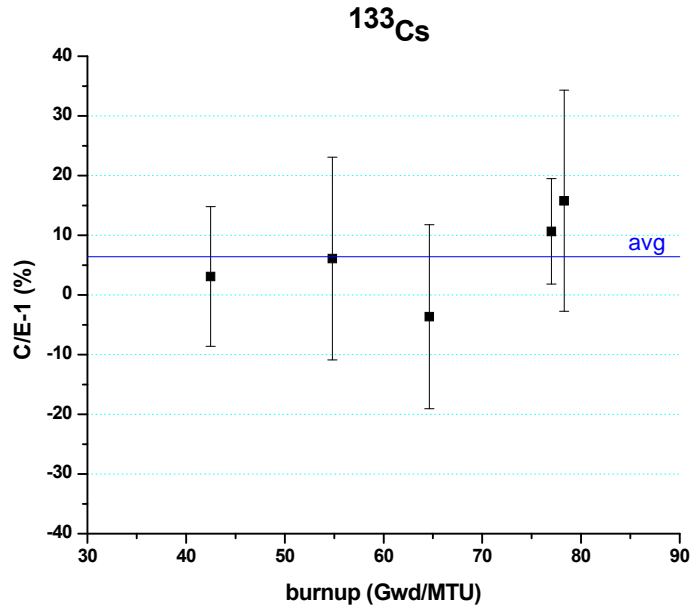


Figure 6.38. Calculation-to-measurement comparison for  $^{133}\text{Cs}$ .

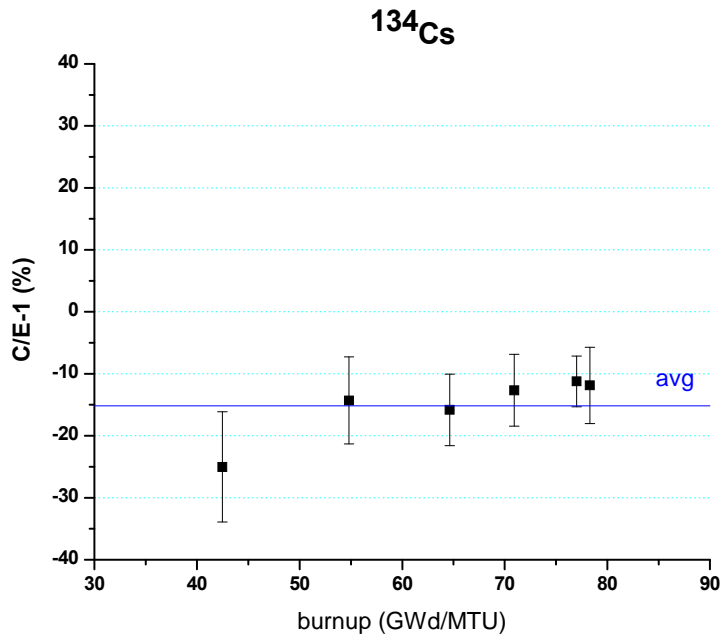


Figure 6.39. Calculation-to-measurement comparison for <sup>134</sup>Cs.

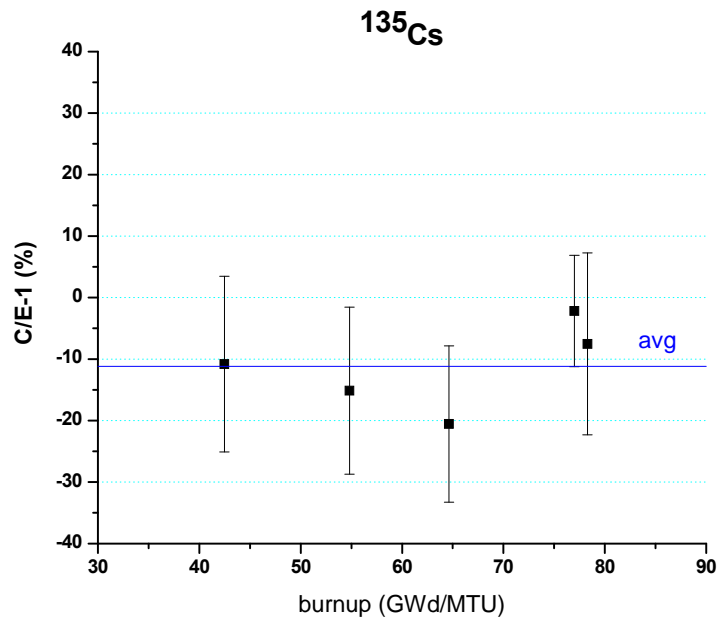


Figure 6.40. Calculation-to-measurement comparison for <sup>135</sup>Cs.



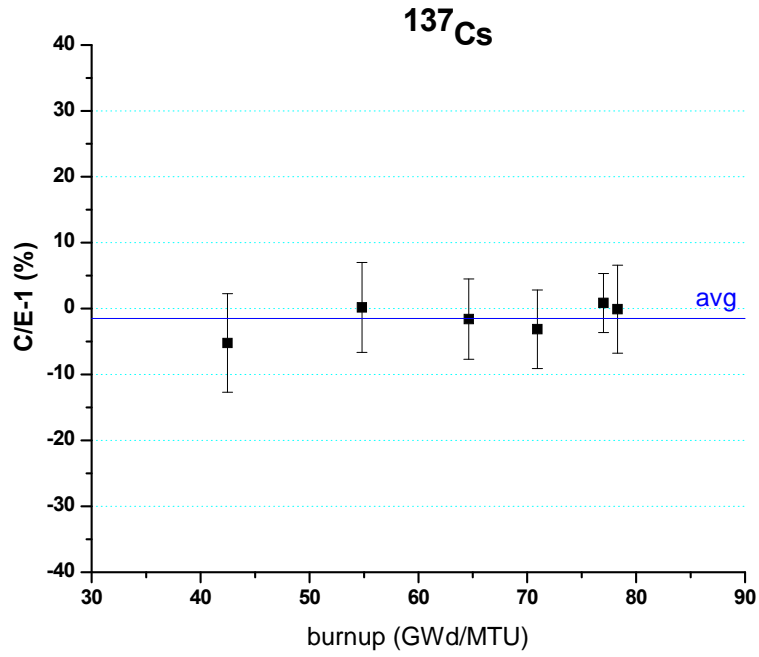


Figure 6.41. Calculation-to-measurement comparison for <sup>137</sup>Cs.

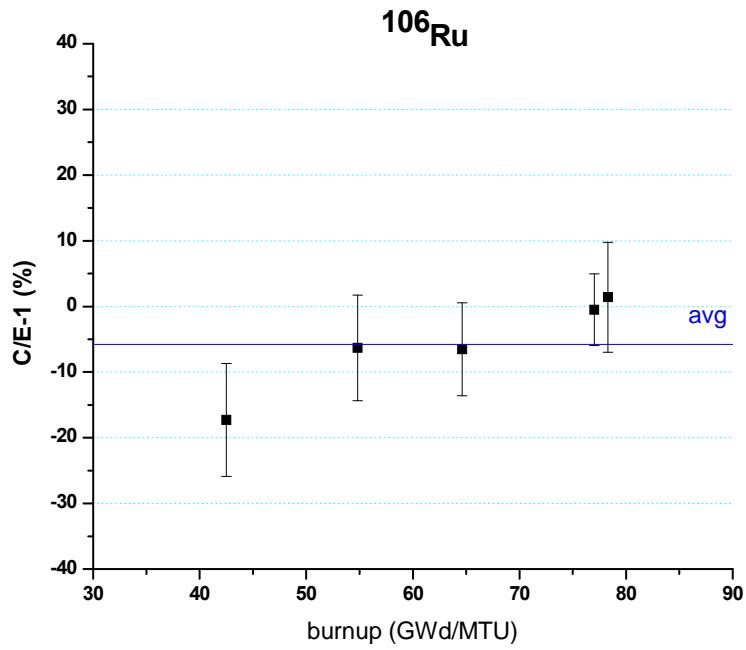


Figure 6.42. Calculation-to-measurement comparison for <sup>106</sup>Ru.

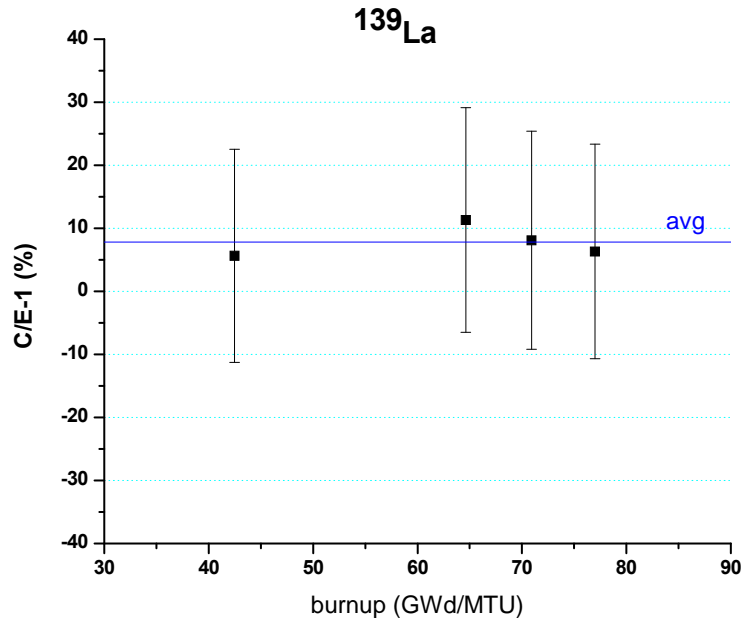


Figure 6.43. Calculation-to-measurement comparison for  $^{139}\text{La}$ .

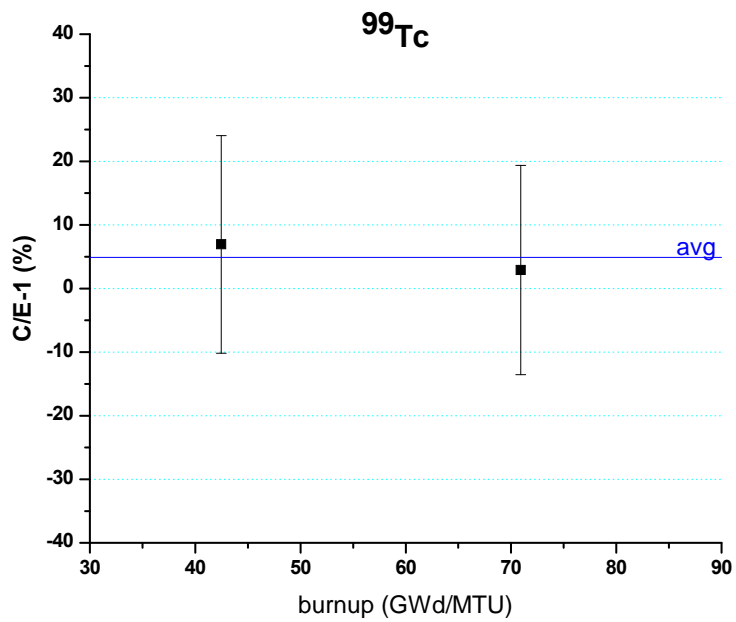


Figure 6.44. Calculation-to-measurement comparison for  $^{99}\text{Tc}$ .

## 7 SUMMARY

This report documents radiochemical assay data for high-burnup spent nuclear fuel that were measured through a high-burnup fuel program coordinated by Spanish organizations. The measurements analyzed in this report include six unique fuel samples with an initial enrichment of 4.5 wt%  $^{235}\text{U}$  that were obtained from three fuel rods irradiated in the Vandellós II PWR operated in Spain. Multiple measurements, available for three of these six samples, were combined using the measurement uncertainty to weight the different measurements, leading to combined datasets with reduced measurement uncertainties. The samples cover a burnup range from 42 to 78 GWd/MTU.

The experimental data were used to validate the 2-D lattice depletion sequence TRITON in the SCALE code system. Individual TRITON models were developed for each of the samples considered. Information on the radiochemical analysis methods and uncertainties, assembly design description and irradiation history, and computational models and results obtained using the SCALE code system are included. The data are presented in sufficient detail to allow an independent analysis to be performed.

The samples measured in this program were obtained from fuel rods that were moved from one assembly to another to obtain very high burnups. The modeling and simulation of these samples for the depletion analysis were very complex compared to typical commercial fuels. Given the fuel reconfiguration during irradiation, the ability to use the data will depend to a large extent on the capabilities of the code used to simulate the reconfigurations. However, for a code with these simulation capabilities, the measurement data are a valuable dataset for validation, as the measurements include extensive isotopic data for the actinides and fission products of high importance to spent fuel safety applications, including burnup credit, decay heat, and radiation source terms.



## 8 REFERENCES

1. J. M. Conde, C. Alejano, and J. M. Rey, *Nuclear Fuel Research Activities of the Consejo de Seguridad Nuclear, Trans. International Meeting on LWR Fuel Performance, Top Fuel 2006*, Salamanca, Spain (2006).
2. J. M. Conde, J. M. Alonso, J. A. Gago, P. González, M. Novo, and L. E. Herranz, *Spanish R&D Program on Spent Fuel Dry Storage, Trans. International Meeting on LWR Fuel Performance, Top Fuel 2006*, Salamanca, Spain (2006).
3. H. U. Zwicky and J. Low, *Fuel Pellet Isotopic Analyses of Vandellós 2 Rods WZtR165 and WZR0058*, Final Report, STUDEVIK/N(H)-03/069, Rev. 1 (2008).
4. H. U. Zwicky and J. Low, *Fuel Pellet Isotopic Analyses of Vandellós 2 Rods WZtR165 and WZR0058: Qualification of Method*, STUDEVIK/N(H)-04/002, Rev. 2 (2008).
5. H. U. Zwicky and J. Low, *Fuel Pellet Isotopic Analyses of Vandellós 2 Rods WZtR165 and WZR0058: Complementary Report*, STUDEVIK/N(H)-04/135, Rev. 1 (2008).
6. H. U. Zwicky, J. Low, and M. Granfors, *Additional Fuel Pellet Isotopic Analyses of Vandellós 2 Rods WZtR160 and WZR0058*, Final Report, STUDEVIK/N-07/140 (2008).
7. P. R. Bevington, *Data Reduction and Error Analysis for the Physical Sciences*, McGraw-Hill Book Company, New York (1969).
8. *ARIANE International Programme—Final Report*, ORNL/SUB/97-XSV750-1, Oak Ridge National Laboratory, Oak Ridge, Tennessee (May 1, 2003).
9. A. Romano, “Irradiation data of the three fuel rods for high burnup fuel isotope determination,” COM-006998 Rev. 2, ENUSA, Spain (2010).
10. *SCALE: A Modular Code System for Performing Standardized Computer Analyses for Licensing Evaluation*, ORNL/TM-2005/39, Version 5.1, Vols. I–III, Oak Ridge National Laboratory, Oak Ridge, Tennessee, November 2006. Available from Radiation Safety Information Computational Center at Oak Ridge National Laboratory as CCC-732.
11. G. Ilas, I. C. Gauld, F. C. Difilippo, and M. B. Emmett, *Analysis of Experimental Data for High Burnup PWR Spent Fuel Isotopic Validation—Calvert Cliffs, Takahama, and Three Mile island Reactors*, NUREG/CR-6968 (ORNL/TM-2008/071), prepared for the U.S. Nuclear Regulatory Commission by Oak Ridge National Laboratory, Oak Ridge, Tennessee (May 2008).
12. G. Ilas and I.C. Gauld, “SCALE 6 Analysis of Isotopic Assay Benchmarks for PWR Spent Fuel,” *Trans. Am. Nucl. Soc.* **101**, 691 (2009).



**APPENDIX A**  
**TRITON INPUT FILES**





## A.1 TRITON INPUT FILE FOR SAMPLE E58-88, CYCLE 7

```
=shell
cp $RTNDIR/s1c7 ./
end
=====
=t-depl parm=(nitawl,addnux=3)
PWR 17x17 pin WZR0058 cycle 7
=====
' model 1/4 host assembly (EC45) + 1/4 E assembly
' E assembly has 22.125 GWD/MTU at BOC, initial enrichment 3.6%
' use the timetable card to model the change in soluble boron
=====
44groupndf5
=====
' Type          = PWR 17x17 design
' TF            = fuel temperature 928 K
' TC            = clad temperature 607 K
' FD            = fuel density 95.016 % TD
' BMD           = boron in moderator at BOC-7 1707 ppm
=====
read alias
$fuel1 10 11 12 13 14 end
$fuel2 15 16          end
$clad1 20 21 22 23 24 end
$clad2 25 26          end
$mod1  30 31 32 33 34 end
$mod2  35 36          end
$gap1  40 41 42 43 44 end
$gap2  45 46          end
end alias
=====
read comp
'host assembly
uo2  $fuel1 0.95016 928 92234 0.0410
      92235 4.4982
      92236 0.0030
      92238 95.4578 end
wtptclad $clad1 6.5 4 40000 97.9
          50000 1.0
          26000 0.1
          41093 1.0 1 607 end
h2o  $mod1 den=0.7421 1 565.4 end
arbm 0.7421 1 1 0 0 5000 100 $mod1 1707e-6 565.4 end
n    $gap1 den=0.00125 1 607 end
' neighbour assembly
<s1c7
wtptclad $clad2 6.5 4 40000 97.9
          50000 1.0
          26000 0.1
          41093 1.0 1 607 end
h2o  $mod2 den=0.7421 1 565.4 end
arbm 0.7421 1 1 0 0 5000 100 $mod2 1707e-6 565.4 end
n    $gap2 den=0.00125 1 607 end
wtptguide 5 6.5 4 40000 97.9
          50000 1.0
```

```

                26000  0.1
                41093  1.0 1 565.4 end
end comp
=====
read celldata
  latticecell squarepitch pitch=1.2600 $mod1
                    fueld=0.8191 $fuel1
                    gapd=0.8356 $gap1
                    cladd=0.9500 $clad1 end
  latticecell squarepitch pitch=1.2600 $mod2
                    fueld=0.8191 $fuel2
                    gapd=0.8356 $gap2
                    cladd=0.9500 $clad2 end

end celldata
=====
read depletion
-10 11 12 13 14 15 16
end depletion
=====
read burndata
power=31.015  burn=358 down=33 nlib=7 end
end burndata
=====
read timetable
density $mod1 2 5010 5011
0  1.000
1  0.988
2  0.931
3  0.860
4  0.825
5  0.802
6  0.776
7  0.809
8  0.851
9  0.781
10 0.777
358 0.000 end
density $mod2 2 5010 5011
0  1.000
1  0.988
2  0.931
3  0.860
4  0.825
5  0.802
6  0.776
7  0.809
8  0.851
9  0.781
10 0.777
358 0.000 end
end timetable
=====
read model
PWR 17x17
read parm
  cmfd=yes  xycmfd=4 run=yes echo=yes drawit=yes
end parm

```

```

read materials
10 1 ! test pin      ! end
20 1 ! clad         ! end
30 2 ! water        ! end
40 0 ! gap          ! end
 5 1 ! guide tube   ! end
11 1 ! N test pin   ! end
12 1 ! W test pin   ! end
13 1 ! S test pin   ! end
14 1 ! test assy    ! end
15 1 ! E test pin   ! end
16 1 ! E assy fuel  ! end
end materials
read geom
unit 1
com='test pin'
cylinder 10 .40955
cylinder 20 .4178
cylinder 30 .475
cuboid 40 4p0.63
media 10 1 10
media 40 1 20 -10
media 20 1 30 -20
media 30 1 40 -30
boundary 40 4 4
unit 2
com='N test pin'
cylinder 10 .40955
cylinder 20 .4178
cylinder 30 .475
cuboid 40 4p0.63
media 11 1 10
media 40 1 20 -10
media 20 1 30 -20
media 30 1 40 -30
boundary 40 4 4
unit 3
com='W test pin'
cylinder 10 .40955
cylinder 20 .4178
cylinder 30 .475
cuboid 40 4p0.63
media 12 1 10
media 40 1 20 -10
media 20 1 30 -20
media 30 1 40 -30
boundary 40 4 4
unit 4
com='S test pin'
cylinder 10 .40955
cylinder 20 .4178
cylinder 30 .475
cuboid 40 4p0.63
media 13 1 10
media 40 1 20 -10
media 20 1 30 -20
media 30 1 40 -30

```

```

boundary 40 4 4
unit 11
com='other pins in test assy'
cylinder 10 .40955
cylinder 20 .4178
cylinder 30 .475
cuboid 40 4p0.63
media 14 1 10
media 40 1 20 -10
media 20 1 30 -20
media 30 1 40 -30
boundary 40 4 4
unit 5
com='E test pin'
cylinder 10 .40955
cylinder 20 .4178
cylinder 30 .475
cuboid 40 4p0.63
media 15 1 10
media 40 1 20 -10
media 20 1 30 -20
media 30 1 40 -30
boundary 40 4 4
unit 21
com='other pins in E assy'
cylinder 10 .40955
cylinder 20 .4178
cylinder 30 .475
cuboid 40 4p0.63
media 16 1 10
media 40 1 20 -10
media 20 1 30 -20
media 30 1 40 -30
boundary 40 4 4
unit 30
com='guide tube'
cylinder 10 .5625
cylinder 20 .6025
cuboid 40 4p0.63
media 30 1 10
media 5 1 20 -10
media 30 1 40 -20
boundary 40 4 4
unit 12
com='right half pin - test assy'
cylinder 10 .40955 chord +x=0
cylinder 20 .4178 chord +x=0
cylinder 30 .475 chord +x=0
cuboid 40 0.63 0.0 2p0.63
media 14 1 10
media 40 1 20 -10
media 20 1 30 -20
media 30 1 40 -30
boundary 40 2 4
unit 13
com='bottom half pin - test assy'
cylinder 10 .40955 chord -y=0

```

```

cylinder 20 .4178 chord -y=0
cylinder 30 .475 chord -y=0
cuboid 40 2p0.63 0.0 -0.63
media 14 1 10
media 40 1 20 -10
media 20 1 30 -20
media 30 1 40 -30
boundary 40 4 2
unit 22
com='left half pin - neighb assy'
cylinder 10 .40955 chord -x=0
cylinder 20 .4178 chord -x=0
cylinder 30 .475 chord -x=0
cuboid 40 0.0 -0.63 2p0.63
media 16 1 10
media 40 1 20 -10
media 20 1 30 -20
media 30 1 40 -30
boundary 40 2 4
unit 23
com='bottom half pin - neighb assy'
cylinder 10 .40955 chord -y=0
cylinder 20 .4178 chord -y=0
cylinder 30 .475 chord -y=0
cuboid 40 2p0.63 0.0 -0.63
media 16 1 10
media 40 1 20 -10
media 20 1 30 -20
media 30 1 40 -30
boundary 40 4 2
unit 31
com='right half of guide tube'
cylinder 10 .5625 chord +x=0
cylinder 20 .6025 chord +x=0
cuboid 40 0.63 0.0 2p0.63
media 30 1 10
media 5 1 20 -10
media 30 1 40 -20
boundary 40 2 4
unit 32
com='left half of guide tube'
cylinder 10 .5625 chord -x=0
cylinder 20 .6025 chord -x=0
cuboid 40 0.0 -0.63 2p0.63
media 30 1 10
media 5 1 20 -10
media 30 1 40 -20
boundary 40 2 4
unit 33
com='bottom half of guide tube'
cylinder 10 .5625 chord -y=0
cylinder 20 .6025 chord -y=0
cuboid 40 2p0.63 0.0 -0.63
media 30 1 10
media 5 1 20 -10
media 30 1 40 -20
boundary 40 4 2

```

```

unit 34
com='1/4 bottom right instrument tube'
cylinder 10 .5625 chord +x=0 chord -y=0
cylinder 20 .6025 chord +x=0 chord -y=0
cuboid 40 0.63 0.0 0.0 -0.63
media 30 1 10
media 5 1 20 -10
media 30 1 40 -20
boundary 40 2 2
unit 35
com='1/4 bottom left instrument tube'
cylinder 10 .5625 chord -x=0 chord -y=0
cylinder 20 .6025 chord -x=0 chord -y=0
cuboid 40 0.0 -0.63 0.0 -0.63
media 30 1 10
media 5 1 20 -10
media 30 1 40 -20
boundary 40 2 2
unit 41
com='1/4 test assy'
cuboid 10 10.752 0.0 10.752 0.0
array 1 10 place 1 1 0.0 0.672
media 30 1 10
boundary 10 17 17
unit 42
com='1/4 neigh assy'
cuboid 10 10.752 0.0 10.752 0.0
array 2 10 place 1 1 0.672 0.672
media 30 1 10
boundary 10 17 17
global unit 50
cuboid 10 21.504 0.0 10.752 0.0
array 3 10 place 1 1 0 0
media 30 1 10
boundary 10 34 34
end geom
read array
ara=1 nux=9 nuy=9 typ=cuboidal
fill
12 11 11 11 11 11 11 11 11
12 11 11 11 11 11 11 11 11
31 11 11 30 11 11 11 11 11
12 11 11 11 11 30 11 11 11
12 11 11 11 11 11 11 11 4
31 11 11 30 11 11 30 3 1
12 11 11 11 11 11 11 11 2
12 11 11 11 11 11 11 11 11
34 13 13 33 13 13 33 13 13 end fill
ara=2 nux=9 nuy=9 typ=cuboidal
fill
21 21 21 21 21 21 21 21 22
21 21 21 21 21 21 21 21 22
21 21 21 21 21 30 21 21 32
21 21 21 30 21 21 21 21 22
21 21 21 21 21 21 21 21 22
5 21 30 21 21 30 21 21 32
21 21 21 21 21 21 21 21 22

```

```
21 21 21 21 21 21 21 21 22
23 23 33 23 23 33 23 23 35 end fill
ara=3 nux=2 nuy=1 typ=cuboidal
fill
  41 42 end fill
end array
read bounds
  all=refl
end bounds
end model
end
```

```
=====
=shell
```

```
cp stdcmp_mix0010 $RTNDIR/E58-088_mix0010_c7
cp stdcmp_mix0011 $RTNDIR/E58-088_mix0011_c7
cp stdcmp_mix0012 $RTNDIR/E58-088_mix0012_c7
cp stdcmp_mix0013 $RTNDIR/E58-088_mix0013_c7
cp stdcmp_mix0014 $RTNDIR/E58-088_mix0014_c7
cp ft71f001 $RTNDIR/E58-088.den
end
```

## A.2 TRITON INPUT FILE FOR SAMPLE E58-88, CYCLE 8

```
=shell
cp $RTNDIR/s1c8 ./
cp $RTNDIR/E58-088_mix0010_c7 ./
cp $RTNDIR/E58-088_mix0011_c7 ./
cp $RTNDIR/E58-088_mix0012_c7 ./
cp $RTNDIR/E58-088_mix0013_c7 ./
cp $RTNDIR/E58-088_mix0014_c7 ./
end
=====
=t-depl parm=(nitawl,addnux=3)
PWR 17x17 pin WZR0058 cycle 8
=====
' model 1/4 host assy (EC45) + 1/4 E assy
' E assy has 31.333 GWd/MTU at BOC, initial enrichment 3.6%
' use the timetable card to model the change in soluble boron
=====
44groupndf5
=====
' Type          = PWR 17x17 design
' TF            = fuel temperature 928 K
' TC            = clad temperature 607 K
' FD            = fuel density 95.016 % TD
' BMD           = boron in moderator at BOC-8 1572 ppm
' BPRs          = no BPRs present
=====
read alias
$fuel1 10 11 12 13 14 end
$fuel2 15 16          end
$clad1 20 21 22 23 24 end
$clad2 25 26          end
$mod1  30 31 32 33 34 end
$mod2  35 36          end
$gap1  40 41 42 43 44 end
$gap2  45 46          end
end alias
=====
read comp
'test assembly
<E58-088_mix0010_c7
<E58-088_mix0011_c7
<E58-088_mix0012_c7
<E58-088_mix0013_c7
<E58-088_mix0014_c7
wtptclad $clad1 6.5 4 40000 97.9
                    50000 1.0
                    26000 0.1
                    41093 1.0 1 607 end
h2o  $mod1 den=0.7421 1 565.4 end
arbbm 0.7421 1 1 0 0 5000 100 $mod1 1572e-6 565.4 end
n  $gap1 den=0.00125 1 607 end
' neighbour assembly
<s1c8
wtptclad $clad2 6.5 4 40000 97.9
                    50000 1.0
```



```

                26000 0.1
                41093 1.0 1 607 end
h2o  $mod2 den=0.7421 1 565.4 end
arbm 0.7421 1 1 0 0 5000 100 $mod2 1572e-6 565.4 end
n    $gap2 den=0.00125 1 607 end
wtptguide 5 6.5 4 40000 97.9
                50000 1.0
                26000 0.1
                41093 1.0 1 565.4 end

end comp
=====
read celldata
  latticecell squarepitch pitch=1.2600 $mod1
                        fueld=0.8191 $fuel1
                        gapd=0.8356 $gap1
                        cladd=0.9500 $clad1 end
  latticecell squarepitch pitch=1.2600 $mod2
                        fueld=0.8191 $fuel2
                        gapd=0.8356 $gap2
                        cladd=0.9500 $clad2 end

end celldata
=====
read depletion
-10 11 12 13 14 15 16
end depletion
=====
read burndata
power=17.415 burn=330 down=35 nlib=7 end
end burndata
=====
read timetable
density $mod1 2 5010 5011
0 1.000
1 1.001
2 0.903
3 0.833
4 0.795
5 0.777
6 0.759
7 0.746
8 0.739
9 0.735
10 0.754
330 0.001 end
density $mod2 2 5010 5011
0 1.000
1 1.001
2 0.903
3 0.833
4 0.795
5 0.777
6 0.759
7 0.746
8 0.739
9 0.735
10 0.754
330 0.001 end

```

```

end timetable
=====
read model
PWR 17x17
read parm
  cmfd=yes xycmfd=4 run=yes echo=yes drawit=no
end parm
read materials
10 1 ! test pin      ! end
20 1 ! clad          ! end
30 2 ! water         ! end
40 0 ! gap           ! end
  5 1 ! guide tube   ! end
11 1 ! N test pin   ! end
12 1 ! W test pin   ! end
13 1 ! S test pin   ! end
14 1 ! test assy    ! end
15 1 ! E test pin   ! end
16 1 ! E assy fuel  ! end
end materials
read geom
unit 1
com='test pin'
  cylinder 10 .40955
  cylinder 20 .4178
  cylinder 30 .475
  cuboid 40 4p0.63
  media 10 1 10
  media 40 1 20 -10
  media 20 1 30 -20
  media 30 1 40 -30
  boundary 40 4 4
unit 2
com='N test pin'
  cylinder 10 .40955
  cylinder 20 .4178
  cylinder 30 .475
  cuboid 40 4p0.63
  media 11 1 10
  media 40 1 20 -10
  media 20 1 30 -20
  media 30 1 40 -30
  boundary 40 4 4
unit 3
com='W test pin'
  cylinder 10 .40955
  cylinder 20 .4178
  cylinder 30 .475
  cuboid 40 4p0.63
  media 12 1 10
  media 40 1 20 -10
  media 20 1 30 -20
  media 30 1 40 -30
  boundary 40 4 4
unit 4
com='S test pin'
  cylinder 10 .40955

```

```

cylinder 20 .4178
cylinder 30 .475
cuboid 40 4p0.63
media 13 1 10
media 40 1 20 -10
media 20 1 30 -20
media 30 1 40 -30
boundary 40 4 4
unit 11
com='other pins in test assy'
cylinder 10 .40955
cylinder 20 .4178
cylinder 30 .475
cuboid 40 4p0.63
media 14 1 10
media 40 1 20 -10
media 20 1 30 -20
media 30 1 40 -30
boundary 40 4 4
unit 5
com='E test pin'
cylinder 10 .40955
cylinder 20 .4178
cylinder 30 .475
cuboid 40 4p0.63
media 15 1 10
media 40 1 20 -10
media 20 1 30 -20
media 30 1 40 -30
boundary 40 4 4
unit 21
com='other pins in E assy'
cylinder 10 .40955
cylinder 20 .4178
cylinder 30 .475
cuboid 40 4p0.63
media 16 1 10
media 40 1 20 -10
media 20 1 30 -20
media 30 1 40 -30
boundary 40 4 4
unit 30
com='guide tube'
cylinder 10 .5625
cylinder 20 .6025
cuboid 40 4p0.63
media 30 1 10
media 5 1 20 -10
media 30 1 40 -20
boundary 40 4 4
unit 12
com='right half pin - test assy'
cylinder 10 .40955 chord +x=0
cylinder 20 .4178 chord +x=0
cylinder 30 .475 chord +x=0
cuboid 40 0.63 0.0 2p0.63
media 14 1 10

```

```

media 40 1 20 -10
media 20 1 30 -20
media 30 1 40 -30
boundary 40 2 4
unit 13
com='bottom half pin - test assy'
cylinder 10 .40955 chord -y=0
cylinder 20 .4178 chord -y=0
cylinder 30 .475 chord -y=0
cuboid 40 2p0.63 0.0 -0.63
media 14 1 10
media 40 1 20 -10
media 20 1 30 -20
media 30 1 40 -30
boundary 40 4 2
unit 22
com='left half pin - neighb assy'
cylinder 10 .40955 chord -x=0
cylinder 20 .4178 chord -x=0
cylinder 30 .475 chord -x=0
cuboid 40 0.0 -0.63 2p0.63
media 16 1 10
media 40 1 20 -10
media 20 1 30 -20
media 30 1 40 -30
boundary 40 2 4
unit 23
com='bottom half pin - neighb assy'
cylinder 10 .40955 chord -y=0
cylinder 20 .4178 chord -y=0
cylinder 30 .475 chord -y=0
cuboid 40 2p0.63 0.0 -0.63
media 16 1 10
media 40 1 20 -10
media 20 1 30 -20
media 30 1 40 -30
boundary 40 4 2
unit 31
com='right half of guide tube'
cylinder 10 .5625 chord +x=0
cylinder 20 .6025 chord +x=0
cuboid 40 0.63 0.0 2p0.63
media 30 1 10
media 5 1 20 -10
media 30 1 40 -20
boundary 40 2 4
unit 32
com='left half of guide tube'
cylinder 10 .5625 chord -x=0
cylinder 20 .6025 chord -x=0
cuboid 40 0.0 -0.63 2p0.63
media 30 1 10
media 5 1 20 -10
media 30 1 40 -20
boundary 40 2 4
unit 33
com='bottom half of guide tube'

```

```

cylinder 10 .5625 chord -y=0
cylinder 20 .6025 chord -y=0
cuboid 40 2p0.63 0.0 -0.63
media 30 1 10
media 5 1 20 -10
media 30 1 40 -20
boundary 40 4 2
unit 34
com='1/4 bottom right instrument tube'
cylinder 10 .5625 chord +x=0 chord -y=0
cylinder 20 .6025 chord +x=0 chord -y=0
cuboid 40 0.63 0.0 0.0 -0.63
media 30 1 10
media 5 1 20 -10
media 30 1 40 -20
boundary 40 2 2
unit 35
com='1/4 bottom left instrument tube'
cylinder 10 .5625 chord -x=0 chord -y=0
cylinder 20 .6025 chord -x=0 chord -y=0
cuboid 40 0.0 -0.63 0.0 -0.63
media 30 1 10
media 5 1 20 -10
media 30 1 40 -20
boundary 40 2 2
unit 41
com='1/4 test assy'
cuboid 10 10.752 0.0 10.752 0.0
array 1 10 place 1 1 0.0 0.672
media 30 1 10
boundary 10 17 17
unit 42
com='1/4 neigh assy'
cuboid 10 10.752 0.0 10.752 0.0
array 2 10 place 1 1 0.672 0.672
media 30 1 10
boundary 10 17 17
global unit 50
cuboid 10 21.504 0.0 10.752 0.0
array 3 10 place 1 1 0 0
media 30 1 10
boundary 10 34 34
end geom
read array
ara=1 nux=9 nuy=9 typ=cuboidal
fill
12 11 11 11 11 11 11 11 11
12 11 11 11 11 11 11 11 11
31 11 11 30 11 11 11 11 11
12 11 11 11 11 30 11 11 11
12 11 11 11 11 11 11 11 4
31 11 11 30 11 11 30 3 1
12 11 11 11 11 11 11 11 2
12 11 11 11 11 11 11 11 11
34 13 13 33 13 13 33 13 13 end fill
ara=2 nux=9 nuy=9 typ=cuboidal
fill

```

```

21 21 21 21 21 21 21 21 22
21 21 21 21 21 21 21 21 22
21 21 21 21 21 30 21 21 32
21 21 21 30 21 21 21 21 22
21 21 21 21 21 21 21 21 22
 5 21 30 21 21 30 21 21 32
21 21 21 21 21 21 21 21 22
21 21 21 21 21 21 21 21 22
23 23 33 23 23 33 23 23 35 end fill
ara=3 nux=2 nuy=1 typ=cuboidal
fill
 41 42 end fill
end array
read bounds
  all=refl
end bounds
end model
end
=====
=shell
cp stdcmp_mix0010 $RTNDIR/E58-088_mix0010_c8
cp stdcmp_mix0011 $RTNDIR/E58-088_mix0011_c8
cp stdcmp_mix0012 $RTNDIR/E58-088_mix0012_c8
cp stdcmp_mix0013 $RTNDIR/E58-088_mix0013_c8
cp stdcmp_mix0014 $RTNDIR/E58-088_mix0014_c8
end

```

### A.3 TRITON INPUT FILE FOR SAMPLE E58-88, CYCLE 9

```
=shell
cp $RTNDIR/E58-088_mix0010_c8 ./
cp $RTNDIR/E58-088_mix0011_c8 ./
cp $RTNDIR/E58-088_mix0012_c8 ./
cp $RTNDIR/E58-088_mix0013_c8 ./
cp $RTNDIR/E58-088_mix0014_c8 ./
end
=====
=t-depl parm=(nitawl,addnux=3)
PWR 17x17 pin WZR0058 cycle 9
=====
' model 1/4 host assy (EC45) + 1/4 E assy (
' E assy has 0 Wd/MTU at BOC, initial enrichment 4.23%
' use the timetable card to model the change in soluble boron
44groupndf5
=====
' Type      = PWR 17x17 design
' TF        = fuel temperature 928 K
' TC        = clad temperature 607 K
' FD        = fuel density 95.016 % TD
' BMD       = boron in moderator at BOC-9 1559 ppm
=====
read alias
$fuel1 10 11 12 13 14 end
$fuel2 15 16          end
$clad1 20 21 22 23 24 end
$clad2 25 26          end
$mod1  30 31 32 33 34 end
$mod2  35 36          end
$gap1  40 41 42 43 44 end
$gap2  45 46          end
end alias
=====
read comp
'test assembly
<E58-088_mix0010_c8
<E58-088_mix0011_c8
<E58-088_mix0012_c8
<E58-088_mix0013_c8
<E58-088_mix0014_c8
wtptclad $clad1 6.5 4 40000 97.9
                    50000 1.0
                    26000 0.1
                    41093 1.0 1 607 end
h2o  $mod1 den=0.7421 1 565.4 end
arbm 0.7421 1 1 0 0 5000 100 $mod1 1559e-6 565.4 end
n  $gap1 den=0.00125 1 607 end
' neighbour assembly
uo2  $fuel2 0.95016 928 92235 4.231
                    92238 95.769 end
wtptclad $clad2 6.5 4 40000 97.9
                    50000 1.0
                    26000 0.1
                    41093 1.0 1 607 end
```

```

h2o $mod2 den=0.7421 1 565.4 end
arbm 0.7421 1 1 0 0 5000 100 $mod2 1559e-6 565.4 end
n $gap2 den=0.00125 1 607 end
wtptguide 5 6.5 4 40000 97.9
          50000 1.0
          26000 0.1
          41093 1.0 1 565.4 end

end comp
=====
read celldata
  latticecell squarepitch pitch=1.2600 $mod1
                    fueld=0.8191 $fuel1
                    gapd=0.8356 $gap1
                    cladd=0.9500 $clad1 end
  latticecell squarepitch pitch=1.2600 $mod2
                    fueld=0.8191 $fuel2
                    gapd=0.8356 $gap2
                    cladd=0.9500 $clad2 end

end celldata
=====
read depletion
-10 11 12 13 14 15 16
end depletion
=====
read burndata
power=28.092 burn=407 down=31 nlib=7 end
end burndata
=====
read timetable
density $mod1 2 5010 5011
0 1.000
1 0.872
2 0.847
3 0.847
4 0.846
5 0.843
6 0.841
7 0.836
8 0.834
9 0.832
10 0.852
407 0.000 end
density $mod2 2 5010 5011
0 1.000
1 0.872
2 0.847
3 0.847
4 0.846
5 0.843
6 0.841
7 0.836
8 0.834
9 0.832
10 0.852
407 0.000 end
end timetable
=====

```



```

read model
PWR 17x17
read parm
  cmfd=yes xycmfd=4 run=yes echo=yes drawit=no
end parm
read materials
10 1 ! test pin      ! end
20 1 ! clad          ! end
30 2 ! water         ! end
40 0 ! gap           ! end
  5 1 ! guide tube   ! end
11 1 ! N test pin   ! end
12 1 ! W test pin   ! end
13 1 ! S test pin   ! end
14 1 ! test assy    ! end
15 1 ! E test pin   ! end
16 1 ! E assy fuel  ! end
end materials
read geom
unit 1
com='test pin'
  cylinder 10 .40955
  cylinder 20 .4178
  cylinder 30 .475
  cuboid 40 4p0.63
  media 10 1 10
  media 40 1 20 -10
  media 20 1 30 -20
  media 30 1 40 -30
  boundary 40 4 4
unit 2
com='N test pin'
  cylinder 10 .40955
  cylinder 20 .4178
  cylinder 30 .475
  cuboid 40 4p0.63
  media 11 1 10
  media 40 1 20 -10
  media 20 1 30 -20
  media 30 1 40 -30
  boundary 40 4 4
unit 3
com='W test pin'
  cylinder 10 .40955
  cylinder 20 .4178
  cylinder 30 .475
  cuboid 40 4p0.63
  media 12 1 10
  media 40 1 20 -10
  media 20 1 30 -20
  media 30 1 40 -30
  boundary 40 4 4
unit 4
com='S test pin'
  cylinder 10 .40955
  cylinder 20 .4178
  cylinder 30 .475

```

```

cuboid 40 4p0.63
media 13 1 10
media 40 1 20 -10
media 20 1 30 -20
media 30 1 40 -30
boundary 40 4 4
unit 11
com='other pins in test assy'
cylinder 10 .40955
cylinder 20 .4178
cylinder 30 .475
cuboid 40 4p0.63
media 14 1 10
media 40 1 20 -10
media 20 1 30 -20
media 30 1 40 -30
boundary 40 4 4
unit 5
com='E test pin'
cylinder 10 .40955
cylinder 20 .4178
cylinder 30 .475
cuboid 40 4p0.63
media 15 1 10
media 40 1 20 -10
media 20 1 30 -20
media 30 1 40 -30
boundary 40 4 4
unit 21
com='other pins in E assy'
cylinder 10 .40955
cylinder 20 .4178
cylinder 30 .475
cuboid 40 4p0.63
media 16 1 10
media 40 1 20 -10
media 20 1 30 -20
media 30 1 40 -30
boundary 40 4 4
unit 30
com='guide tube'
cylinder 10 .5625
cylinder 20 .6025
cuboid 40 4p0.63
media 30 1 10
media 5 1 20 -10
media 30 1 40 -20
boundary 40 4 4
unit 12
com='right half pin - test assy'
cylinder 10 .40955 chord +x=0
cylinder 20 .4178 chord +x=0
cylinder 30 .475 chord +x=0
cuboid 40 0.63 0.0 2p0.63
media 14 1 10
media 40 1 20 -10
media 20 1 30 -20

```

```

media 30 1 40 -30
boundary 40 2 4
unit 13
com='bottom half pin - test assy'
cylinder 10 .40955 chord -y=0
cylinder 20 .4178 chord -y=0
cylinder 30 .475 chord -y=0
cuboid 40 2p0.63 0.0 -0.63
media 14 1 10
media 40 1 20 -10
media 20 1 30 -20
media 30 1 40 -30
boundary 40 4 2
unit 22
com='left half pin - neighb assy'
cylinder 10 .40955 chord -x=0
cylinder 20 .4178 chord -x=0
cylinder 30 .475 chord -x=0
cuboid 40 0.0 -0.63 2p0.63
media 16 1 10
media 40 1 20 -10
media 20 1 30 -20
media 30 1 40 -30
boundary 40 2 4
unit 23
com='bottom half pin - neighb assy'
cylinder 10 .40955 chord -y=0
cylinder 20 .4178 chord -y=0
cylinder 30 .475 chord -y=0
cuboid 40 2p0.63 0.0 -0.63
media 16 1 10
media 40 1 20 -10
media 20 1 30 -20
media 30 1 40 -30
boundary 40 4 2
unit 31
com='right half of guide tube'
cylinder 10 .5625 chord +x=0
cylinder 20 .6025 chord +x=0
cuboid 40 0.63 0.0 2p0.63
media 30 1 10
media 5 1 20 -10
media 30 1 40 -20
boundary 40 2 4
unit 32
com='left half of guide tube'
cylinder 10 .5625 chord -x=0
cylinder 20 .6025 chord -x=0
cuboid 40 0.0 -0.63 2p0.63
media 30 1 10
media 5 1 20 -10
media 30 1 40 -20
boundary 40 2 4
unit 33
com='bottom half of guide tube'
cylinder 10 .5625 chord -y=0
cylinder 20 .6025 chord -y=0

```

```

cuboid 40 2p0.63 0.0 -0.63
media 30 1 10
media 5 1 20 -10
media 30 1 40 -20
boundary 40 4 2
unit 34
com='1/4 bottom right instrument tube'
cylinder 10 .5625 chord +x=0 chord -y=0
cylinder 20 .6025 chord +x=0 chord -y=0
cuboid 40 0.63 0.0 0.0 -0.63
media 30 1 10
media 5 1 20 -10
media 30 1 40 -20
boundary 40 2 2
unit 35
com='1/4 bottom left instrument tube'
cylinder 10 .5625 chord -x=0 chord -y=0
cylinder 20 .6025 chord -x=0 chord -y=0
cuboid 40 0.0 -0.63 0.0 -0.63
media 30 1 10
media 5 1 20 -10
media 30 1 40 -20
boundary 40 2 2
unit 41
com='1/4 test assy'
cuboid 10 10.752 0.0 10.752 0.0
array 1 10 place 1 1 0.0 0.672
media 30 1 10
boundary 10 17 17
unit 42
com='1/4 neigh assy'
cuboid 10 10.752 0.0 10.752 0.0
array 2 10 place 1 1 0.672 0.672
media 30 1 10
boundary 10 17 17
global unit 50
cuboid 10 21.504 0.0 10.752 0.0
array 3 10 place 1 1 0 0
media 30 1 10
boundary 10 34 34
end geom
read array
ara=1 nux=9 nuy=9 typ=cuboidal
fill
12 11 11 11 11 11 11 11 11
12 11 11 11 11 11 11 11 11
31 11 11 30 11 11 11 11 11
12 11 11 11 11 30 11 11 11
12 11 11 11 11 11 11 11 4
31 11 11 30 11 11 30 3 1
12 11 11 11 11 11 11 11 2
12 11 11 11 11 11 11 11 11
34 13 13 33 13 13 33 13 13 end fill
ara=2 nux=9 nuy=9 typ=cuboidal
fill
21 21 21 21 21 21 21 21 22
21 21 21 21 21 21 21 21 22

```

```

21 21 21 21 21 30 21 21 32
21 21 21 30 21 21 21 21 22
21 21 21 21 21 21 21 21 22
  5 21 30 21 21 30 21 21 32
21 21 21 21 21 21 21 21 22
21 21 21 21 21 21 21 21 22
23 23 33 23 23 33 23 23 35 end fill
ara=3 nux=2 nuy=1 typ=cuboidal
fill
  41 42 end fill
end array
read bounds
  all=refl
end bounds
end model
end
=====
=shell
cp stdcmp_mix0010 $RTNDIR/E58-088_mix0010_c9
cp stdcmp_mix0011 $RTNDIR/E58-088_mix0011_c9
cp stdcmp_mix0012 $RTNDIR/E58-088_mix0012_c9
cp stdcmp_mix0013 $RTNDIR/E58-088_mix0013_c9
cp stdcmp_mix0014 $RTNDIR/E58-088_mix0014_c9
end

```

#### A.4 TRITON INPUT FILE FOR SAMPLE E58-88, CYCLE 10

```
=shell
cp $RTNDIR/s1c0 ./
cp $RTNDIR/E58-088_mix0010_c9 ./
cp $RTNDIR/E58-088_mix0011_c9 ./
cp $RTNDIR/E58-088_mix0012_c9 ./
cp $RTNDIR/E58-088_mix0013_c9 ./
cp $RTNDIR/E58-088_mix0014_c9 ./
end
=====
=t-depl parm=(nitawl,addnux=3)
PWR 17x17 pin WZR0058 cycle 9
=====
' model 1/4 host assy (EC45) + 1/4 E assy + water at the edge of the core
' E assy has 34.678Gwd/MTU at BOC, initial enrichment 3.6%
' use the timetable card to model the change in soluble boron
=====
44groupndf5
=====
' Type          = PWR 17x17 design
' TF            = fuel temperature 928 K
' TC            = clad temperature 607 K
' FD            = fuel density 95.016 % TD
' BMD           = boron in moderator at BOC-10 2237 ppm
=====
read alias
  $fuel1 10 11 12 13 14 end
  $fuel2 15 16          end
  $clad1 20 21 22 23 24 end
  $clad2 25 26          end
  $mod1  30 31 32 33 34 end
  $mod2  35 36          end
  $gap1  40 41 42 43 44 end
  $gap2  45 46          end
end alias
=====
read comp
'test assembly
<E58-088_mix0010_c9
<E58-088_mix0011_c9
<E58-088_mix0012_c9
<E58-088_mix0013_c9
<E58-088_mix0014_c9
wtptclad $clad1 6.5 4 40000 97.9
                    50000 1.0
                    26000 0.1
                    41093 1.0 1 607 end
h2o  $mod1 den=0.7425 1 565.4 end
arbbm 0.7425 1 1 0 0 5000 100 $mod1 2237e-6 565.4 end
n  $gap1 den=0.00125 1 607 end
' neighbour assembly
<s1c0
wtptclad $clad2 6.5 4 40000 97.9
                    50000 1.0
                    26000 0.1
```

```

                                41093  1.0 1 607 end
h2o   $mod2 den=0.7425 1 565.4 end
arbm  0.7425 1 1 0 0 5000 100 $mod2 2237e-6 565.4 end
n      $gap2 den=0.00125 1 607 end
wtptguide 5 6.5 4 40000 97.9
                                50000  1.0
                                26000  0.1
                                41093  1.0 1 565.4 end
end comp
=====
read celldata
  latticecell squarepitch pitch=1.2600 $mod1
                                fueld=0.8191 $fuel1
                                gapd=0.8356 $gap1
                                cladd=0.9500 $clad1 end
  latticecell squarepitch pitch=1.2600 $mod2
                                fueld=0.8191 $fuel2
                                gapd=0.8356 $gap2
                                cladd=0.9500 $clad2 end
end celldata
=====
read depletion
-10 11 12 13 14 15 16
end depletion
=====
read burndata
power=7.3720 burn=535 down=50 nlib=2 end
end burndata
=====
read timetable
density $mod1 2 5010 5011
0  1.000
1  0.959
2  0.904
3  0.895
4  0.872
5  0.843
6  0.836
7  0.834
8  0.821
9  0.813
10 0.843
535 0.002 end
density $mod2 2 5010 5011
0  1.000
1  0.959
2  0.904
3  0.895
4  0.872
5  0.843
6  0.836
7  0.834
8  0.821
9  0.813
10 0.843
535 0.002 end
end timetable

```

```

=====
read model
PWR 17x17
read parm
  cmfd=yes xycmfd=4 run=yes echo=yes drawit=no converg=mix
end parm
read materials
10 1 ! test pin      ! end
20 1 ! clad         ! end
30 2 ! water        ! end
40 0 ! gap          ! end
  5 1 ! guide tube  ! end
11 1 ! N test pin  ! end
12 1 ! W test pin  ! end
13 1 ! S test pin  ! end
14 1 ! test assy   ! end
15 1 ! E test pin  ! end
16 1 ! E assy fuel ! end
end materials
read geom
unit 1
com='test pin'
  cylinder 10 .40955
  cylinder 20 .4178
  cylinder 30 .475
  cuboid 40 4p0.63
  media 10 1 10
  media 40 1 20 -10
  media 20 1 30 -20
  media 30 1 40 -30
  boundary 40 4 4
unit 2
com='N test pin'
  cylinder 10 .40955
  cylinder 20 .4178
  cylinder 30 .475
  cuboid 40 4p0.63
  media 11 1 10
  media 40 1 20 -10
  media 20 1 30 -20
  media 30 1 40 -30
  boundary 40 4 4
unit 3
com='W test pin'
  cylinder 10 .40955
  cylinder 20 .4178
  cylinder 30 .475
  cuboid 40 4p0.63
  media 12 1 10
  media 40 1 20 -10
  media 20 1 30 -20
  media 30 1 40 -30
  boundary 40 4 4
unit 4
com='S test pin'
  cylinder 10 .40955
  cylinder 20 .4178

```



```

cylinder 30 .475
cuboid 40 4p0.63
media 13 1 10
media 40 1 20 -10
media 20 1 30 -20
media 30 1 40 -30
boundary 40 4 4
unit 11
com='other pins in test assy'
cylinder 10 .40955
cylinder 20 .4178
cylinder 30 .475
cuboid 40 4p0.63
media 14 1 10
media 40 1 20 -10
media 20 1 30 -20
media 30 1 40 -30
boundary 40 4 4
unit 5
com='E test pin'
cylinder 10 .40955
cylinder 20 .4178
cylinder 30 .475
cuboid 40 4p0.63
media 15 1 10
media 40 1 20 -10
media 20 1 30 -20
media 30 1 40 -30
boundary 40 4 4
unit 6
com='water cell'
cuboid 40 4p0.63
media 30 1 40
boundary 40 4 4
unit 61
com='half water cell'
cuboid 40 0.63 0. 2p0.63
media 30 1 40
boundary 40 2 4
unit 21
com='other pins in E assy'
cylinder 10 .40955
cylinder 20 .4178
cylinder 30 .475
cuboid 40 4p0.63
media 16 1 10
media 40 1 20 -10
media 20 1 30 -20
media 30 1 40 -30
boundary 40 4 4
unit 30
com='guide tube'
cylinder 10 .5625
cylinder 20 .6025
cuboid 40 4p0.63
media 30 1 10
media 5 1 20 -10

```

```

media 30 1 40 -20
boundary 40 4 4
unit 12
com='right half pin - test assy'
cylinder 10 .40955 chord +x=0
cylinder 20 .4178 chord +x=0
cylinder 30 .475 chord +x=0
cuboid 40 0.63 0.0 2p0.63
media 14 1 10
media 40 1 20 -10
media 20 1 30 -20
media 30 1 40 -30
boundary 40 2 4
unit 13
com='bottom half pin - test assy'
cylinder 10 .40955 chord -y=0
cylinder 20 .4178 chord -y=0
cylinder 30 .475 chord -y=0
cuboid 40 2p0.63 0.0 -0.63
media 14 1 10
media 40 1 20 -10
media 20 1 30 -20
media 30 1 40 -30
boundary 40 4 2
unit 22
com='left half pin - neighb assy'
cylinder 10 .40955 chord -x=0
cylinder 20 .4178 chord -x=0
cylinder 30 .475 chord -x=0
cuboid 40 0.0 -0.63 2p0.63
media 16 1 10
media 40 1 20 -10
media 20 1 30 -20
media 30 1 40 -30
boundary 40 2 4
unit 23
com='bottom half pin - neighb assy'
cylinder 10 .40955 chord -y=0
cylinder 20 .4178 chord -y=0
cylinder 30 .475 chord -y=0
cuboid 40 2p0.63 0.0 -0.63
media 16 1 10
media 40 1 20 -10
media 20 1 30 -20
media 30 1 40 -30
boundary 40 4 2
unit 31
com='right half of guide tube'
cylinder 10 .5625 chord +x=0
cylinder 20 .6025 chord +x=0
cuboid 40 0.63 0.0 2p0.63
media 30 1 10
media 5 1 20 -10
media 30 1 40 -20
boundary 40 2 4
unit 32
com='left half of guide tube'

```

```

cylinder 10 .5625 chord -x=0
cylinder 20 .6025 chord -x=0
cuboid 40 0.0 -0.63 2p0.63
media 30 1 10
media 5 1 20 -10
media 30 1 40 -20
boundary 40 2 4
unit 33
com='bottom half of guide tube'
cylinder 10 .5625 chord -y=0
cylinder 20 .6025 chord -y=0
cuboid 40 2p0.63 0.0 -0.63
media 30 1 10
media 5 1 20 -10
media 30 1 40 -20
boundary 40 4 2
unit 34
com='1/4 bottom right instrument tube'
cylinder 10 .5625 chord +x=0 chord -y=0
cylinder 20 .6025 chord +x=0 chord -y=0
cuboid 40 0.63 0.0 0.0 -0.63
media 30 1 10
media 5 1 20 -10
media 30 1 40 -20
boundary 40 2 2
unit 35
com='1/4 bottom left instrument tube'
cylinder 10 .5625 chord -x=0 chord -y=0
cylinder 20 .6025 chord -x=0 chord -y=0
cuboid 40 0.0 -0.63 0.0 -0.63
media 30 1 10
media 5 1 20 -10
media 30 1 40 -20
boundary 40 2 2
unit 41
com='1/4 test assy'
cuboid 10 10.752 0.0 10.752 0.0
array 1 10 place 1 1 0.0 0.672
media 30 1 10
boundary 10 17 17
unit 42
com='1/4 neigh assy'
cuboid 10 10.752 0.0 10.752 0.0
array 2 10 place 1 1 0.672 0.672
media 30 1 10
boundary 10 17 17
unit 43
com='water below test assy'
cuboid 10 10.752 0.0 3.822 0.0
array 4 10 place 1 1 0.0 0.672
media 30 1 10
boundary 10 17 6
unit 44
com='water below E of test assy'
cuboid 10 10.752 0.0 3.822 0.0
array 5 10 place 1 1 0.672 0.672
media 30 1 10

```

```

boundary 10 17 6
global unit 50
cuboid 10 21.504 0.0 14.574 0.0
array 3 10 place 1 1 0 0
media 30 1 10
boundary 10 34 34
end geom
read array
ara=1 nux=9 nuy=9 typ=cuboidal
fill
12 11 11 11 11 11 11 11 11
12 11 11 11 11 11 11 11 11
31 11 11 30 11 11 11 11 11
12 11 11 11 11 30 11 11 11
12 11 11 11 11 11 11 11 4
31 11 11 30 11 11 30 3 1
12 11 11 11 11 11 11 11 2
12 11 11 11 11 11 11 11 11
34 13 13 33 13 13 33 13 13 end fill
ara=2 nux=9 nuy=9 typ=cuboidal
fill
21 21 21 21 21 21 21 21 22
21 21 21 21 21 21 21 21 22
21 21 21 21 21 30 21 21 32
21 21 21 30 21 21 21 21 22
21 21 21 21 21 21 21 21 22
5 21 30 21 21 30 21 21 32
21 21 21 21 21 21 21 21 22
21 21 21 21 21 21 21 21 22
23 23 33 23 23 33 23 23 35 end fill
ara=3 nux=2 nuy=2 typ=cuboidal
fill
43 44
41 42 end fill
ara=4 nux=9 nuy=3 typ=cuboidal
fill
61 6 6 6 6 6 6 6 6
61 6 6 6 6 6 6 6 6
61 6 6 6 6 6 6 6 6 end fill
ara=5 nux=9 nuy=3 typ=cuboidal
fill
6 6 6 6 6 6 6 6 61
6 6 6 6 6 6 6 6 61
6 6 6 6 6 6 6 6 61 end fill
end array
read bounds
all=refl
end bounds
end model
end
=shell
cp stdcmp_mix0010 $RTNDIR/E58-088_mix0010_c0
cp stdcmp_mix0011 $RTNDIR/E58-088_mix0011_c0
cp stdcmp_mix0012 $RTNDIR/E58-088_mix0012_c0
cp stdcmp_mix0013 $RTNDIR/E58-088_mix0013_c0
cp stdcmp_mix0014 $RTNDIR/E58-088_mix0014_c0
end

```

## A.5 TRITON INPUT FILE FOR SAMPLE E58-88, CYCLE 11

```

=shell
cp $RTNDIR/E58-088_mix0010_c0 ./
cp $RTNDIR/EF05s1 ./
end
=====
=t-depl parm=(nitawl,addnux=3)
PWR 17x17 pin WZR0058 cycle 10
=====
' model 1/4 rebuilt assy (EF05)
' EF05 has 26.529Gwd/MTU at BOC, initial enrichment 4.24%
' use the timetable card to model the change in soluble boron
=====
44groupndf5
=====
' Type          = PWR 17x17 design
' TF            = fuel temperature 928 K
' TC            = clad temperature 607 K
' FD            = fuel density 95.016 % TD
' BMD           = boron in moderator at BOC-11 2570 ppm
=====
read alias
$fuell 10          end
$fuel2 11 12 13 15 end
$clad1 20          end
$clad2 21 22 23 25 end
$mod1  30          end
$mod2  31 32 33 35 end
$gap1  40          end
$gap2  41 42 43 45 end
end alias
=====
read comp
'test pin
<E58-088_mix0010_c0
wtptclad $clad1 6.5 4 40000 97.9
                    50000  1.0
                    26000  0.1
                    41093  1.0 1 607 end
h2o  $mod1 den=0.7456 1 563.7 end
arbm 0.7456 1 1 0 0 5000 100 $mod1 2570e-6 563.7 end
n  $gap1 den=0.00125 1 607 end
' host assembly
<EF05s1
wtptclad $clad2 6.5 4 40000 97.9
                    50000  1.0
                    26000  0.1
                    41093  1.0 1 607 end
h2o  $mod2 den=0.7456 1 563.7 end
arbm 0.7456 1 1 0 0 5000 100 $mod2 2570e-6 563.7 end
n  $gap2 den=0.00125 1 607 end
wtptguide 5 6.5 4 40000 97.9
                    50000  1.0
                    26000  0.1
                    41093  1.0 1 563.7 end

```

```

end comp
=====
read celldata
  latticecell squarepitch pitch=1.2600 $mod1
                                fueld=0.8191 $fuel1
                                gapd=0.8356 $gap1
                                cladd=0.9500 $clad1 end
  latticecell squarepitch pitch=1.2600 $mod2
                                fueld=0.8191 $fuel2
                                gapd=0.8356 $gap2
                                cladd=0.9500 $clad2 end

end celldata
=====
read depletion
-10 11 12 13 15
end depletion
=====
read burndata
power=24.368 burn=496 down=0 nlib=7 end
end burndata
=====
read timetable
density $mod1 2 5010 5011
0 1.000
2 0.843
3 0.821
4 0.787
5 0.745
6 0.699
7 0.672
8 0.750
9 0.772
10 0.858
11 0.763
12 0.698
13 0.688
14 0.674
15 0.723
496 0.002 end
density $mod2 2 5010 5011
0 1.000
2 0.843
3 0.821
4 0.787
5 0.745
6 0.699
7 0.672
8 0.750
9 0.772
10 0.858
11 0.763
12 0.698
13 0.688
14 0.674
15 0.723
496 0.002 end
end timetable

```

```

=====
read model
PWR 17x17
read parm
  cmfd=yes xycmfd=4 run=yes echo=yes drawit=no
end parm
read materials
10 1 ! test pin      ! end
20 1 ! clad         ! end
30 2 ! water        ! end
40 0 ! gap          ! end
  5 1 ! guide tube  ! end
11 1 ! N test pin  ! end
12 1 ! W test pin  ! end
13 1 ! E test pin  ! end
15 1 ! assy fuel   ! end
end materials
read geom
unit 1
com='test pin'
  cylinder 10 .40955
  cylinder 20 .4178
  cylinder 30 .475
  cuboid   40 4p0.63
  media 10 1 10
  media 40 1 20 -10
  media 20 1 30 -20
  media 30 1 40 -30
  boundary 40 4 4
unit 2
com='N test pin'
  cylinder 10 .40955
  cylinder 20 .4178
  cylinder 30 .475
  cuboid   40 4p0.63
  media 11 1 10
  media 40 1 20 -10
  media 20 1 30 -20
  media 30 1 40 -30
  boundary 40 4 4
unit 3
com='W test pin'
  cylinder 10 .40955
  cylinder 20 .4178
  cylinder 30 .475
  cuboid   40 4p0.63
  media 12 1 10
  media 40 1 20 -10
  media 20 1 30 -20
  media 30 1 40 -30
  boundary 40 4 4
unit 4
com='S test pin'
  cylinder 10 .40955
  cylinder 20 .4178
  cylinder 30 .475
  cuboid   40 4p0.63

```

```

media 13 1 10
media 40 1 20 -10
media 20 1 30 -20
media 30 1 40 -30
boundary 40 4 4
unit 11
com='other pins in host assy'
cylinder 10 .40955
cylinder 20 .4178
cylinder 30 .475
cuboid 40 4p0.63
media 15 1 10
media 40 1 20 -10
media 20 1 30 -20
media 30 1 40 -30
boundary 40 4 4
unit 30
com='guide tube'
cylinder 10 .5625
cylinder 20 .6025
cuboid 40 4p0.63
media 30 1 10
media 5 1 20 -10
media 30 1 40 -20
boundary 40 4 4
unit 12
com='left half pin - host assy'
cylinder 10 .40955 chord -x=0
cylinder 20 .4178 chord -x=0
cylinder 30 .475 chord -x=0
cuboid 40 0.0 -0.63 2p0.63
media 15 1 10
media 40 1 20 -10
media 20 1 30 -20
media 30 1 40 -30
boundary 40 2 4
unit 13
com='top half pin - host assy'
cylinder 10 .40955 chord +y=0
cylinder 20 .4178 chord +y=0
cylinder 30 .475 chord +y=0
cuboid 40 2p0.63 0.63 0.0
media 15 1 10
media 40 1 20 -10
media 20 1 30 -20
media 30 1 40 -30
boundary 40 4 2
unit 32
com='left half of guide tube'
cylinder 10 .5625 chord -x=0
cylinder 20 .6025 chord -x=0
cuboid 40 0.0 -0.63 2p0.63
media 30 1 10
media 5 1 20 -10
media 30 1 40 -20
boundary 40 2 4
unit 33

```



```

com='top half of guide tube'
  cylinder 10 .5625 chord +y=0
  cylinder 20 .6025 chord +y=0
  cuboid 40 2p0.63 0.63 0.0
  media 30 1 10
  media 5 1 20 -10
  media 30 1 40 -20
  boundary 40 4 2
unit 35
com='1/4 top left instrument tube'
  cylinder 10 .5625 chord -x=0 chord +y=0
  cylinder 20 .6025 chord -x=0 chord +y=0
  cuboid 40 0.0 -0.63 0.63 0.0
  media 30 1 10
  media 5 1 20 -10
  media 30 1 40 -20
  boundary 40 2 2
global unit 50
com='1/4 assy'
  cuboid 10 10.752 0.0 10.752 0.0
  array 1 10 place 1 1 0.672 0.0
  media 30 1 10
  boundary 10 17 17
end geom
read array
  ara=1 nux=9 nuy=9 typ=cuboidal
  fill
  13 13 33 13 13 33 13 13 35
  11 11 11 11 11 11 11 11 12
  11 11 11 11 11 11 11 11 12
  11 11 30 11 11 30 11 11 32
  11 11 11 11 11 11 11 11 12
  11 11 11 30 4 11 11 11 12
  11 11 11 3 1 30 11 11 32
  11 11 11 11 2 11 11 11 12
  11 11 11 11 11 11 11 11 12 end fill
end array
read bounds
  all=refl
end bounds
end model
end
=====
=shell
  cp stdcmp_mix0010 $RTNDIR/E58-088_mix0010_c11
  cp ft71f001 $RTNDIR/E58-088_den_c11
end

```



NUREG/CR-7013  
ORNL/TM-2009/321